Astro 7B: Introduction to Astrophysics

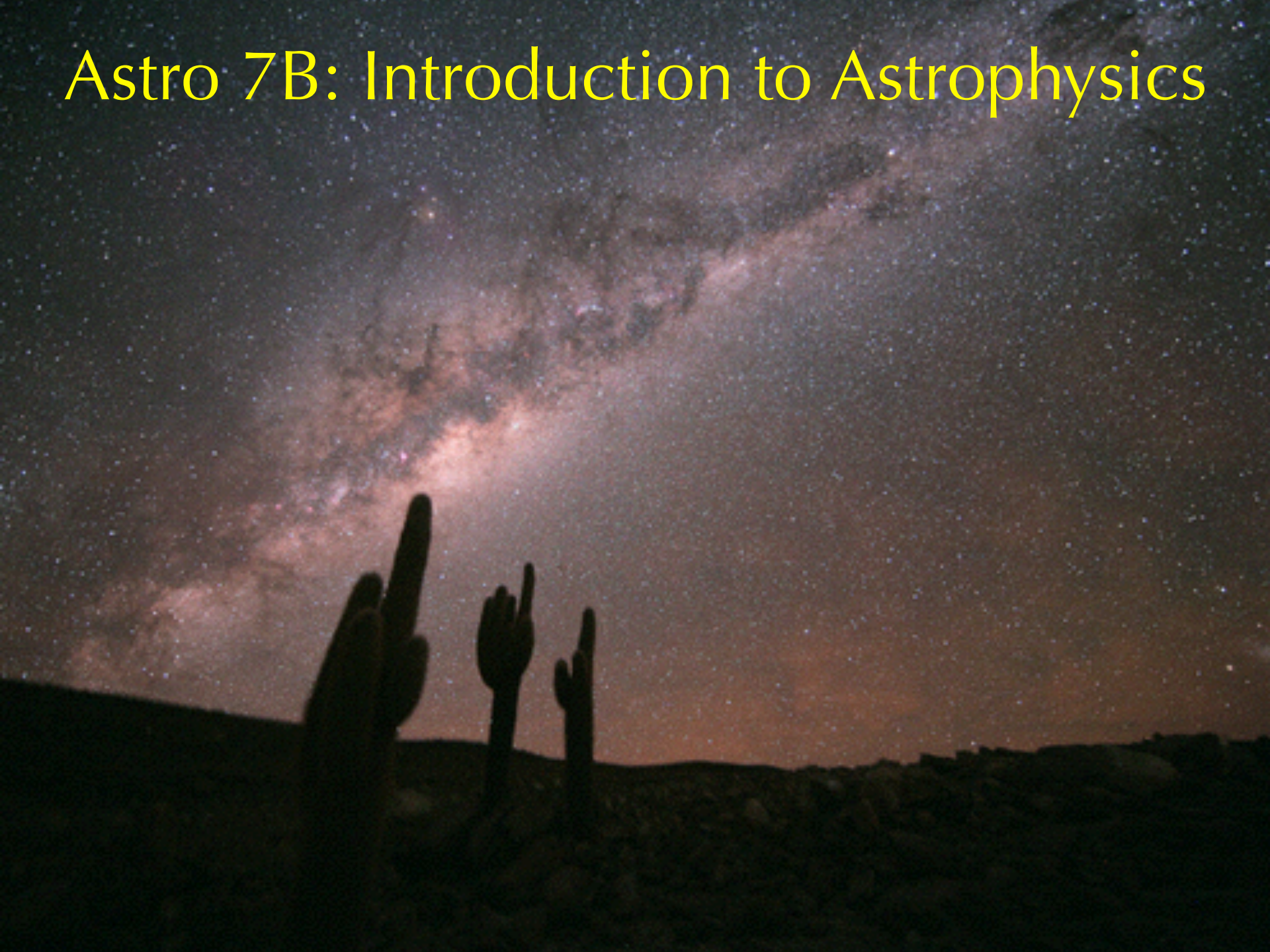


Milky Way Galaxy
Diameter ~ 20 kpc
Number of stars ~ 2 x 10^{11}
(and more planets)
M ~ 10^{11} $M_\odot$
Rotation period at Sun's location ≈ 250 Myr (too fast!)
8 +/- 0.5 kpc
Sun

Supermassive Black Hole and Young Stars at Galactic Center

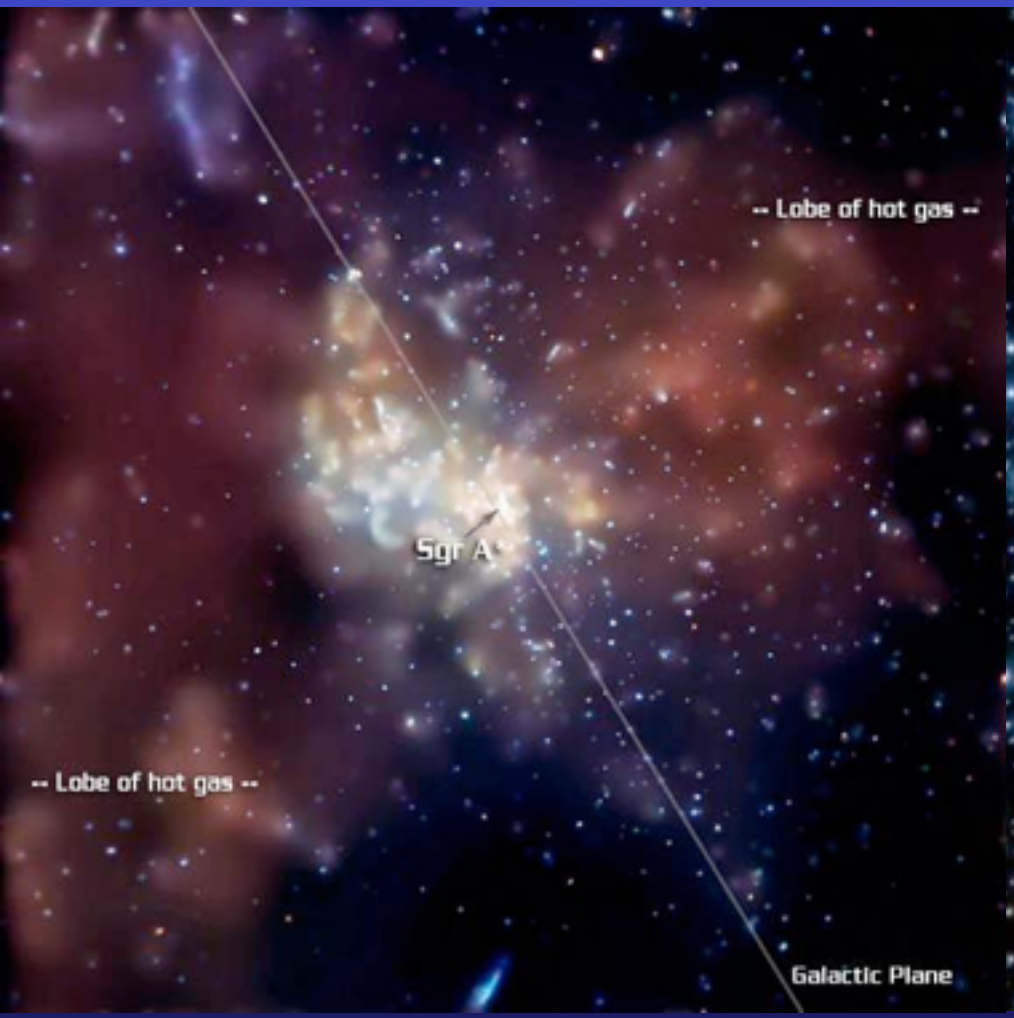

Central ~10 pc

Central ~1 pc

M87: Elliptical galaxy with Active Galactic Nucleus

All galaxies have black hole nuclei

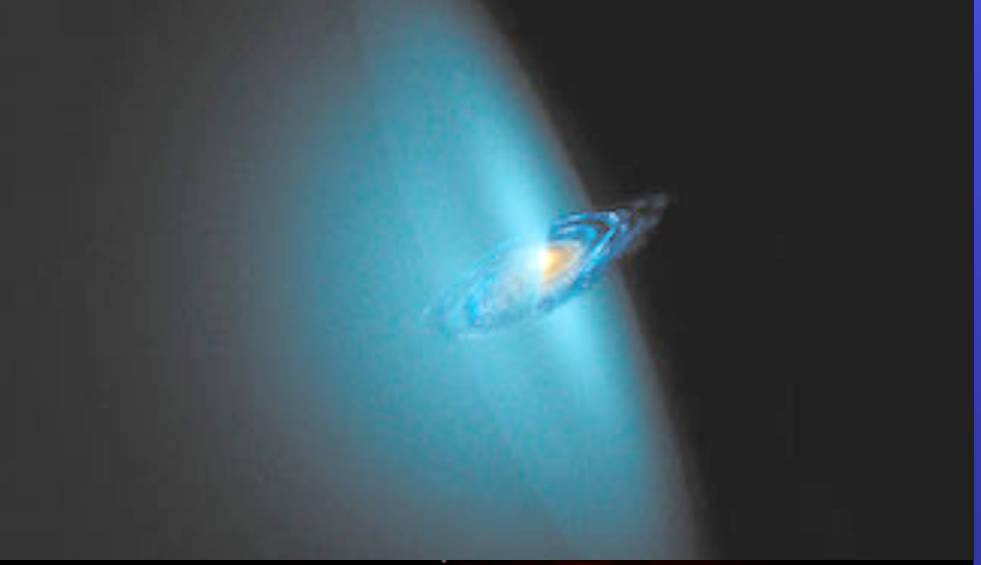

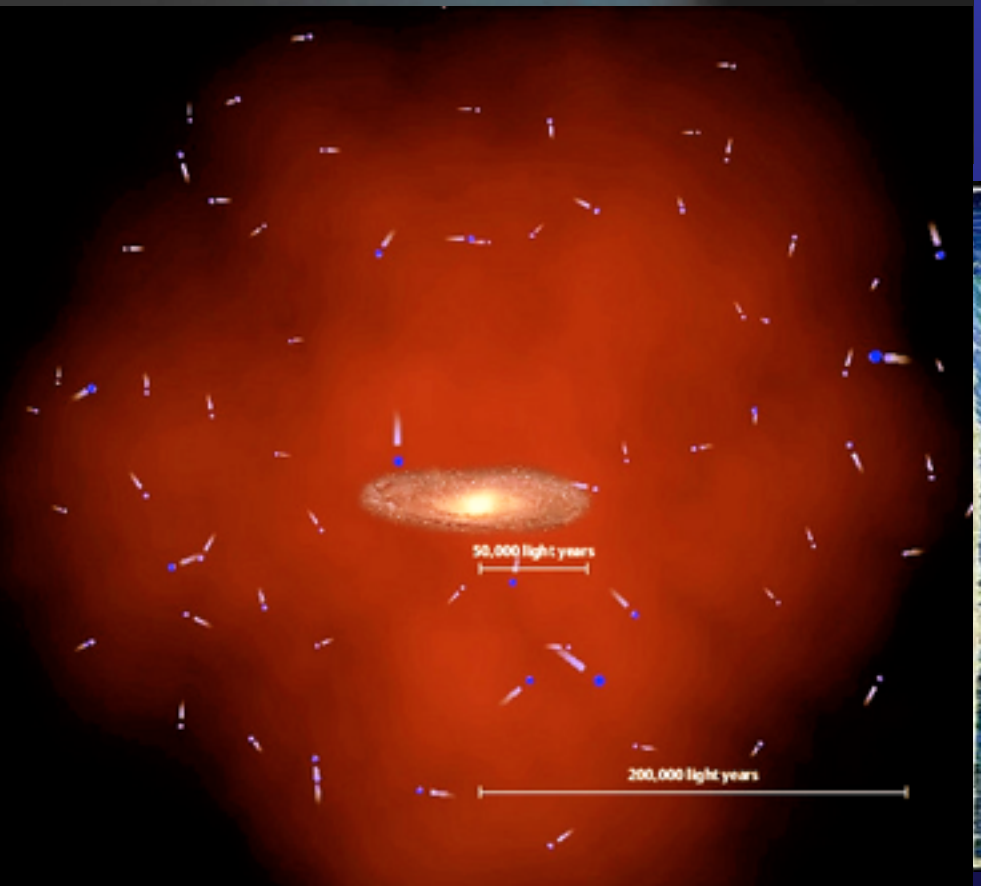

Dark Matter Halos

$M \sim 20 \times M_{stars}$

$R \sim Mpc$

~80% of matter consists neither of protons nor neutrons, but some "cold" (non-relativistic) particle, to be identified

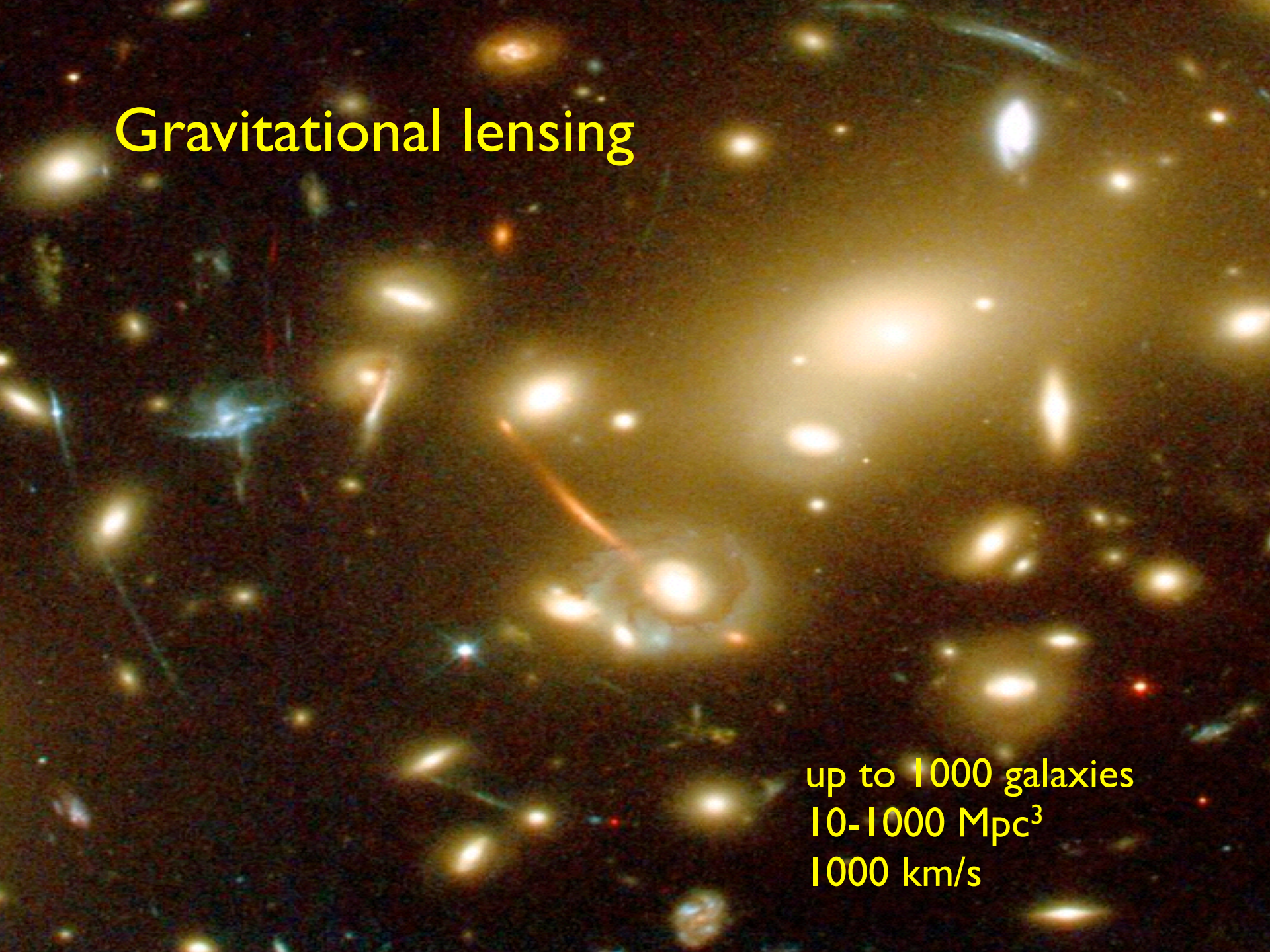
Gravitational lensing
up to 1000 galaxies
10-1000 Mpc^3
1000 km/s

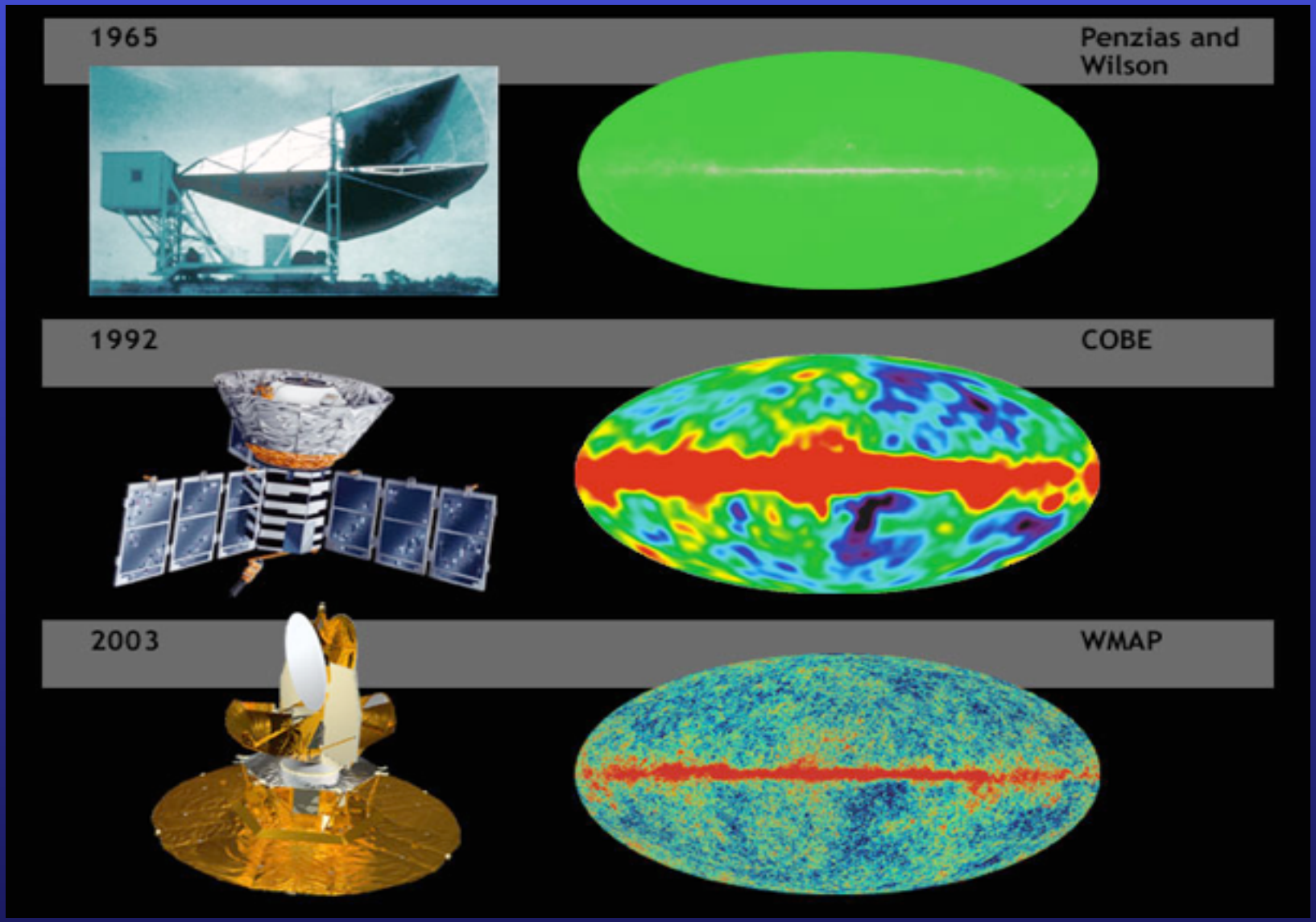

Universe is flat in space and has a finite age (14 Gyr)

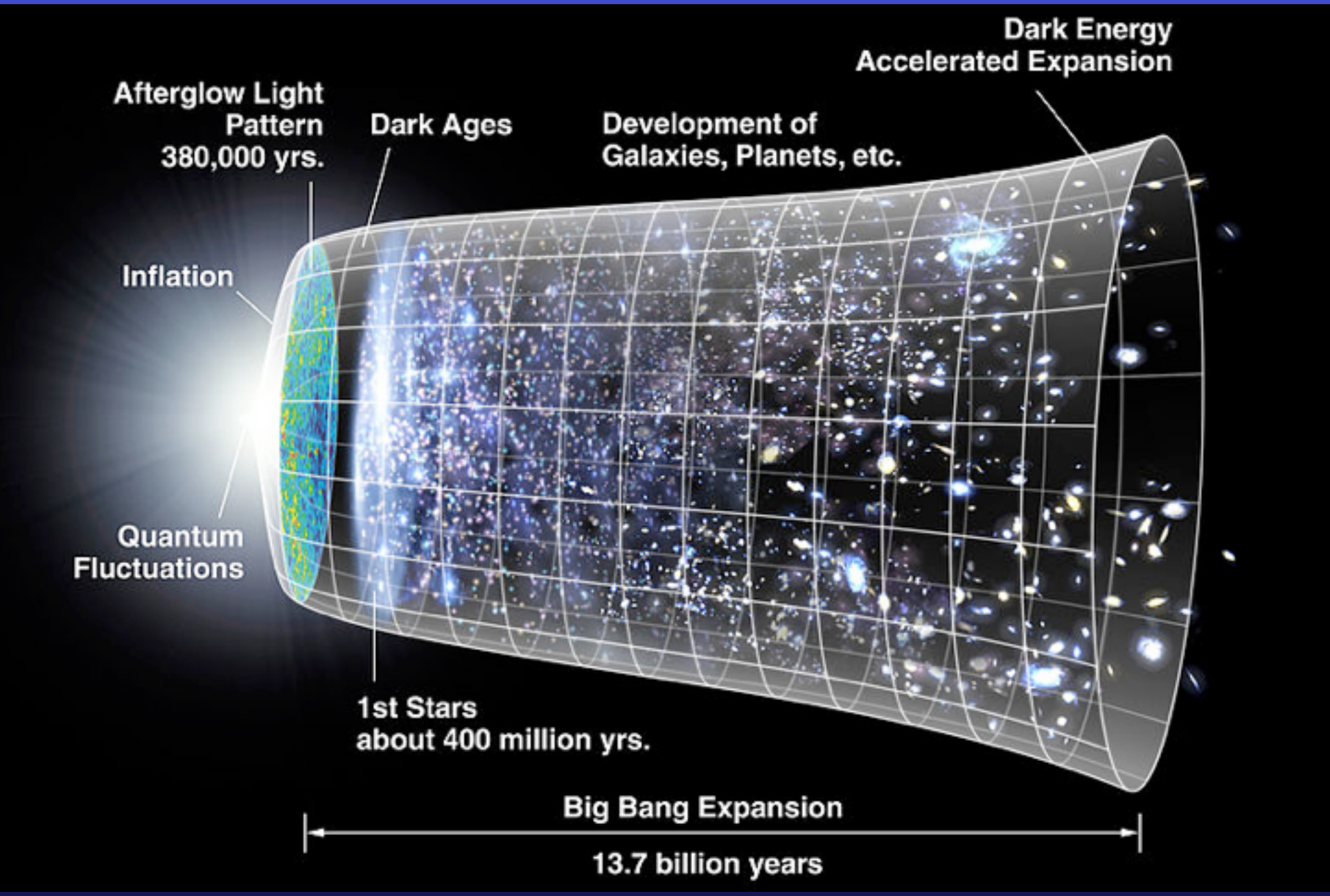
Dark Energy
Accelerated Expansion
Afterglow Light
Pattern
380,000 yrs.
Dark Ages
Development of
Galaxies, Planets, etc.
Inflation
Quantum
Fluctuations
1st Stars
about 400 million yrs.
Big Bang Expansion
13.7 billion years

Kepler 2-body problem

Binary Stars: Some Interacting

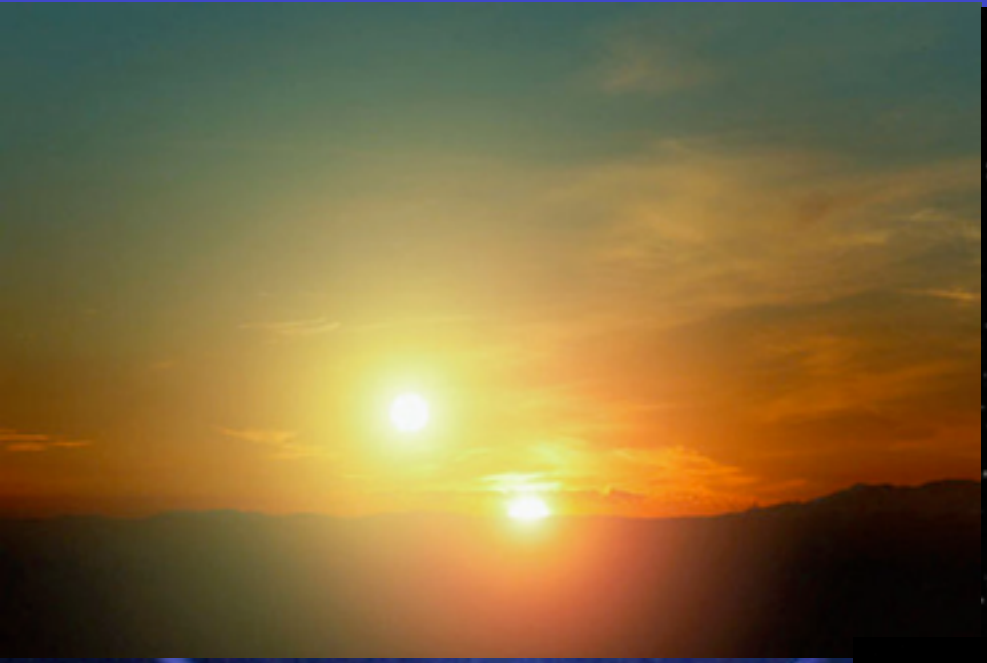

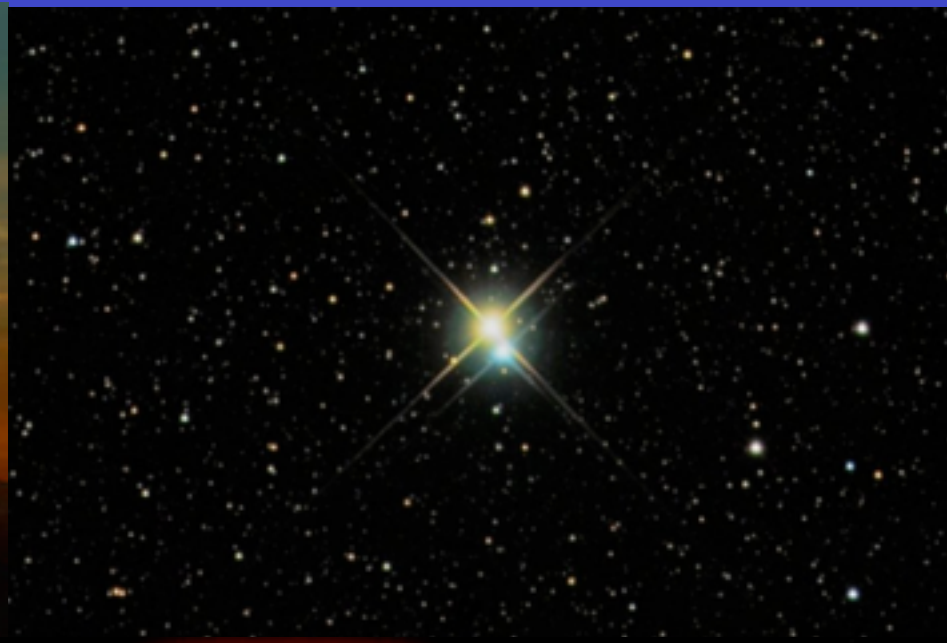

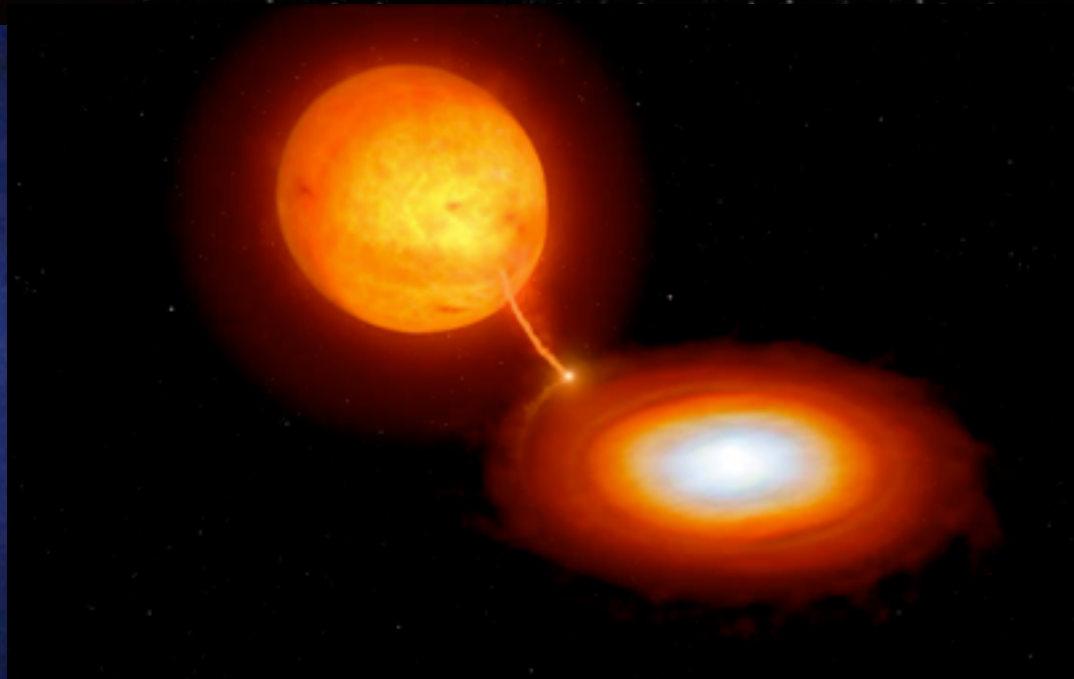

Shifted tidal bulge → Tidal torque

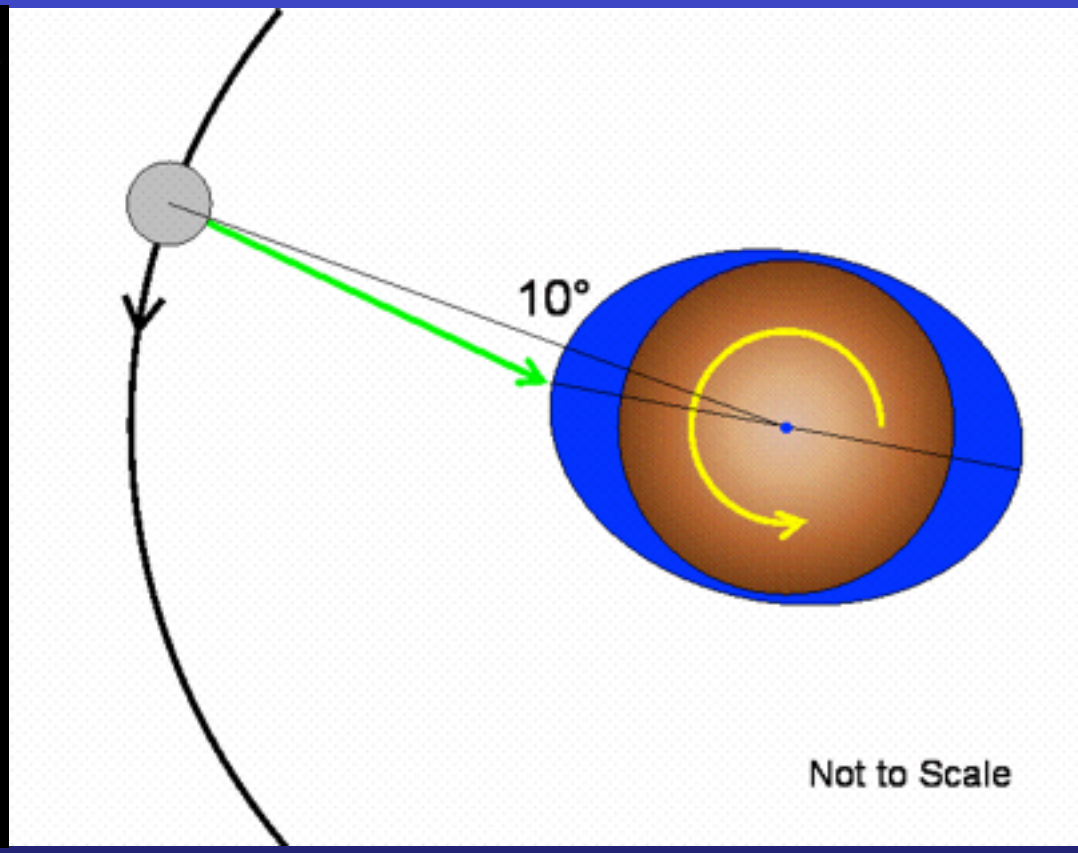

Earth is not yet synchronous with orbit
→ tidal torque and continued tidal spin-orbit evolution
Moon has already synchronized

Galilean moons of Jupiter

Moons have synchronized.
Jupiter has not.

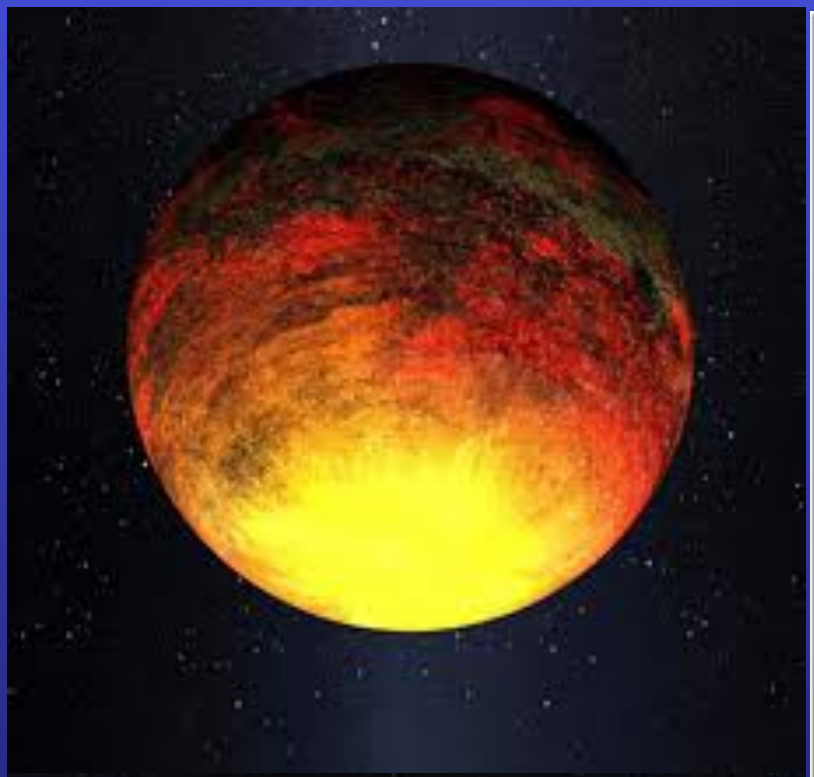

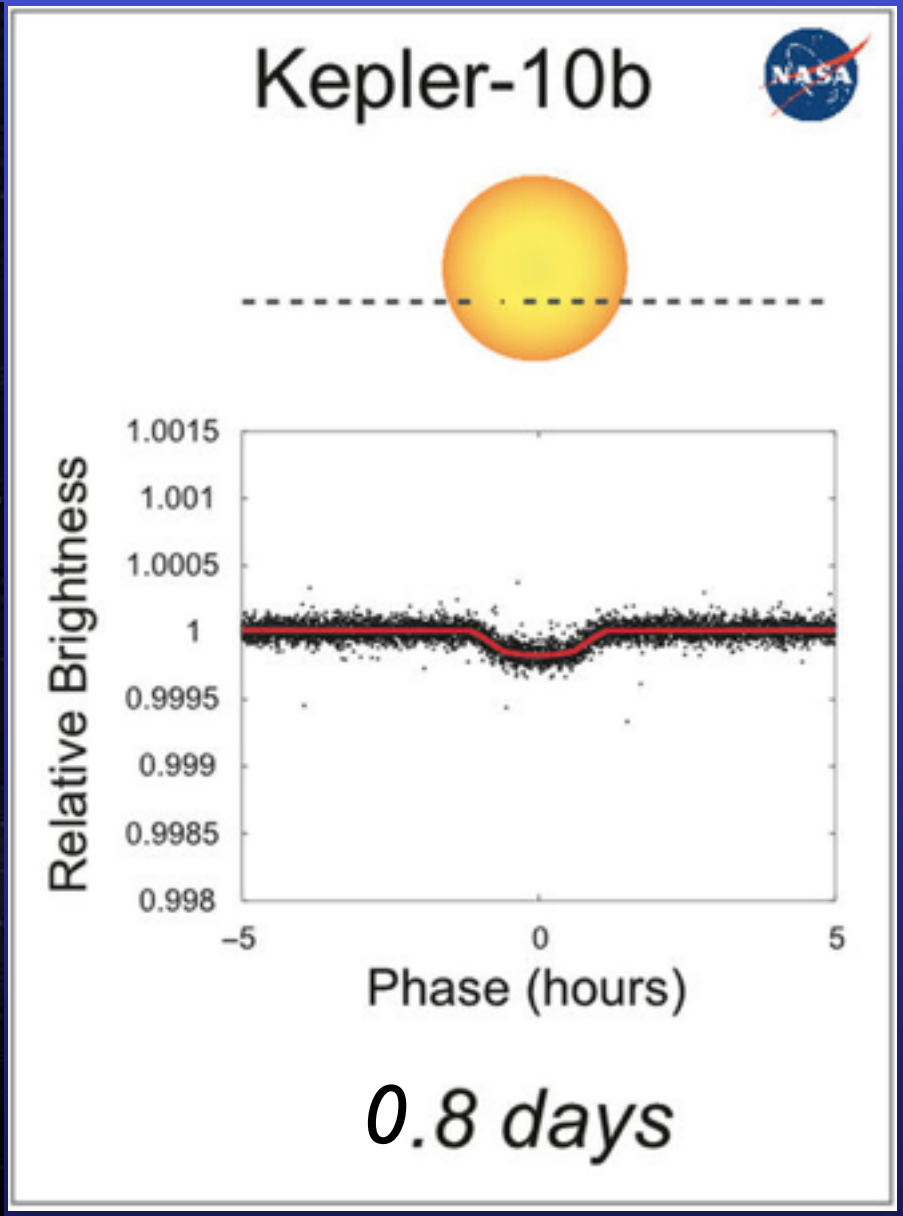

A (Probably) Tidally Locked Extrasolar Planet

Tidal melting of Io

1. Jupiter's asynchronous tide repels Io
2. Io approaches Europa
3. Europa forces Io onto eccentric orbit
4. Io's eccentricity tide stresses Io

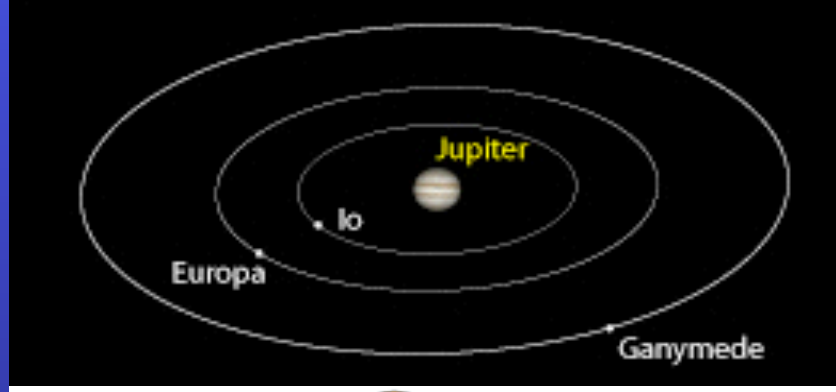

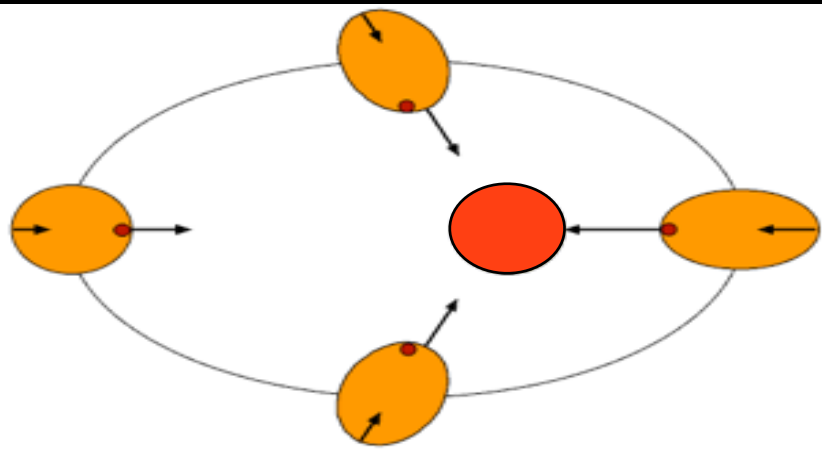

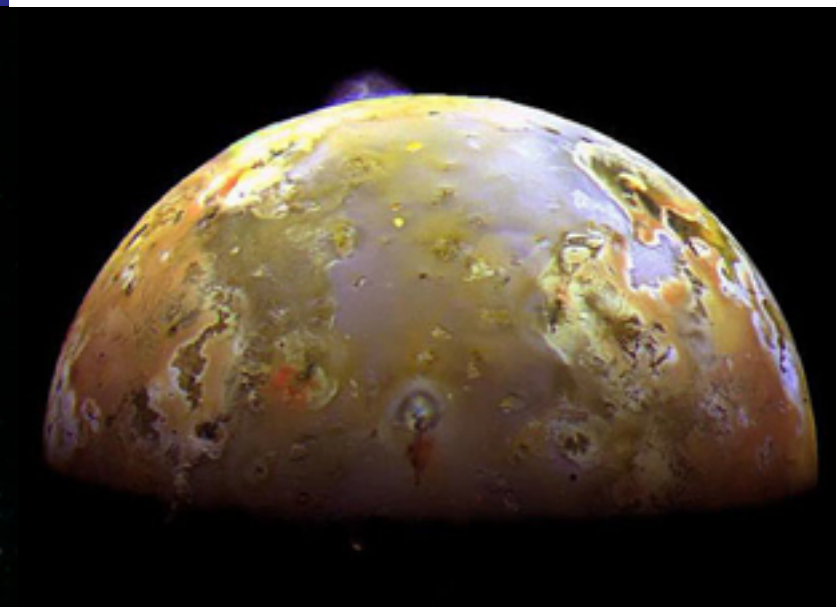

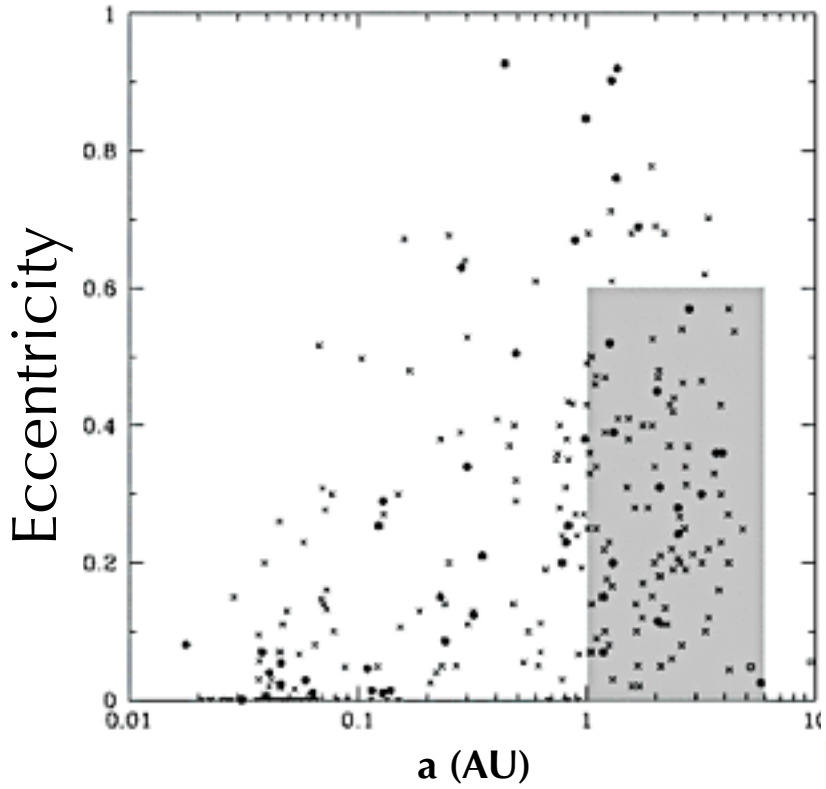

Extrasolar planets detected by radial velocity (> Neptune mass)

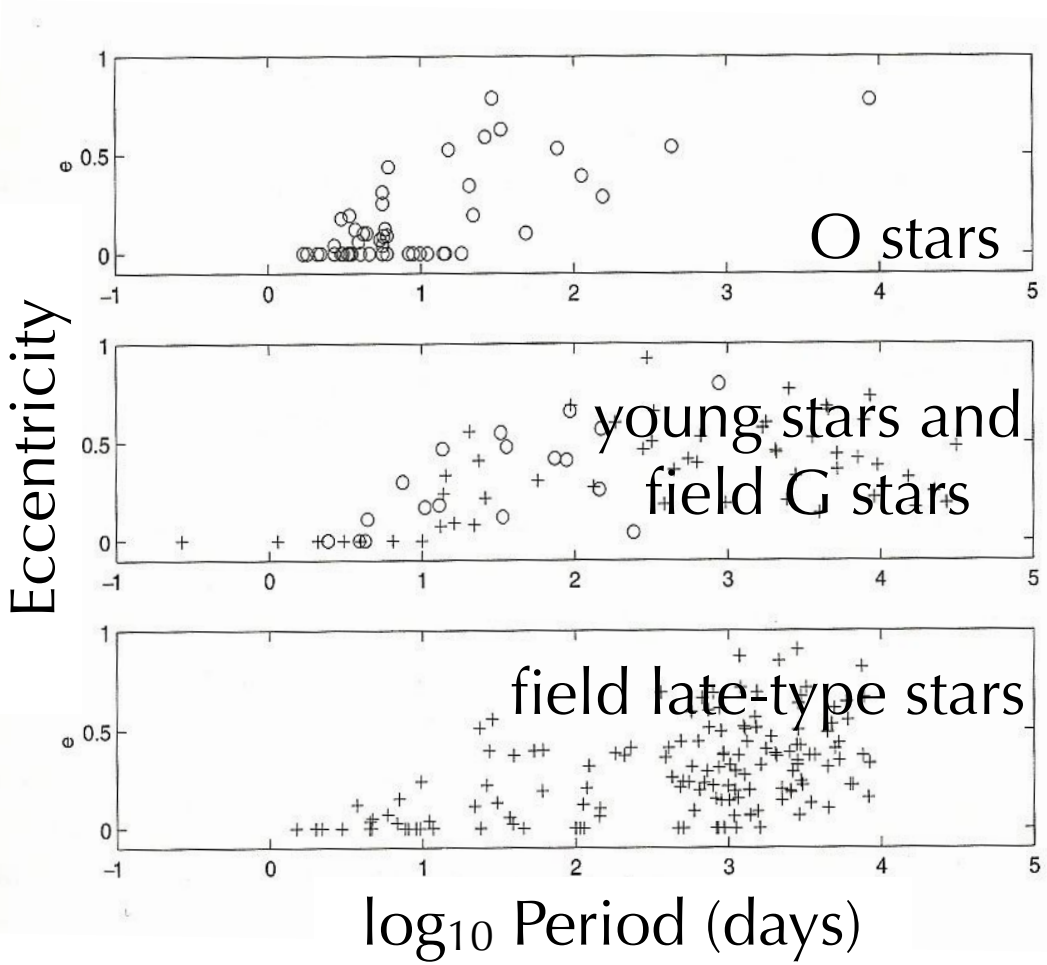

Tidal interactions (circularization + synchronization) most important close-in

■ **Figure 18.5** The Roche limit. A satellite (far right) in orbit around a planet is slightly deformed by tides. If it moves closer to the planet, it is deformed even more and finally disintegrates when it passes within the Roche limit *(dotted line)*, located 2.44 times the planet's radius from its center.

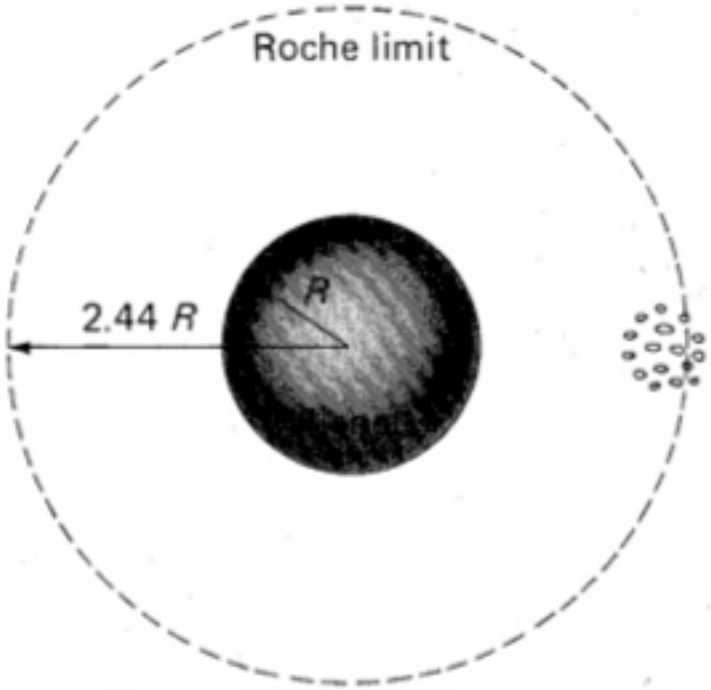

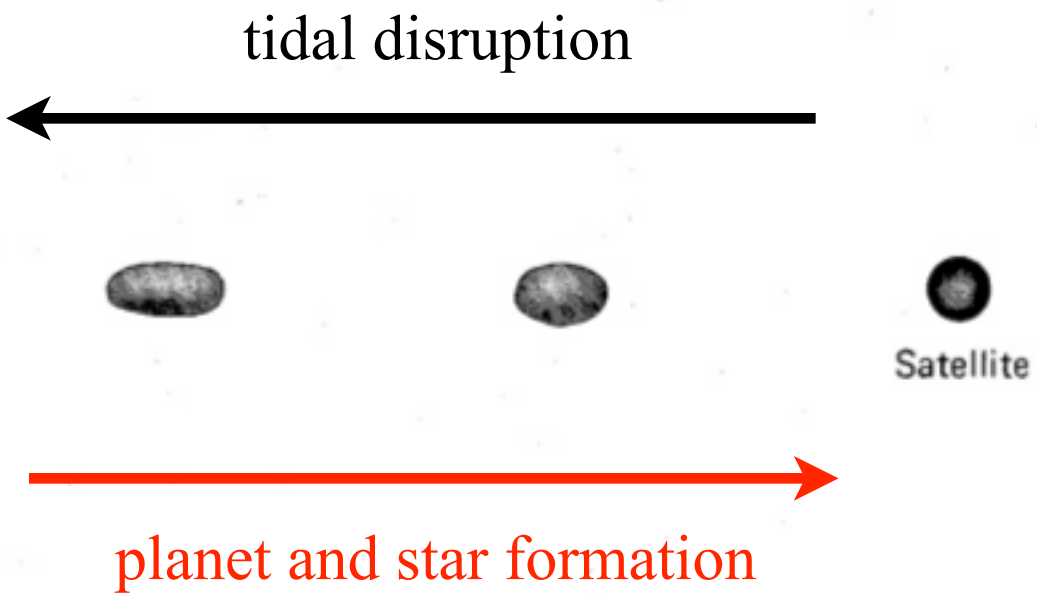

Comet Shoemaker-Levy 9: Tidally disrupted by Jupiter

Planetary rings are *inside* the Roche disruption zone.

Satellites are always *outside*.

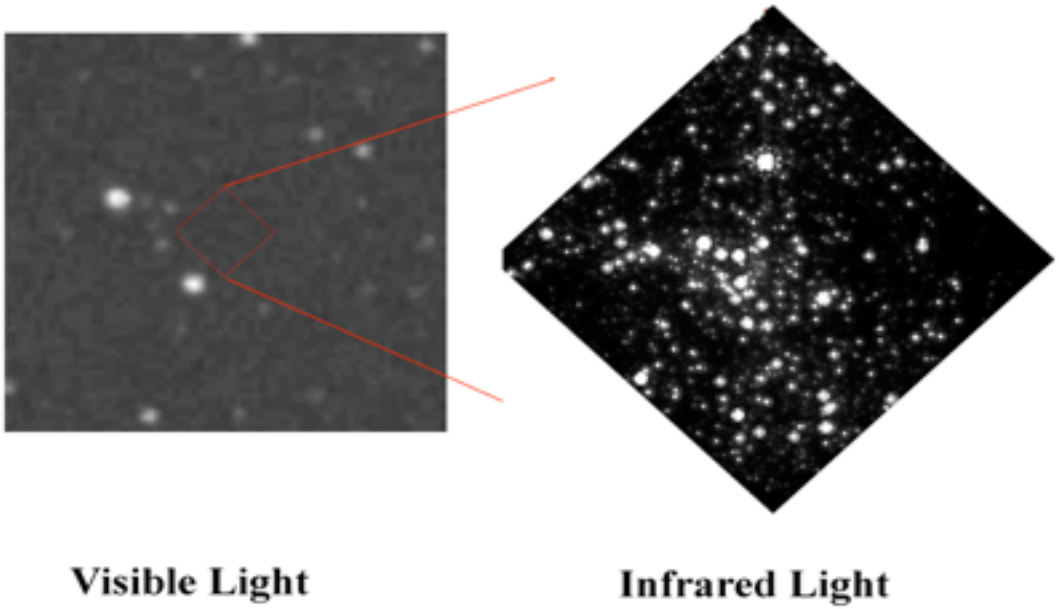

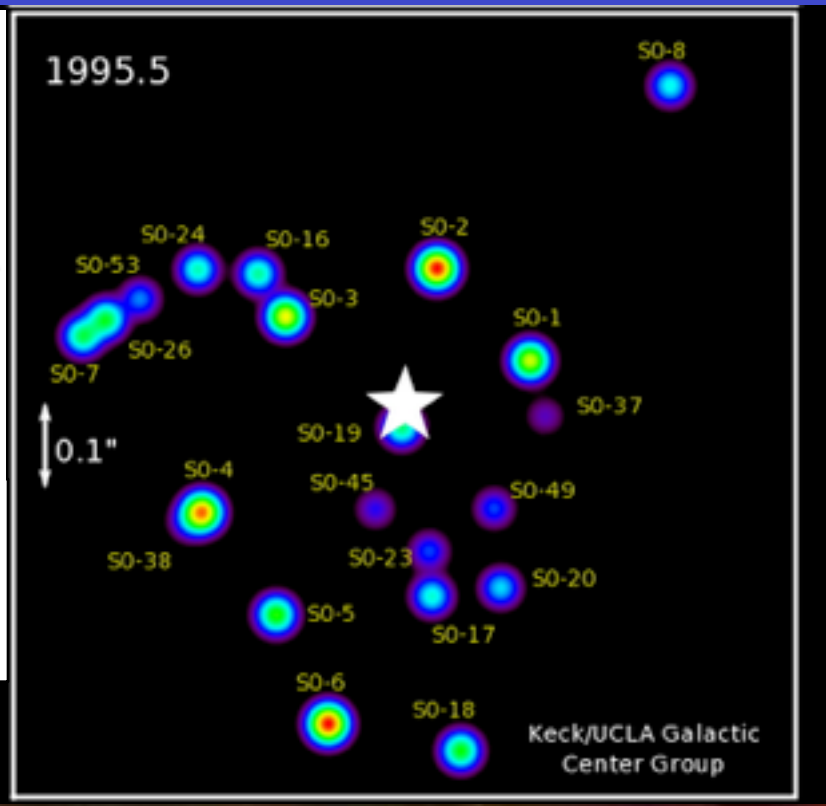

The Supermassive Black Hole at the Galactic Center

$M \approx 3.5 \times 10^6 M_\odot$

$R \approx 0.07$ AU

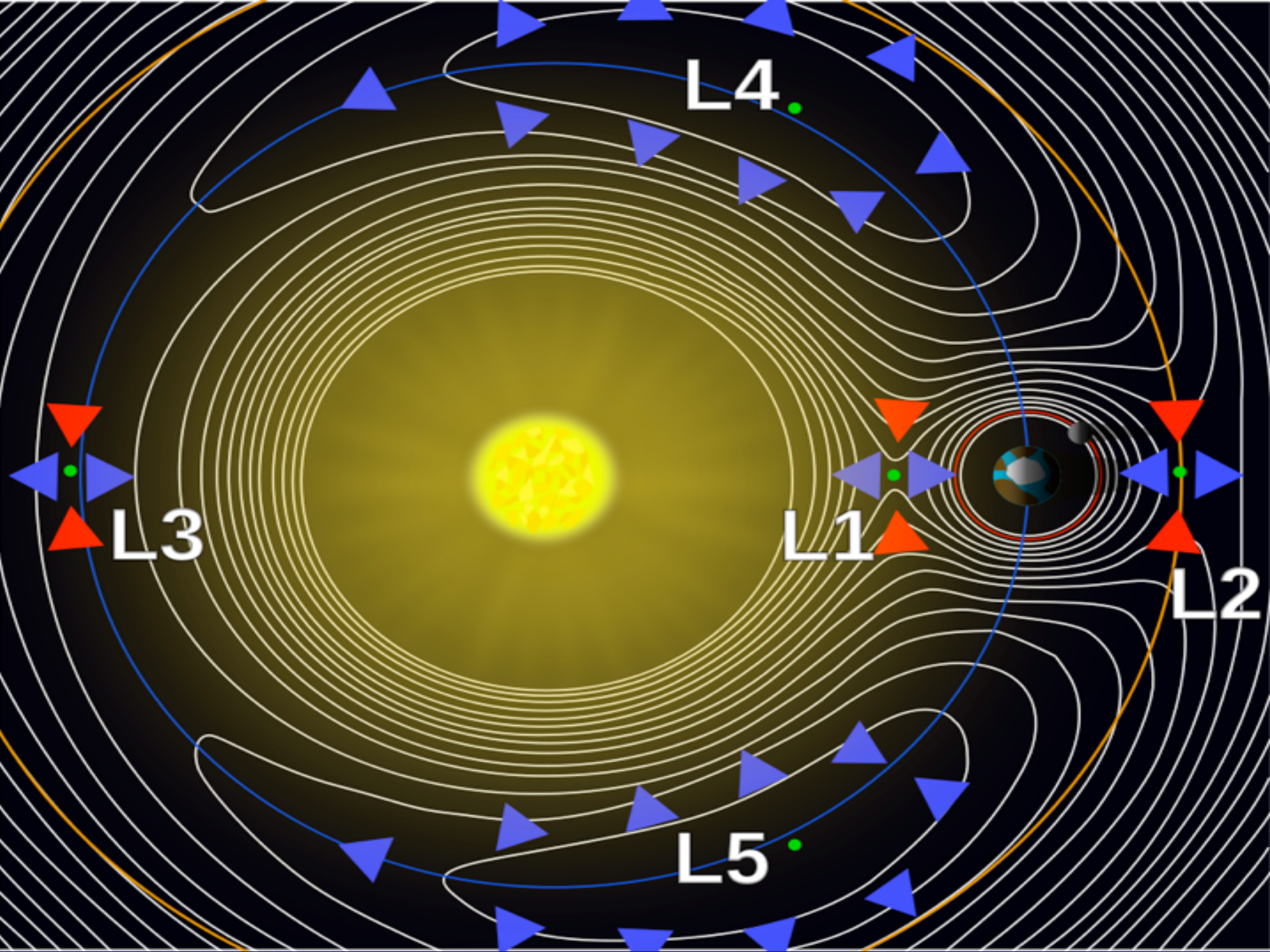
L4
L3
L1
L2
L5

LMXB = "Low-Mass X-ray Binary"

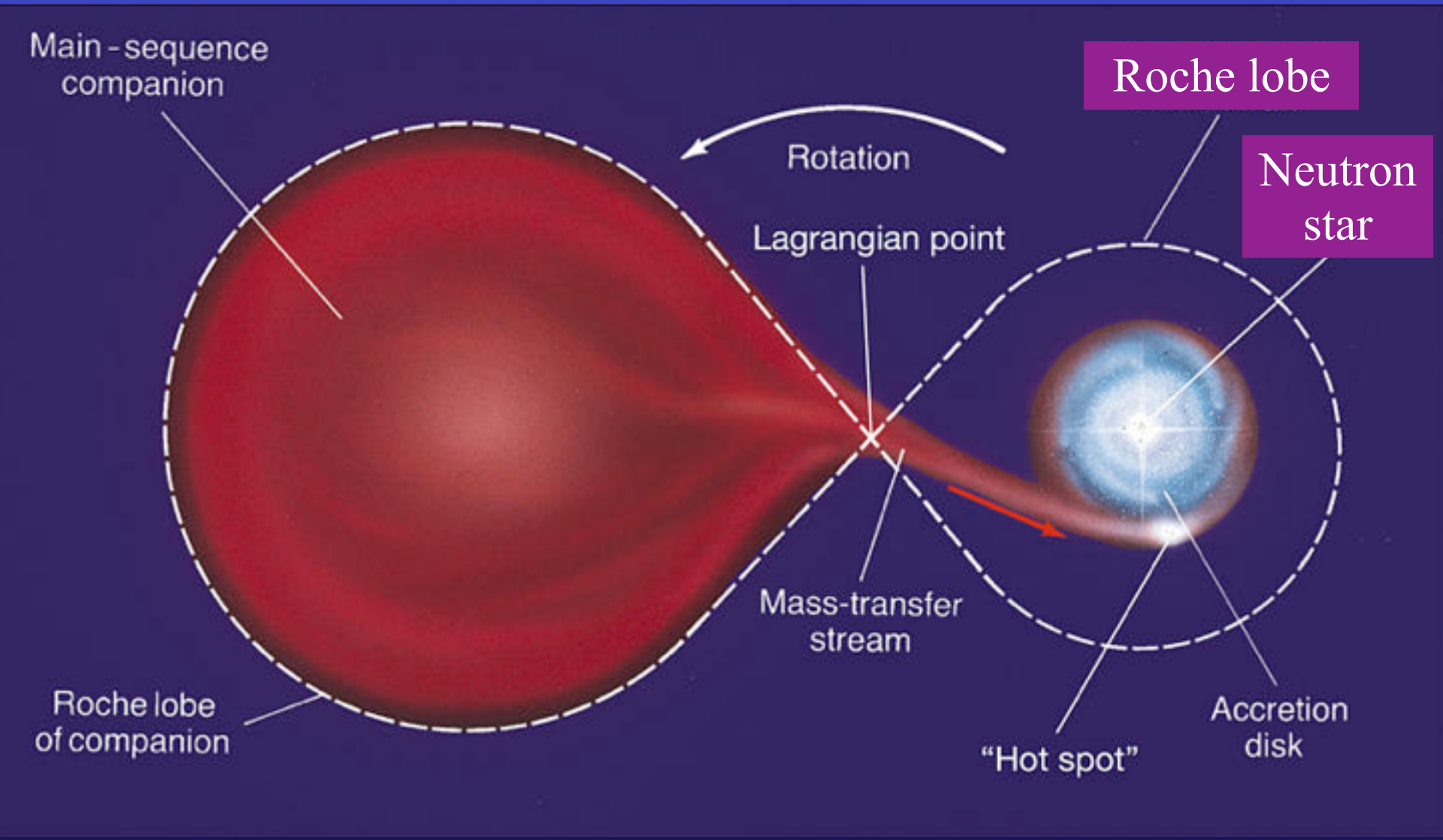

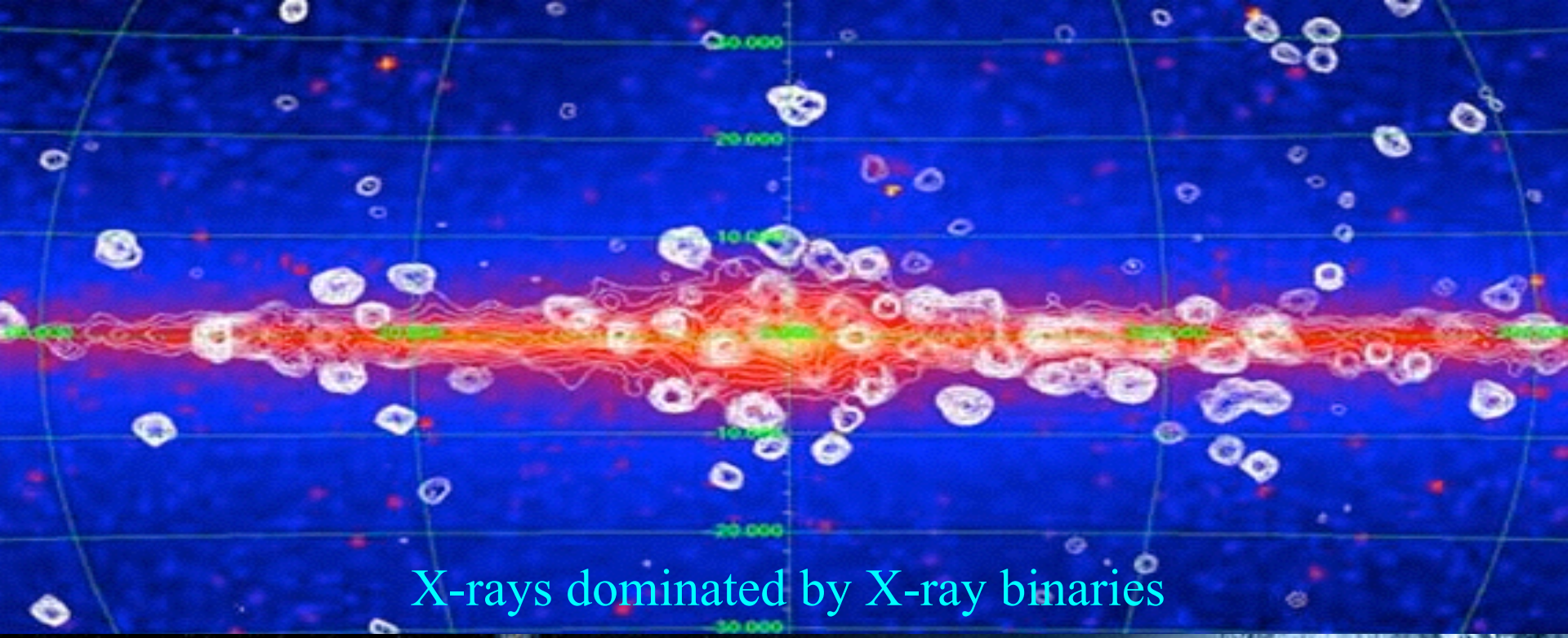

X-rays dominated by X-ray binaries

Accretion Disk

Turbulence driven by Magneto-Rotational Instability

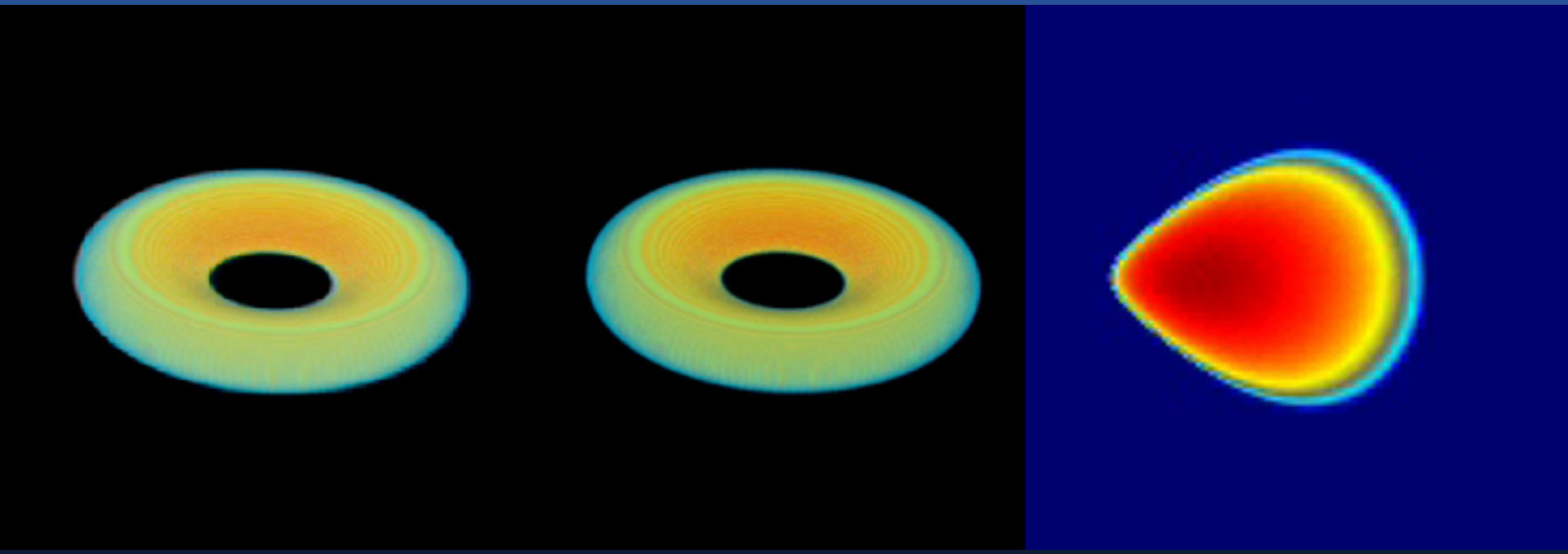

Hawley 2000

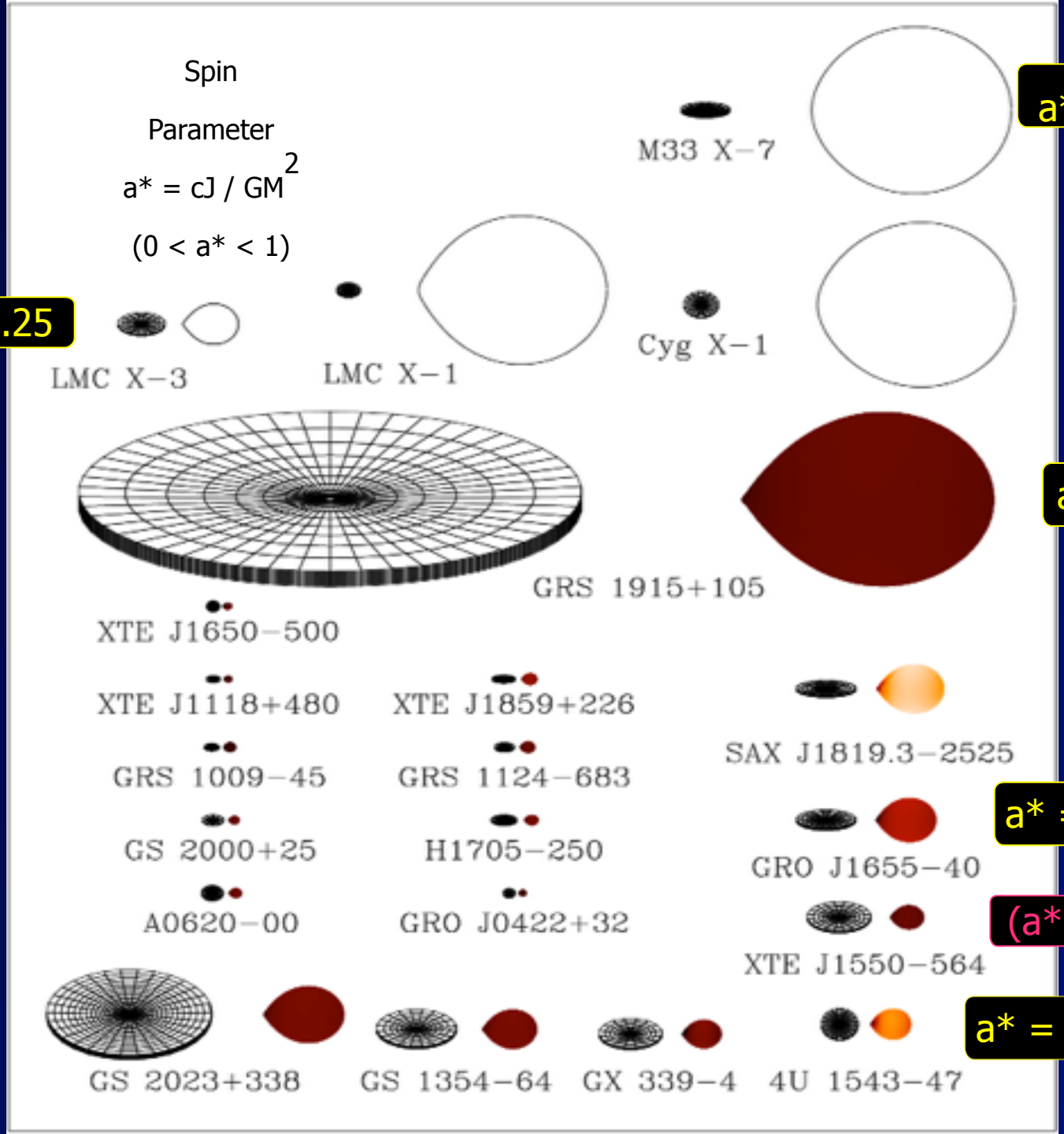
Spin
Parameter
a* = cJ / GM2
(0 < a* < 1)
M33 X−7
a* = 0.77 ± 0.05
a* ~ 0.25
LMC X−3
LMC X−1
Cyg X−1
GRS 1915+105
a* = 0.98 - 1.0
XTE J1650−500
XTE J1118+480
XTE J1859+226
SAX J1819.3−2525
GRS 1009−45
GRS 1124−683
GS 2000+25
H1705−250
GRO J1655−40
a* = 0.65 - 0.75
A0620−00
GRO J0422+32
(a* ~ 0.5)
XTE J1550−564
GS 2023+338
GS 1354−64
GX 339−4
4U 1543−47
a* = 0.75 - 0.85

Blackbody-Like Spectral State in BH Accretion Disk

LMC X-3: Beppo-SAX
(Davis, Done & Blaes 2006)

Up to 10 keV, the only component seen is the disk. Beyond that, a weak PL tail

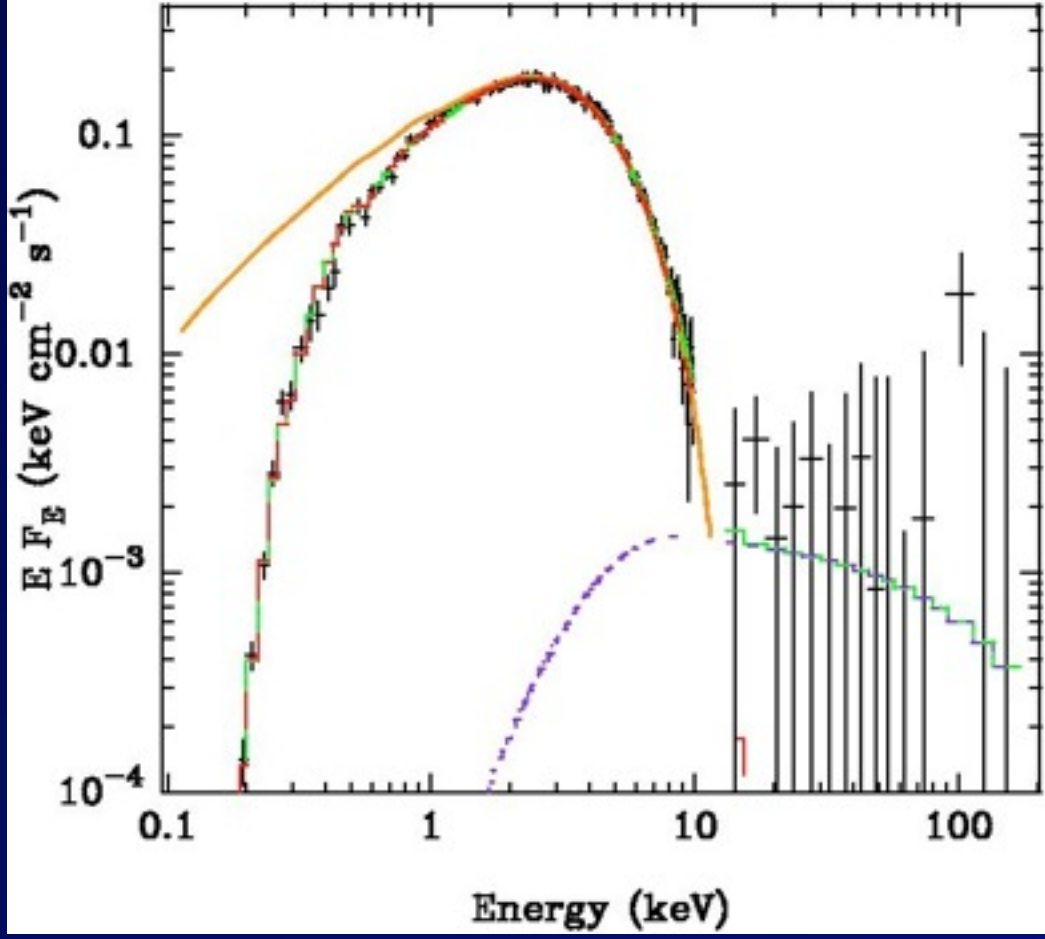

- Perfect for estimating inner radius of accretion disk → BH spin
- Just need to estimate L_X, T_X (and N_H) from X-ray continuum
- Use full relativistic model (Novikov-Thorne 1973; KERRBB, Li et al. 2005)

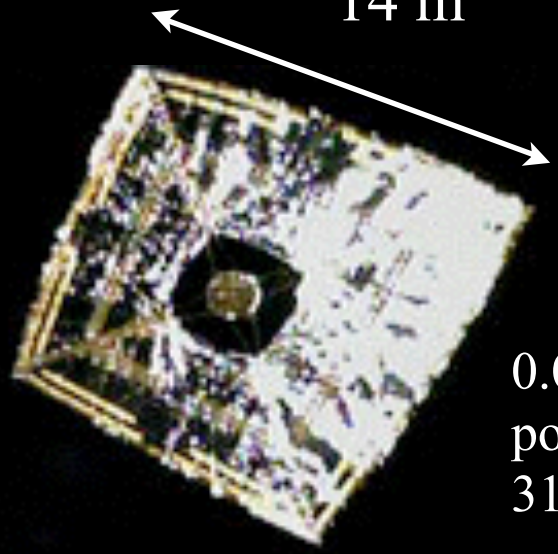

0.0075 mm
polyimide sheet
310 kg

© JAXA

IKAROS
"Interplanetary Kite-craft
Accelerated by Radiation of the Sun"

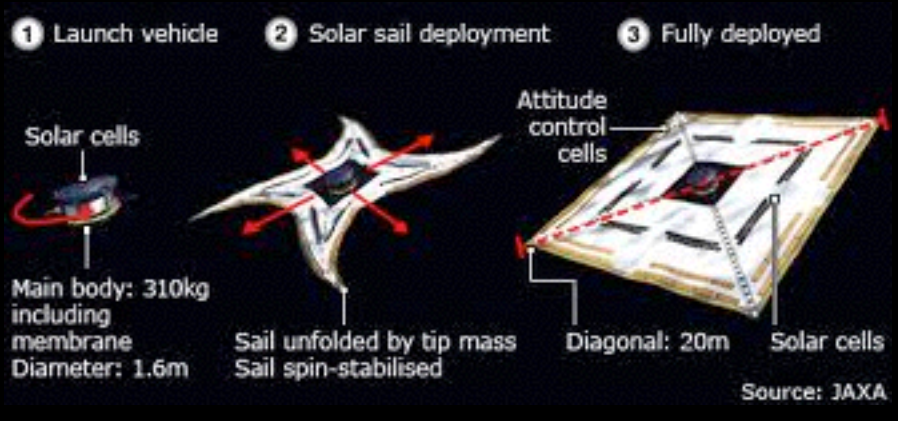

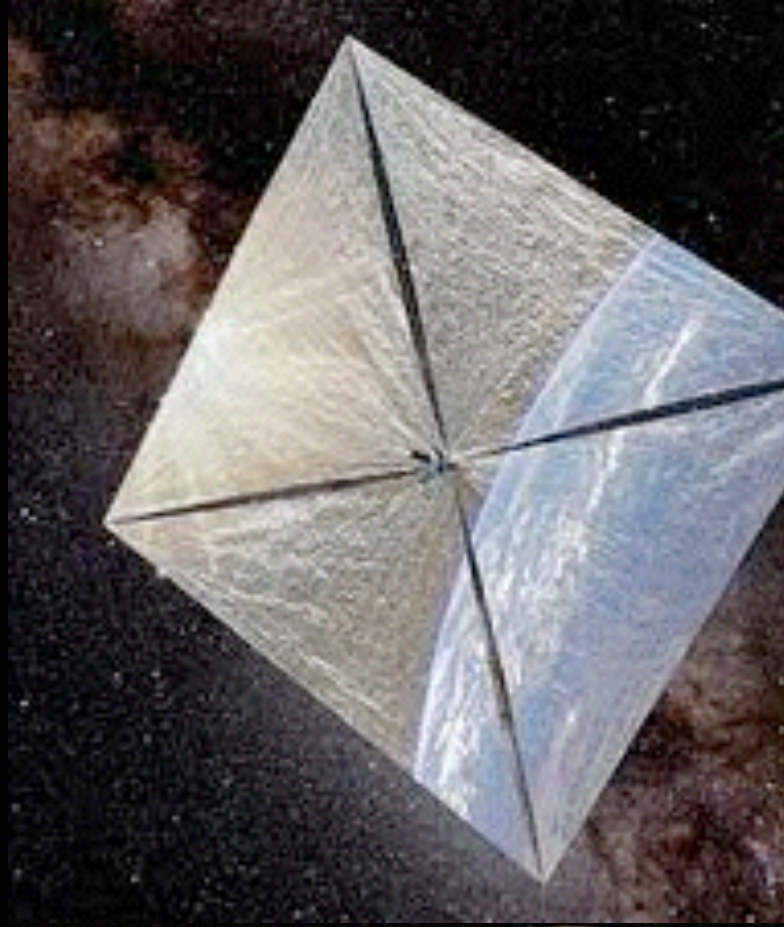

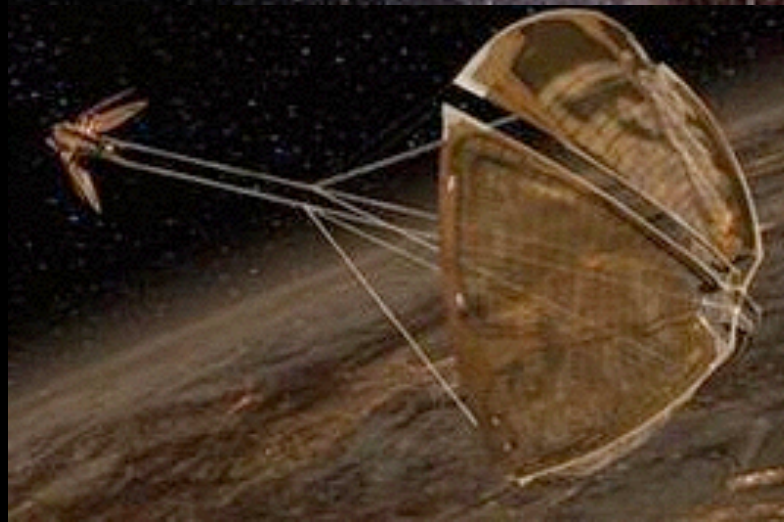

"Superstar" Eta Carina: 100-150 $M_\odot$
lost ~30 $M_\odot$ in previous eruptions
Eruptions driven by radiation pressure

29. If there ſhould really exiſt in nature any bodies, whoſe denſity is not leſs than that of the ſun, and whoſe diameters are more than 500 times the diameter of the ſun, ſince their light could not arrive at us; or if there ſhould exiſt any other bodies of a ſomewhat ſmaller ſize, which are not naturally luminous; of the exiſtence of bodies under either of theſe circumſtances, we could have no information from ſight; yet, if any other luminous bodies ſhould happen to revolve about them we might ſtill perhaps from the motions of theſe revolving bodies infer the exiſtence of the central ones with ſome degree of probability, as this might afford a clue to ſome of the apparent irregularities of the revolving bodies, which would not be eaſily explicable on any other hypotheſis; but as the conſequences of ſuch a ſuppoſition are very obvious, and the conſideration of them ſomewhat beſide my preſent purpoſe, I ſhall not proſecute them any farther.

John Michell

$$G_{\mu\nu} + g_{\mu\nu}\Lambda = \frac{8\pi G}{c^4} T_{\mu\nu}.$$

Albert Einstein

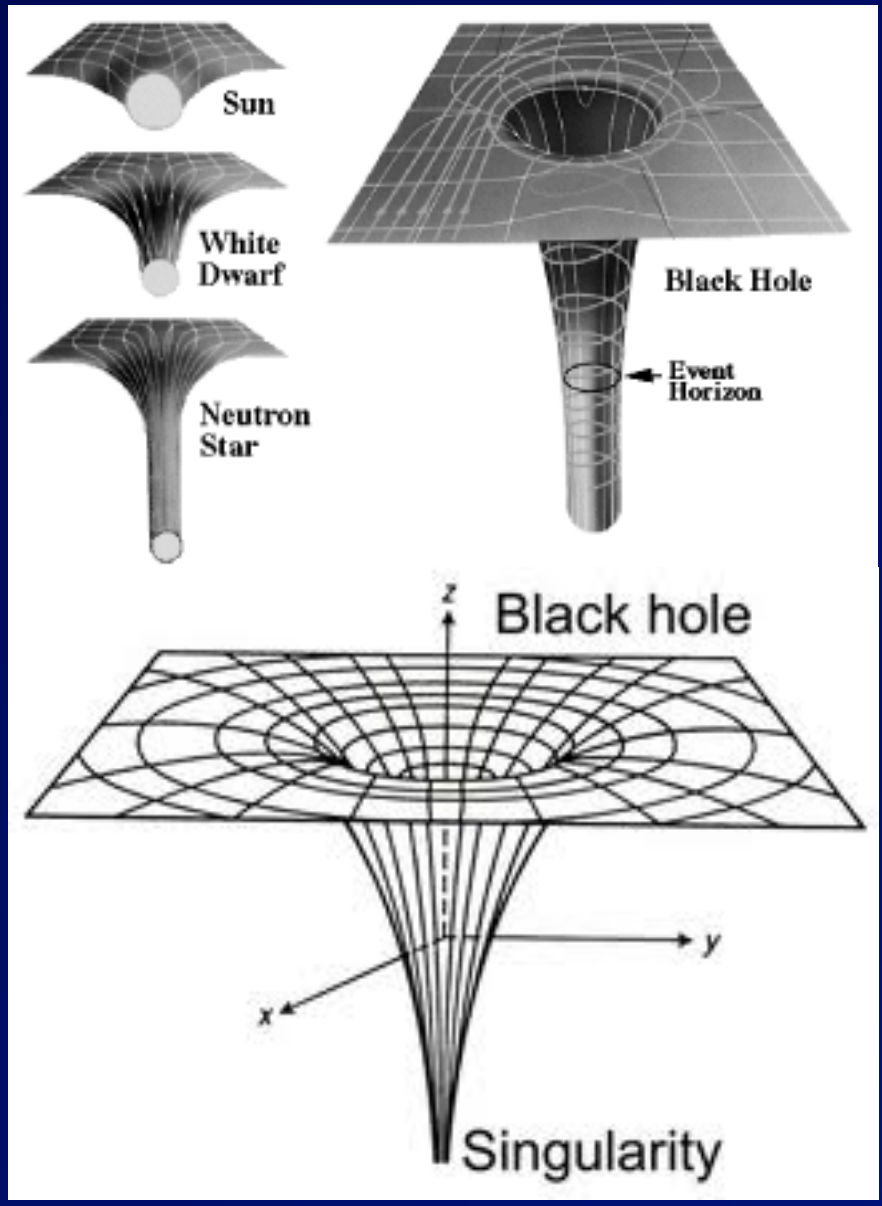

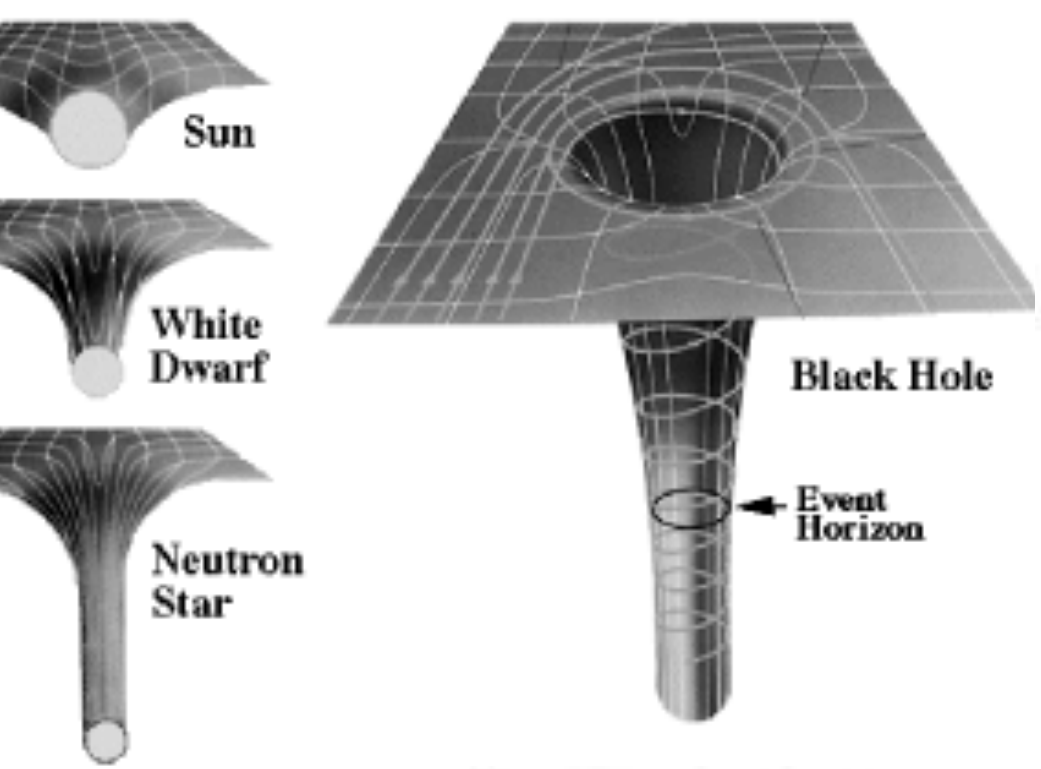
Sun
White Dwarf
Neutron Star
Black Hole
Event Horizon

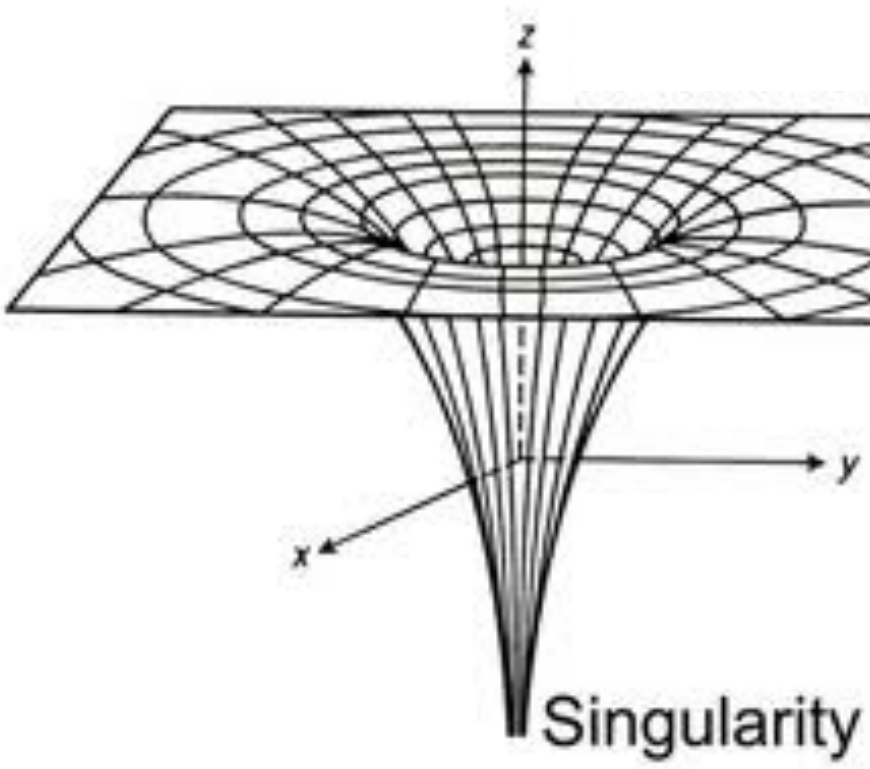
z
y
x
Singularity

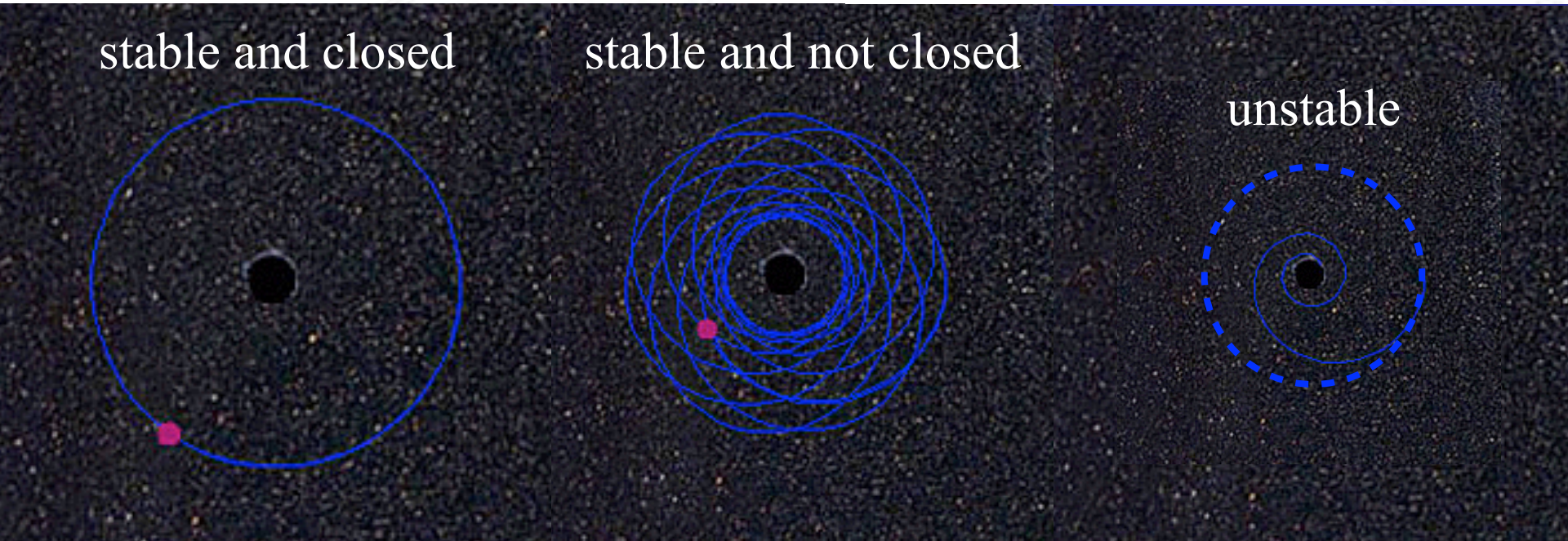
stable and closed
stable and not closed
unstable

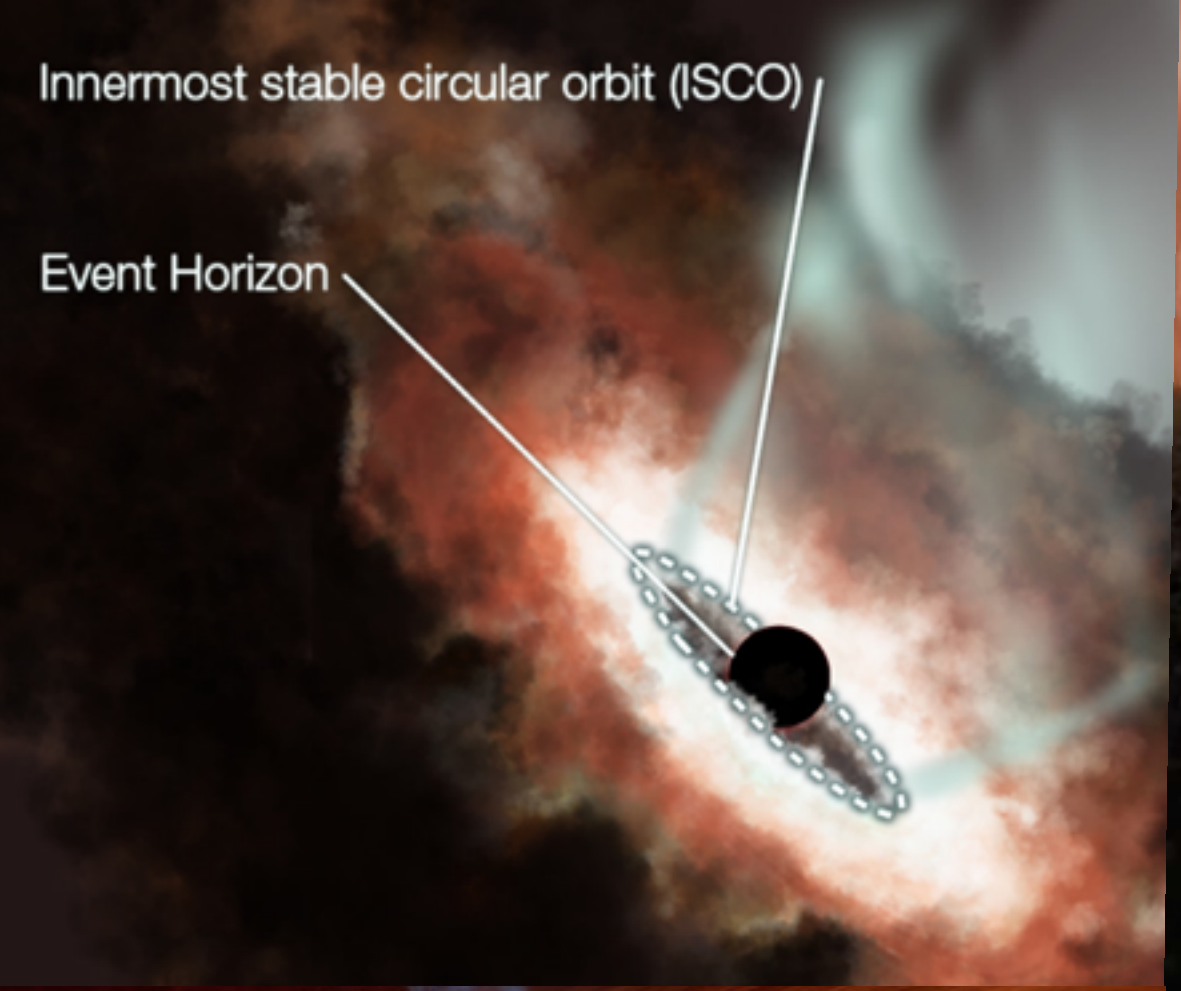
Innermost stable circular orbit (ISCO)
Event Horizon

Measuring spin for stellar-mass black holes

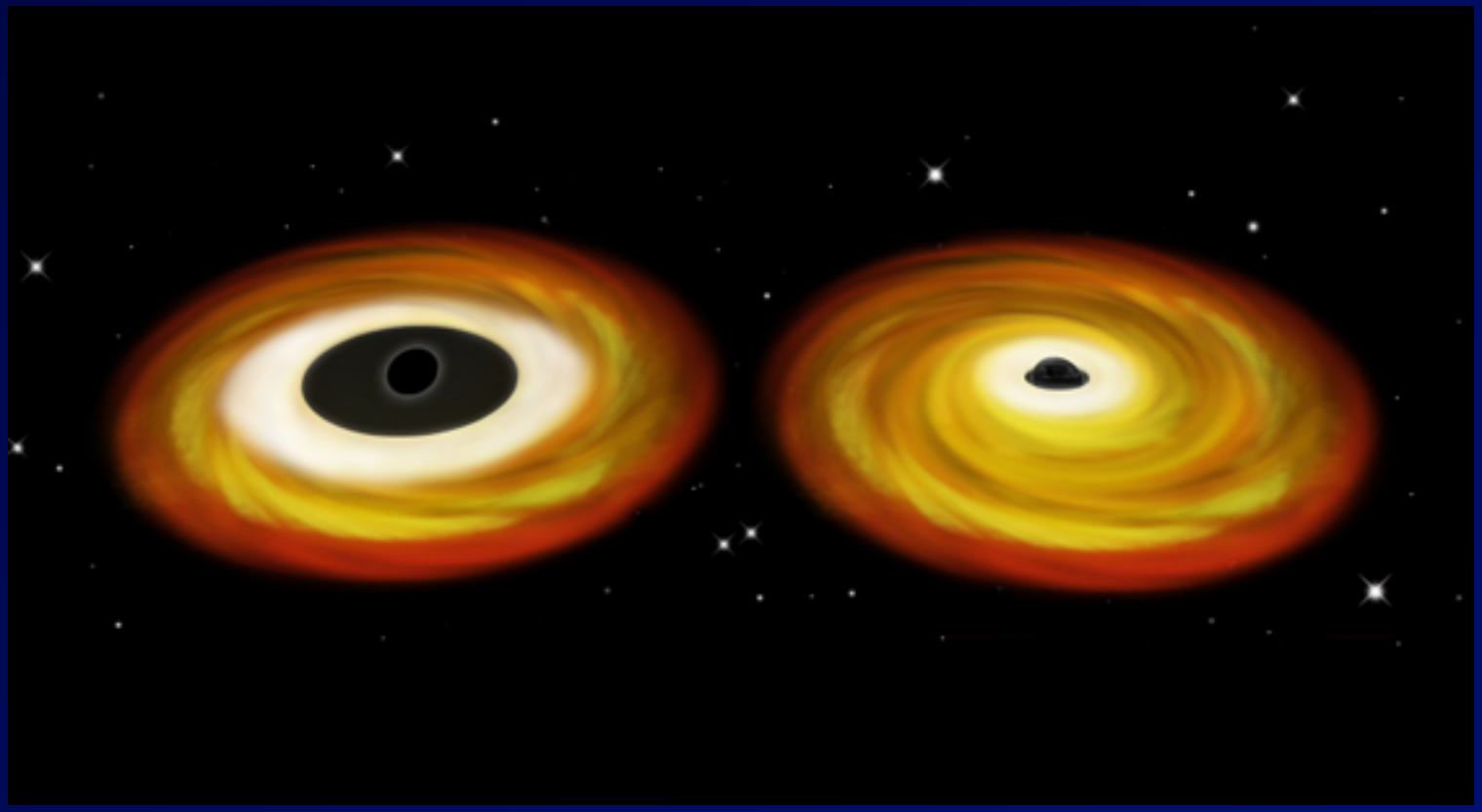

Measure Radius of the Hole in the disk by estimating the area of the bright inner disk using X-ray Data in the Thermal State: L_X and T_X

Zhang et al. (1997); Shafee et al. (2006); Davis et al. (2006); McClintock et al. (2006); Middleton et al. (2006); Liu et al. (2008)

Blackbody-Like Spectral State in BH Accretion Disk

LMC X-3: Beppo-SAX
(Davis, Done & Blaes 2006)

Up to 10 keV, the only component seen is the disk. Beyond that, a weak PL tail

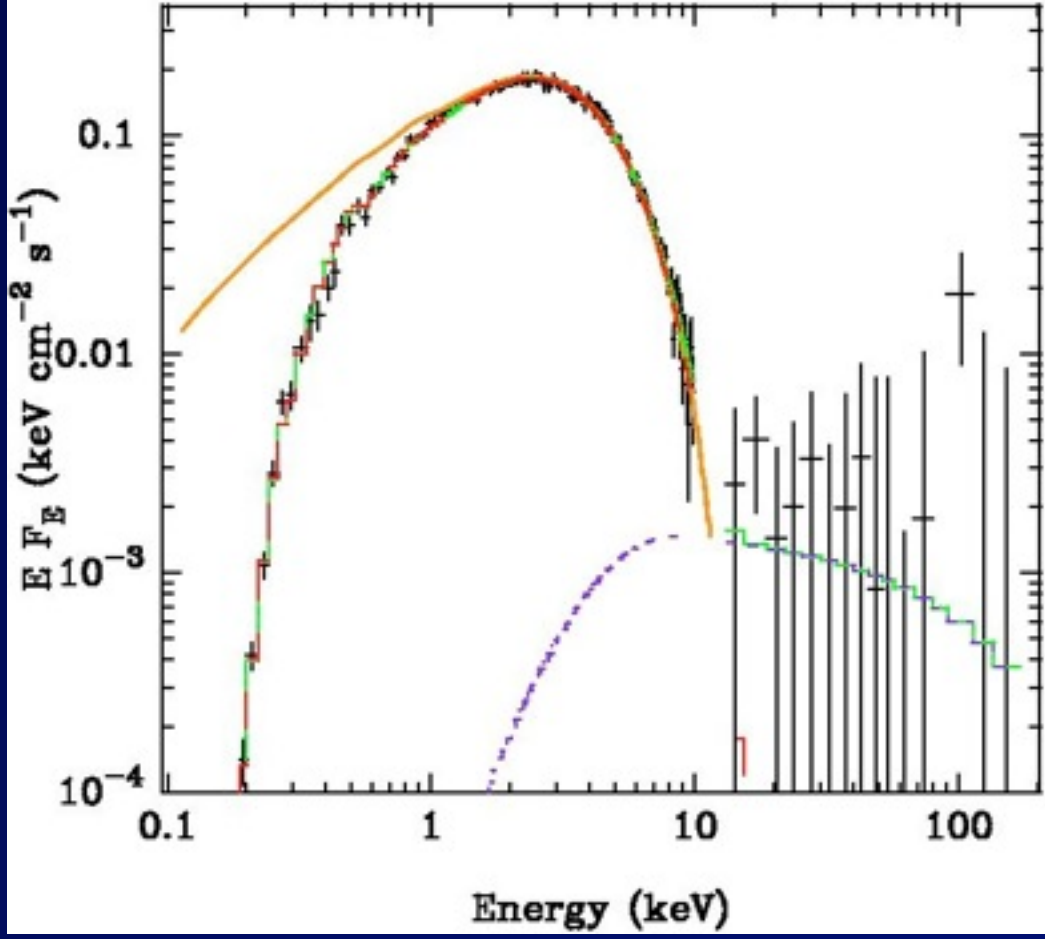

- Perfect for estimating inner radius of accretion disk → BH spin
- Just need to estimate L_X, T_X (and N_H) from X-ray continuum
- Use full relativistic model (Novikov-Thorne 1973; KERRBB, Li et al. 2005)

A Test of the Blackbody Assumption

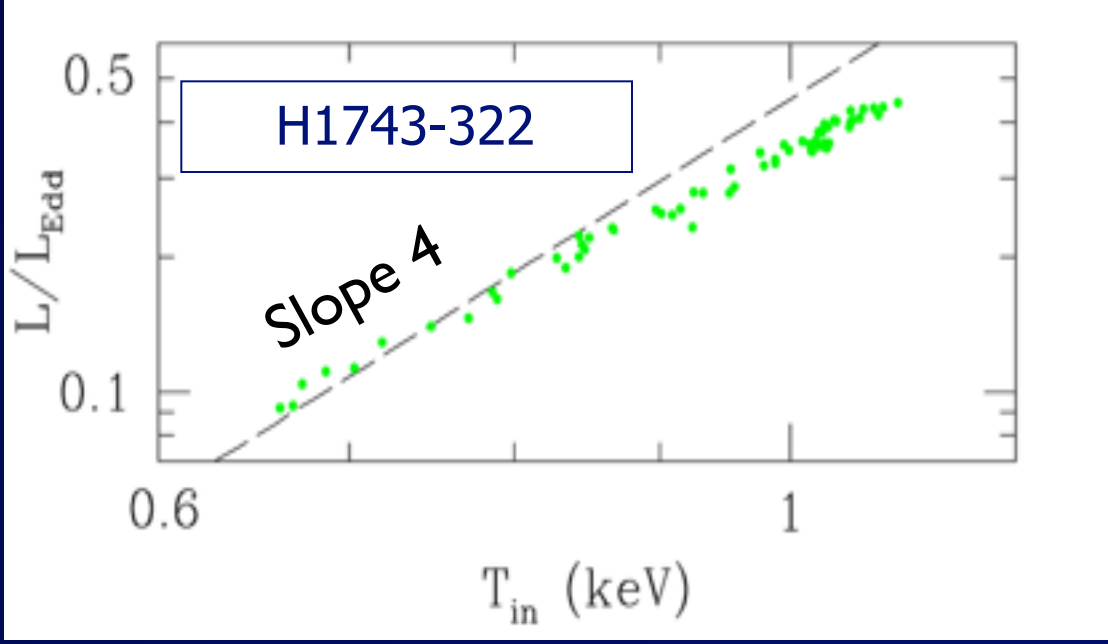

Kubota et al. (2002)

McClintock et al. (2008)

- For a blackbody, L scales as T^4
- BH accretion disks vary a lot in their luminosity
- If a disk is a good blackbody, L should vary as T^4
- **Looks reasonable**

$$L = A\sigma T^4$$

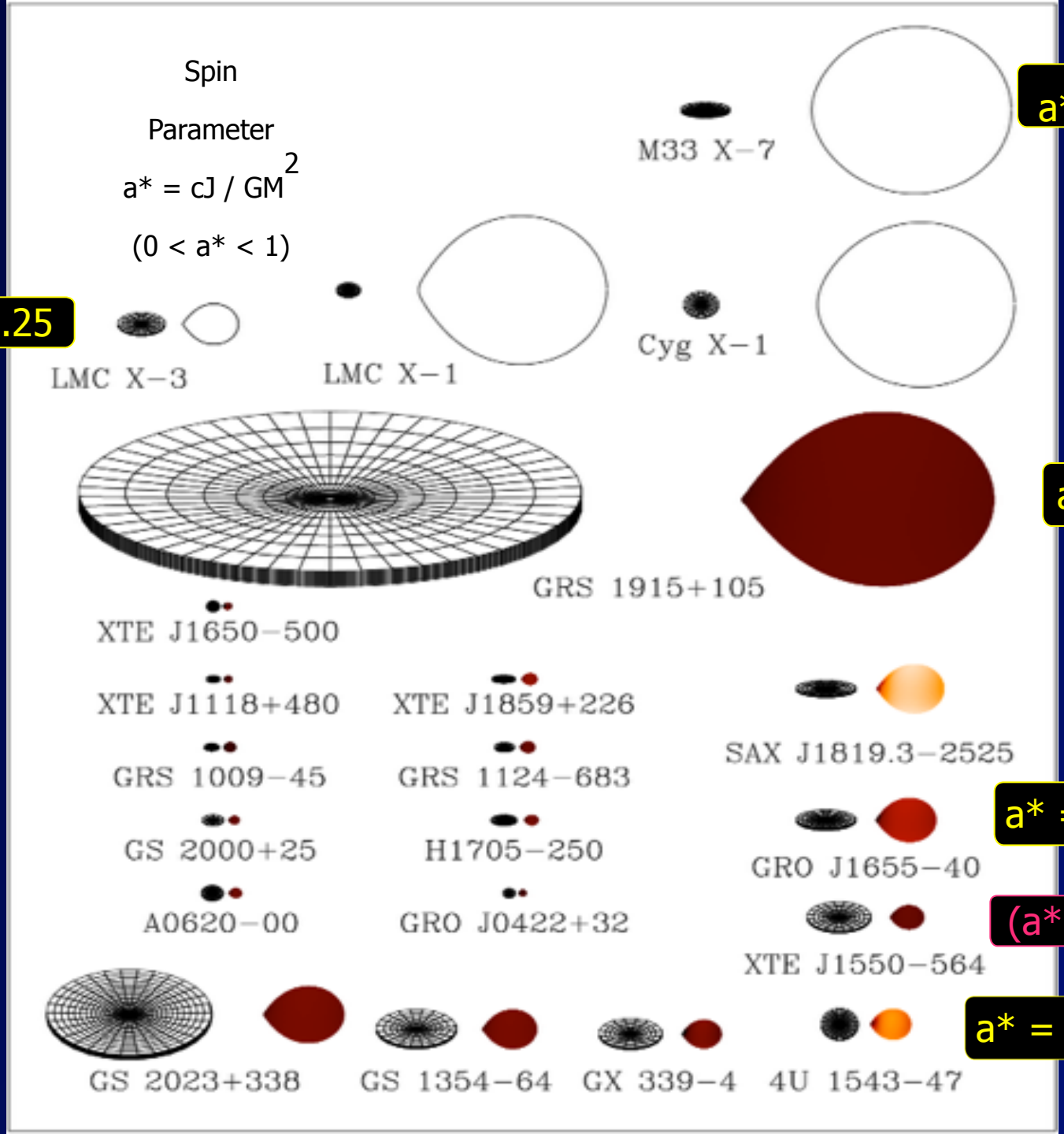
Spin
Parameter
a* = cJ / GM2
(0 < a* < 1)
M33 X−7
a* = 0.77 ± 0.05
a* ~ 0.25
LMC X−3
LMC X−1
Cyg X−1
GRS 1915+105
a* = 0.98 - 1.0
XTE J1650−500
XTE J1118+480
XTE J1859+226
SAX J1819.3−2525
GRS 1009−45
GRS 1124−683
GS 2000+25
H1705−250
GRO J1655−40
a* = 0.65 - 0.75
A0620−00
GRO J0422+32
(a* ~ 0.5)
XTE J1550−564
GS 2023+338
GS 1354−64
GX 339−4
4U 1543−47
a* = 0.75 - 0.85

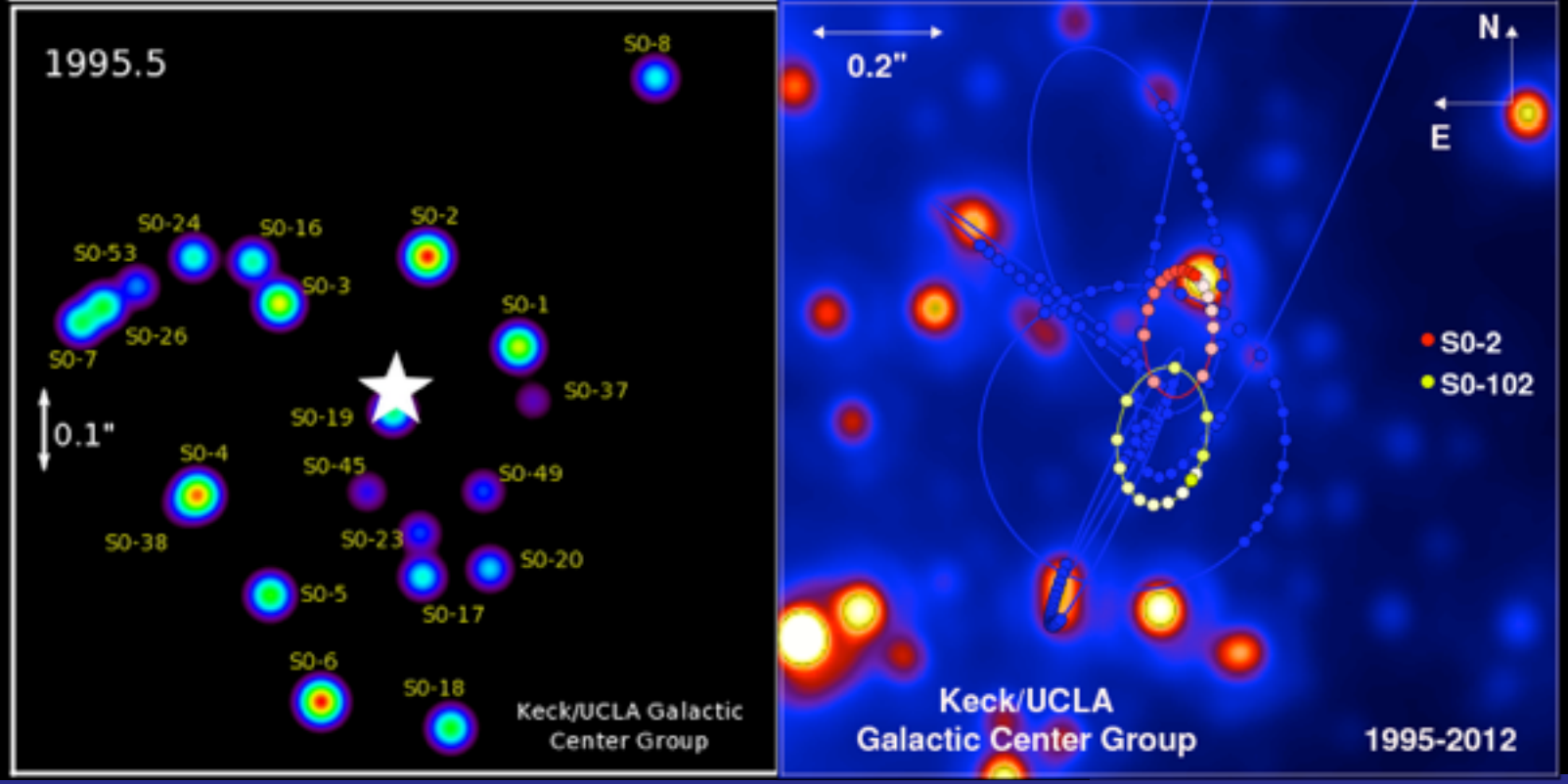

Sgr A*

= The Supermassive Black Hole at the Galactic Center

$M \approx 4 \times 10^6 M_\odot$

$R_g \approx 0.04$ AU

$q_{star} \approx 0.01$ arcsec x 8 kpc $\approx$ 80 AU

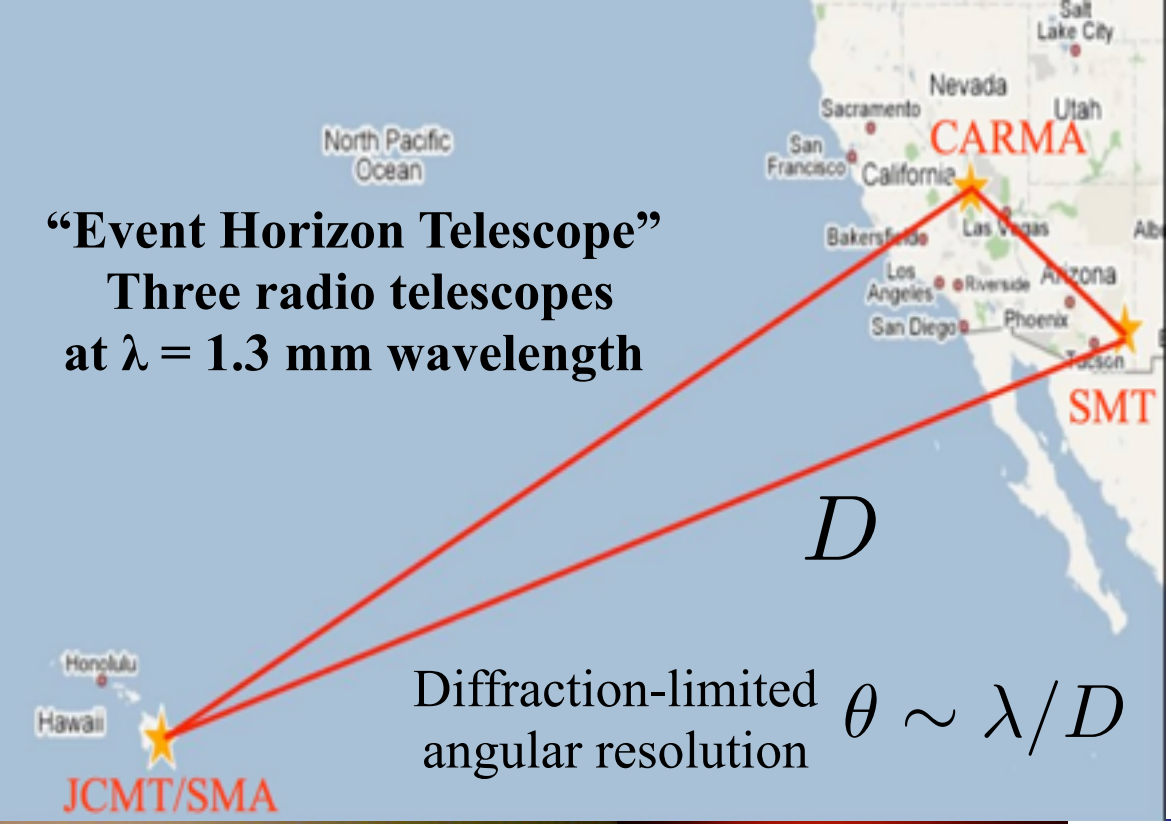

"Event Horizon Telescope"
Three radio telescopes
at λ = 1.3 mm wavelength

D

Diffraction-limited angular resolution $\theta \sim \lambda / D$

"The data presented here confirm structure in Sgr A* on linear scales of $4R_{Sch}$, but the exact nature of this structure is not well determined."

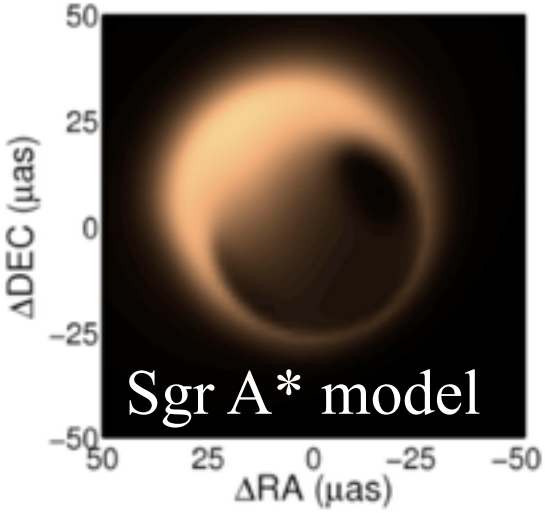

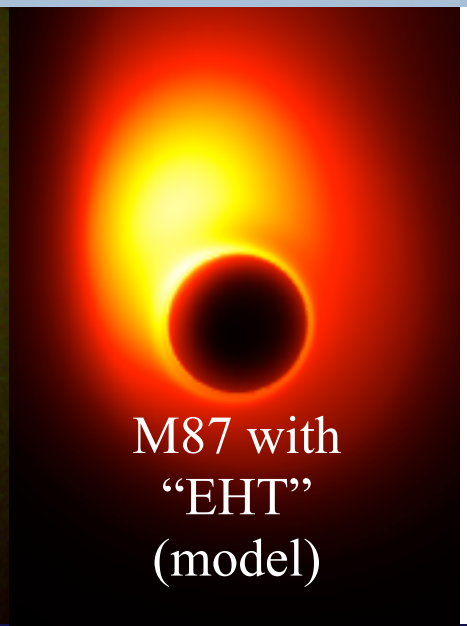

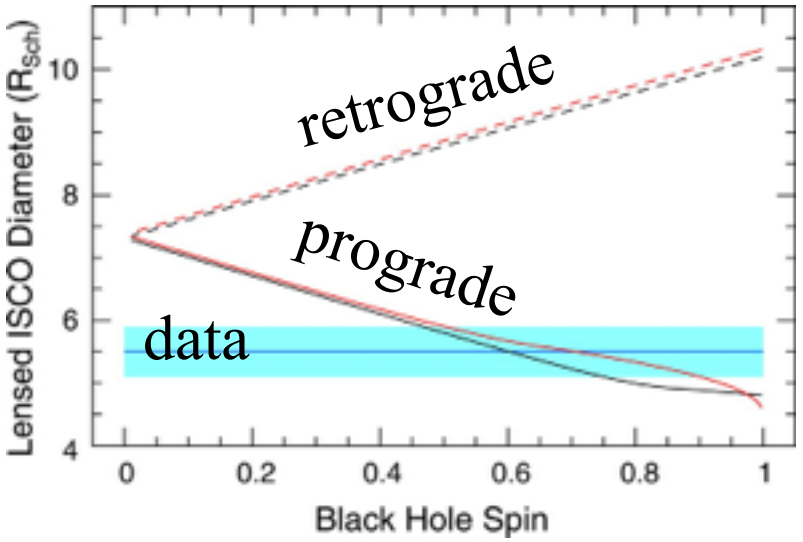

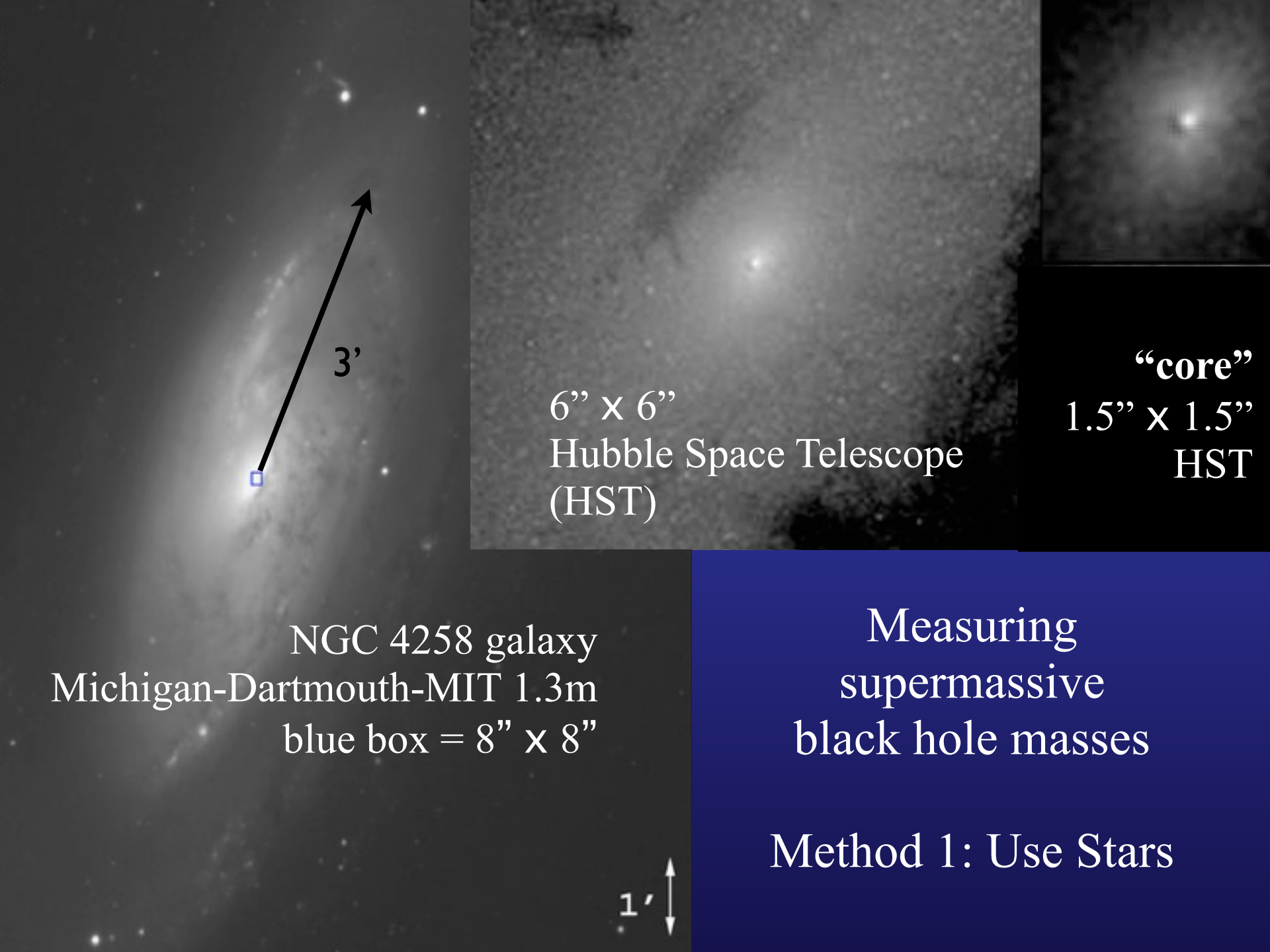

Measuring supermassive black hole masses

Method 1: Use Stars

Answer: $M = 3.3 \times 10^7 M_\odot$

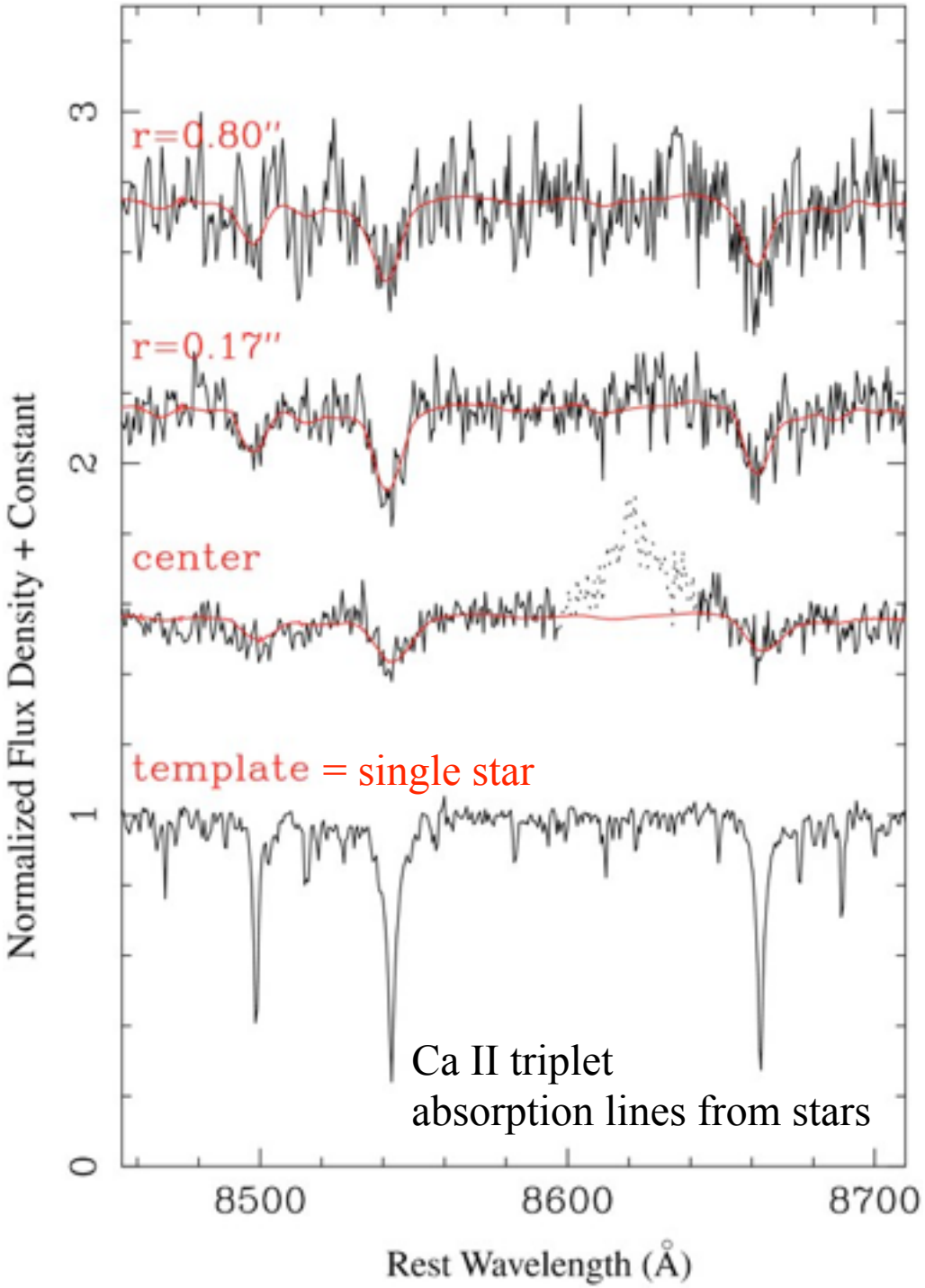

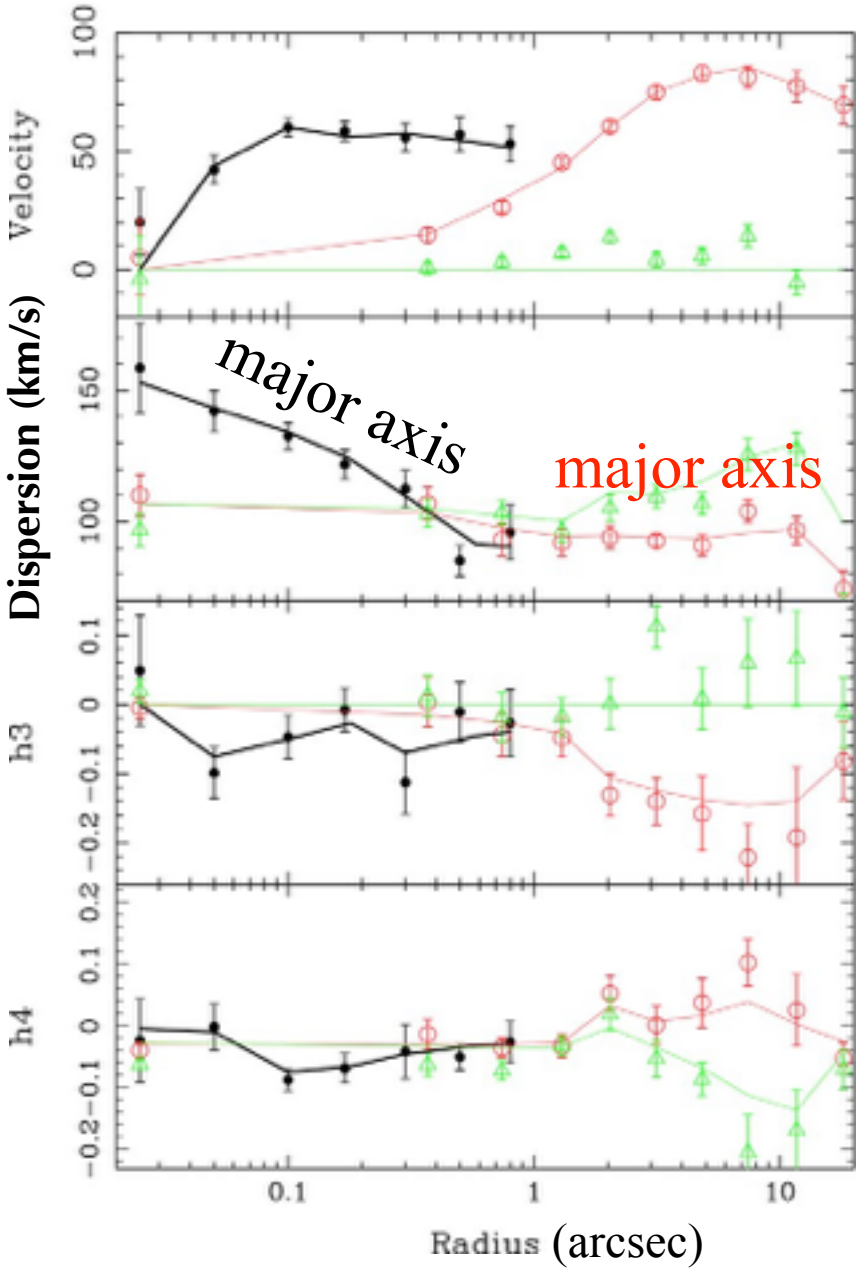

Method 2: Use Accretion Disk (Reverberation Mapping)

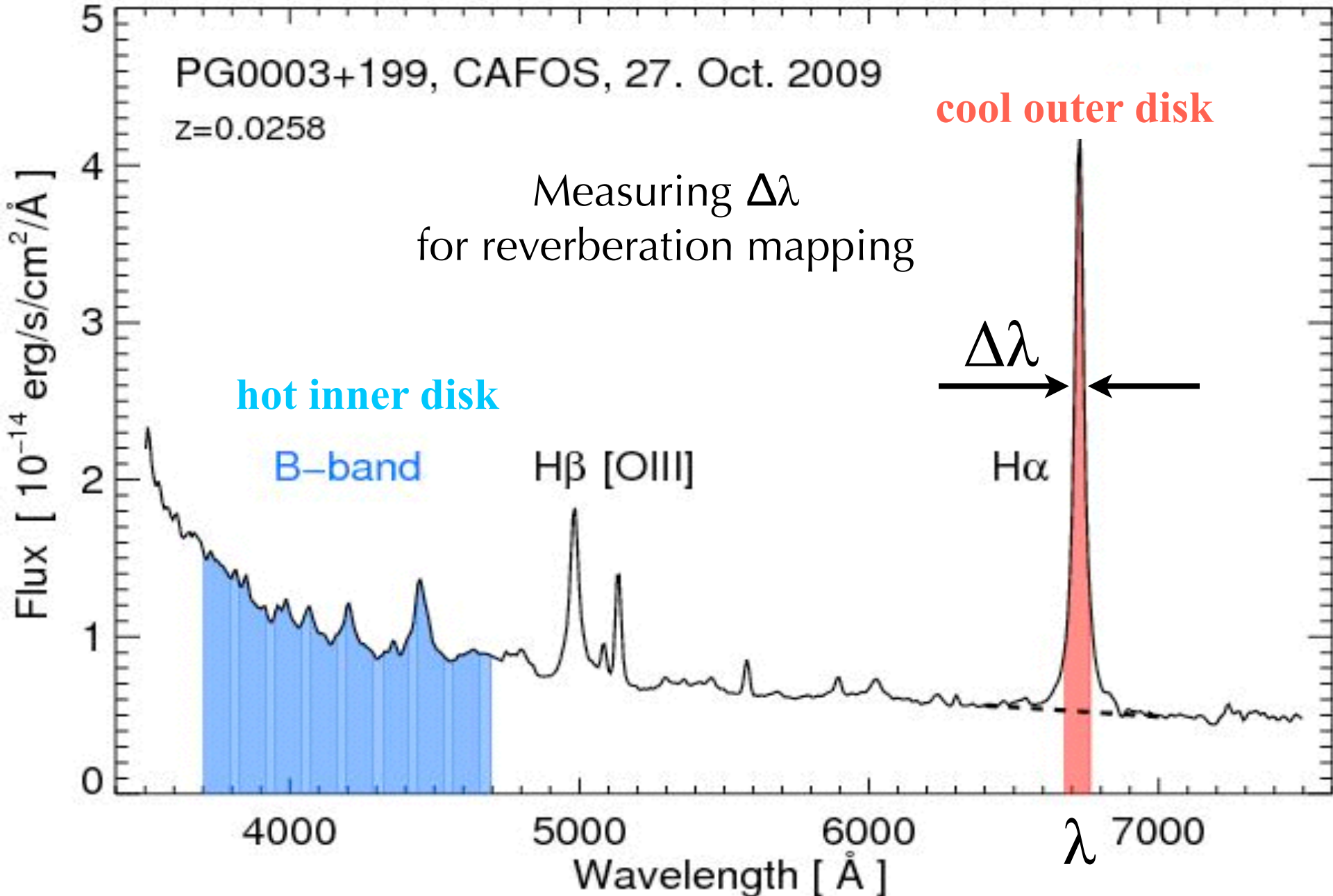

Method 2: Use Accretion Disk (Reverberation Mapping)

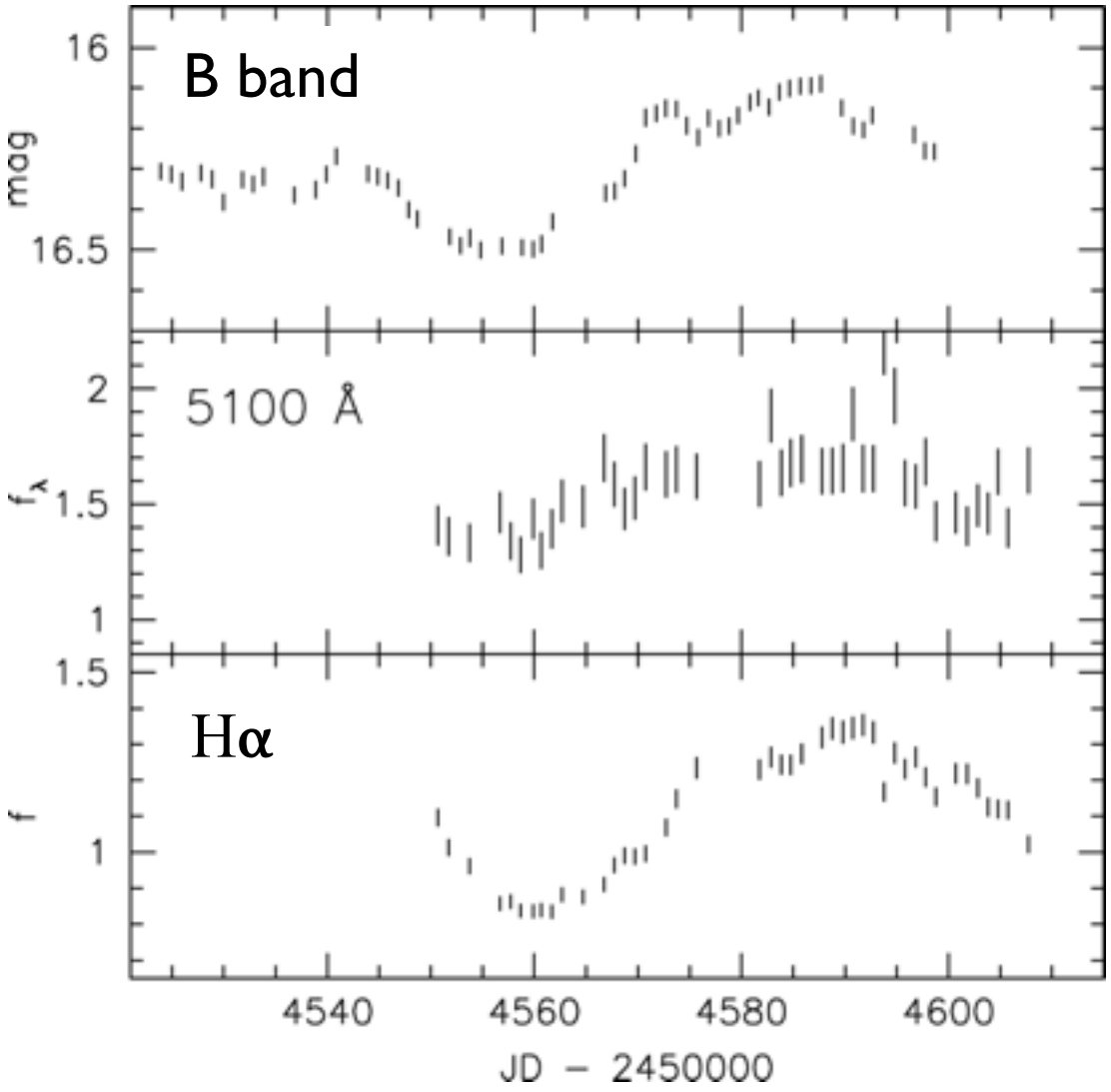

$\Delta t_{lag} \sim 4$ days

Quasars: the most luminous objects in the universe

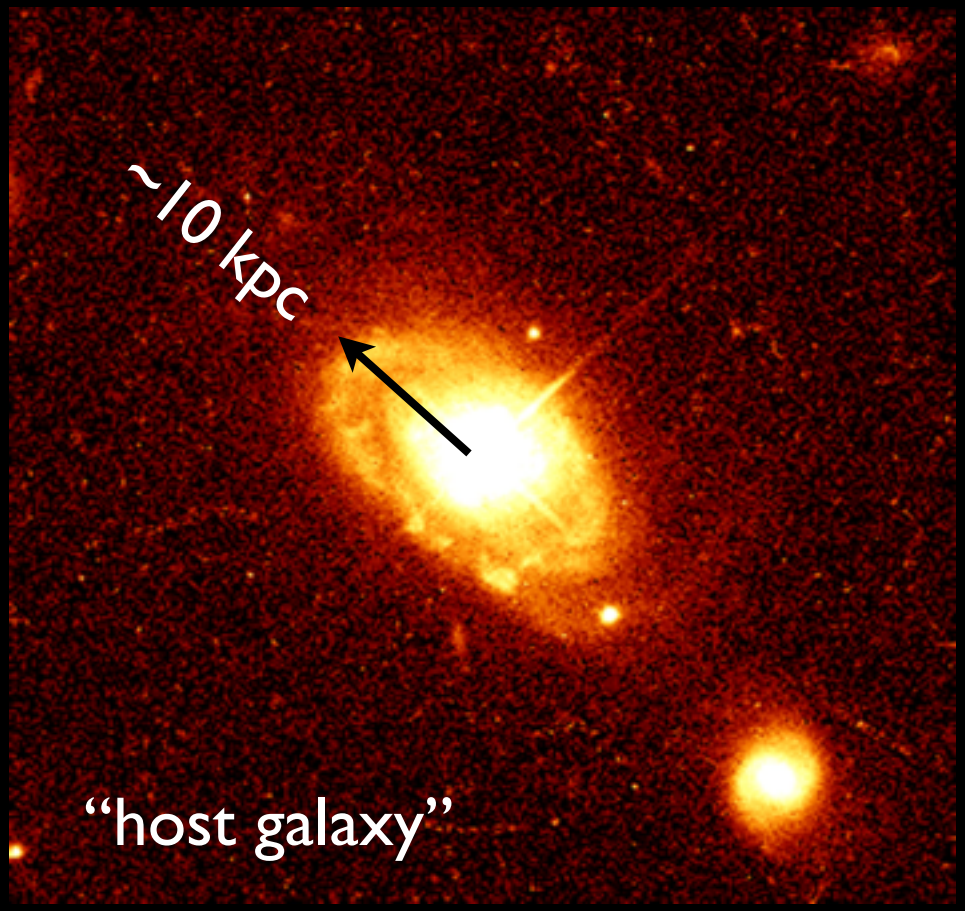

"host galaxy"

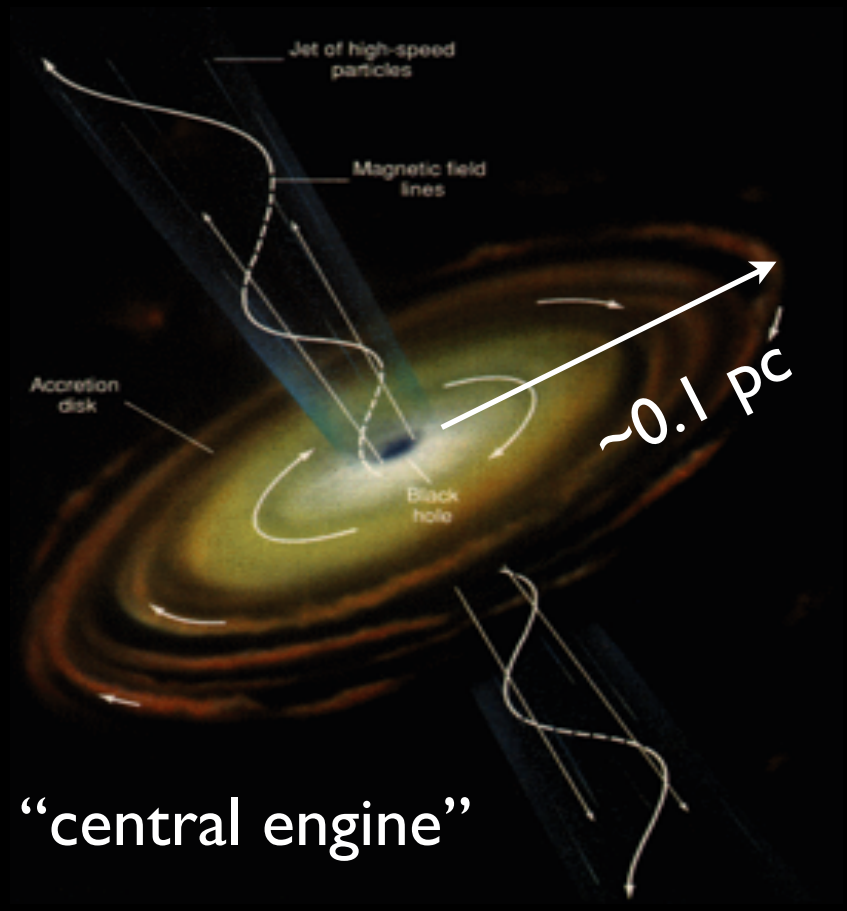

"central engine"

Quasars = accreting supermassive black holes in the nuclei of galaxies

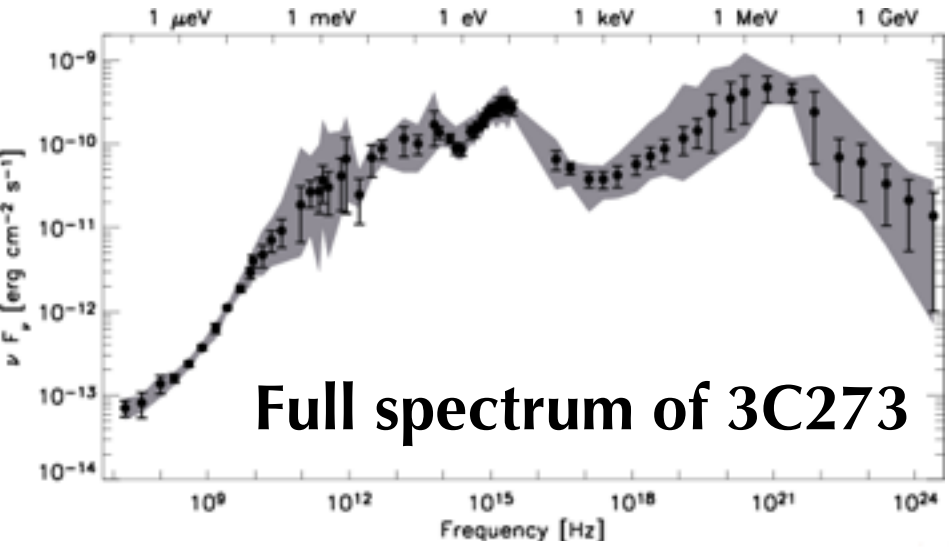

Full spectrum of 3C273

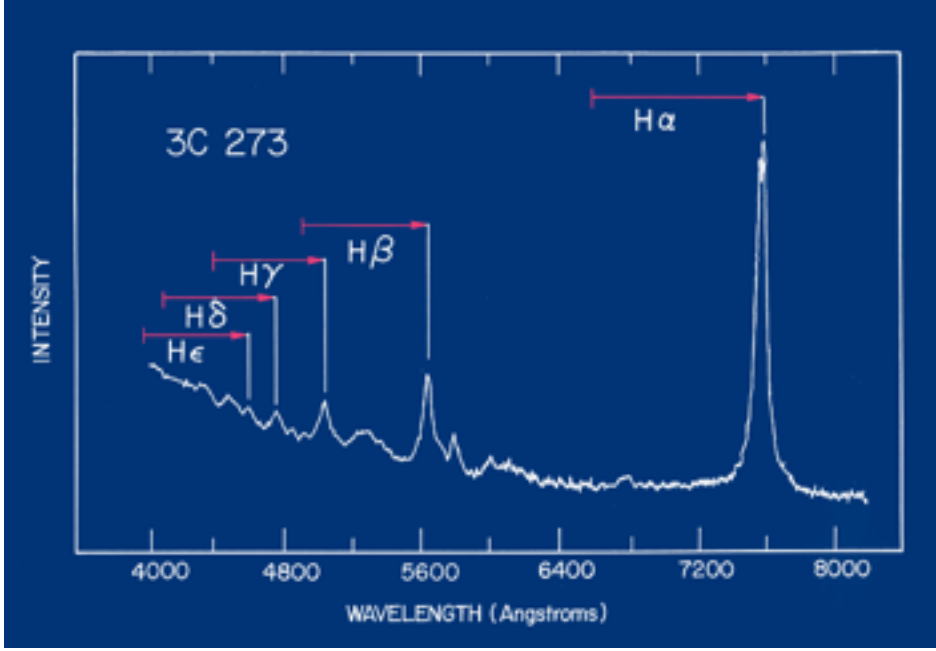

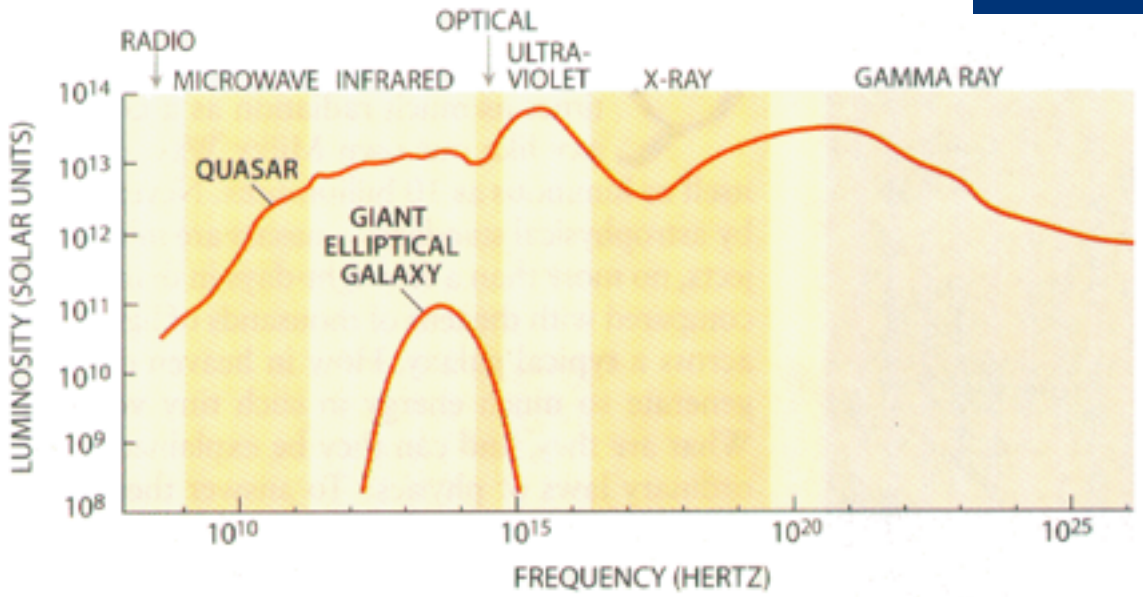

QUASAR SPECTRUM of 3C273—one of the brightest quasars and the first to be discovered—is far broader than the spectrum of a typical giant elliptical galaxy (*left*). In the optical range, the quasar is hundreds of times more luminous. Quasars were most numerous when the universe was two to four billion years old

Luminosity of 3C273
~ 10^{47} erg/s

Luminosity of host galaxy
~ 10^{44} erg/s

Quasar Masses from Reverberation Mapping

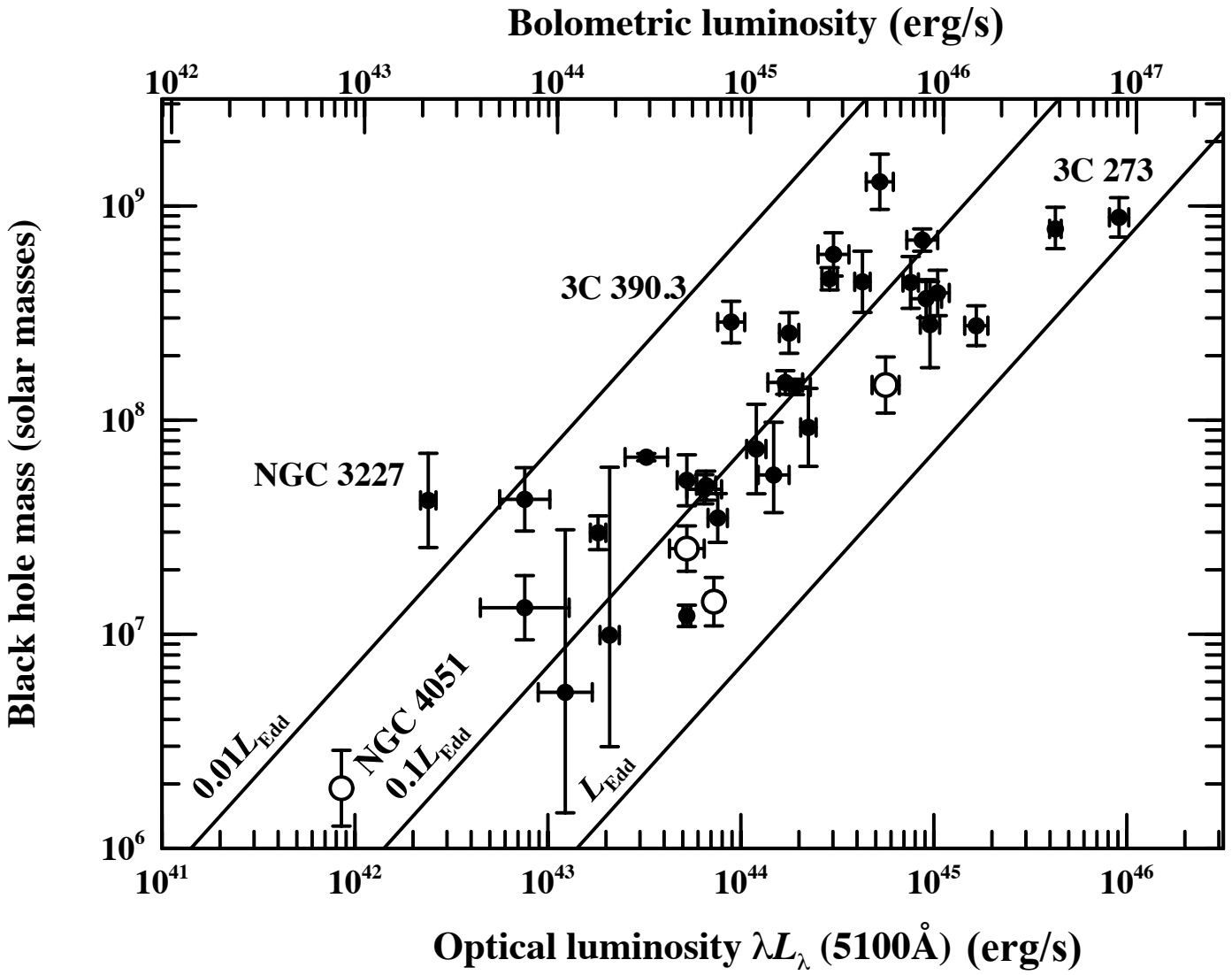

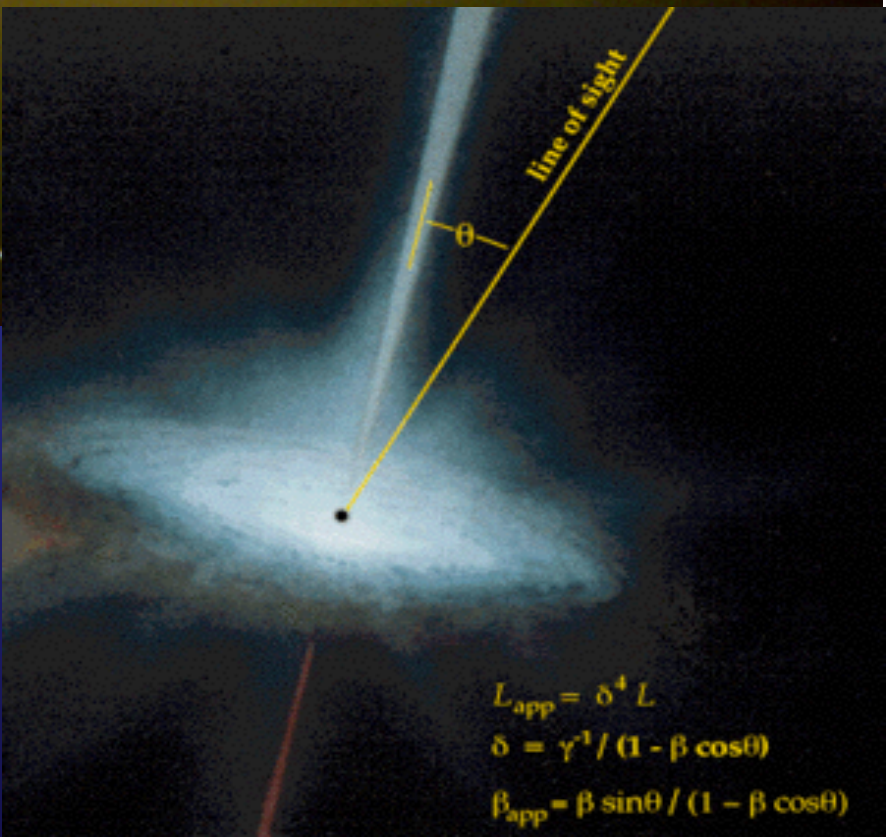

Superluminal Motion in the M87 Jet

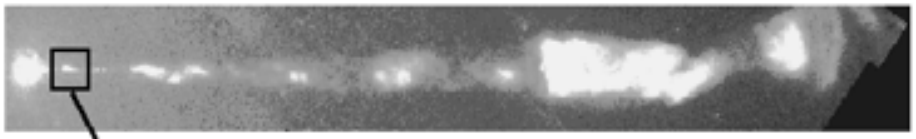

proper motion μ ~ 25 milliarcsecond/yr
distance to M87 = d = 16 Mpc
apparent transverse velocity v = μ d = 6c > c!

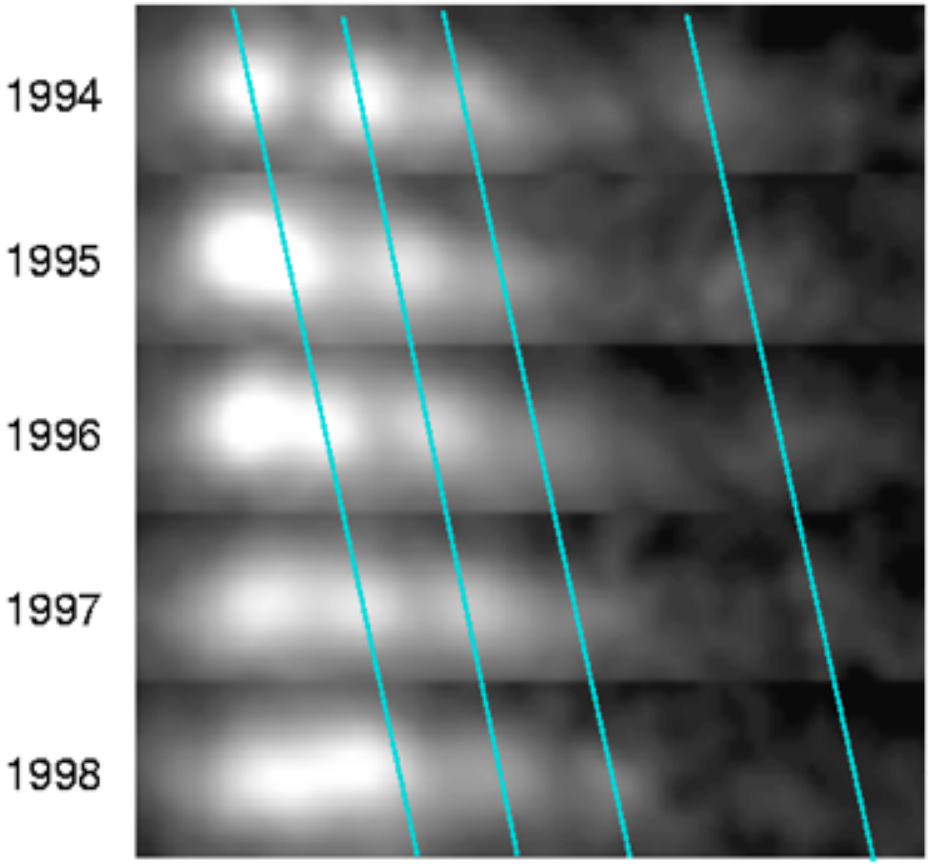

Gravitational Lensing

Resolved "strong" lensing

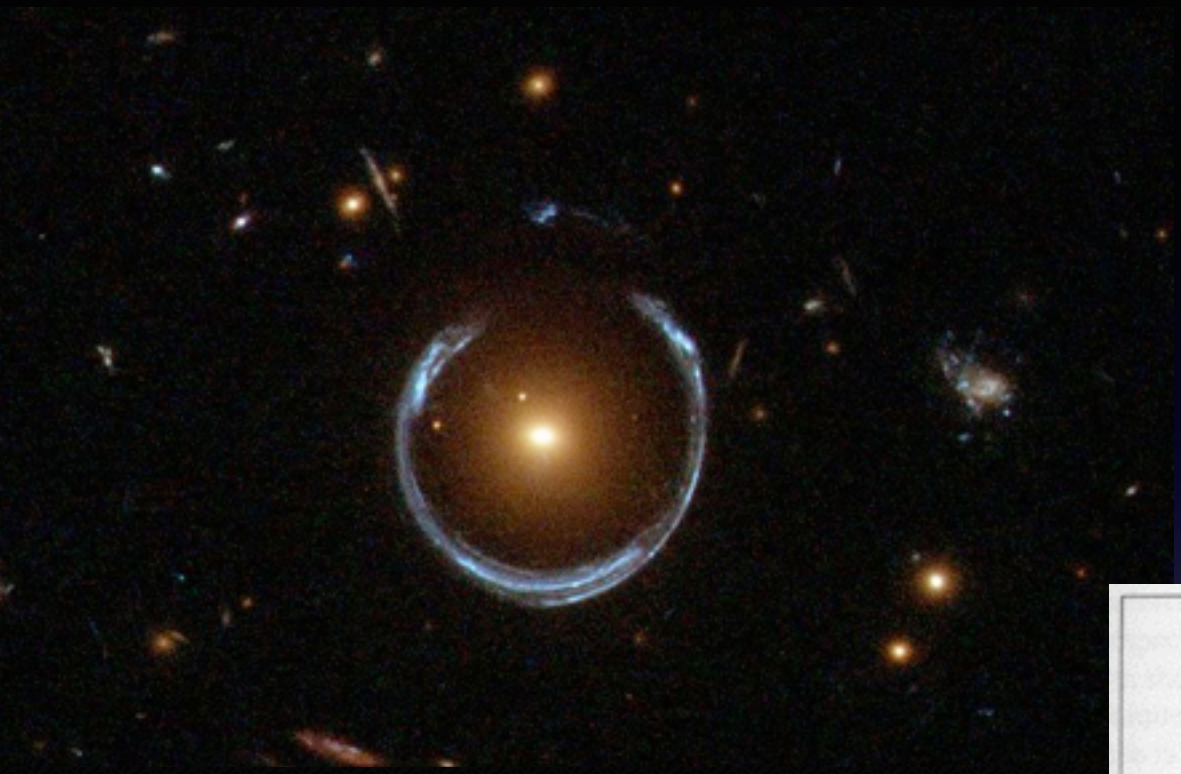

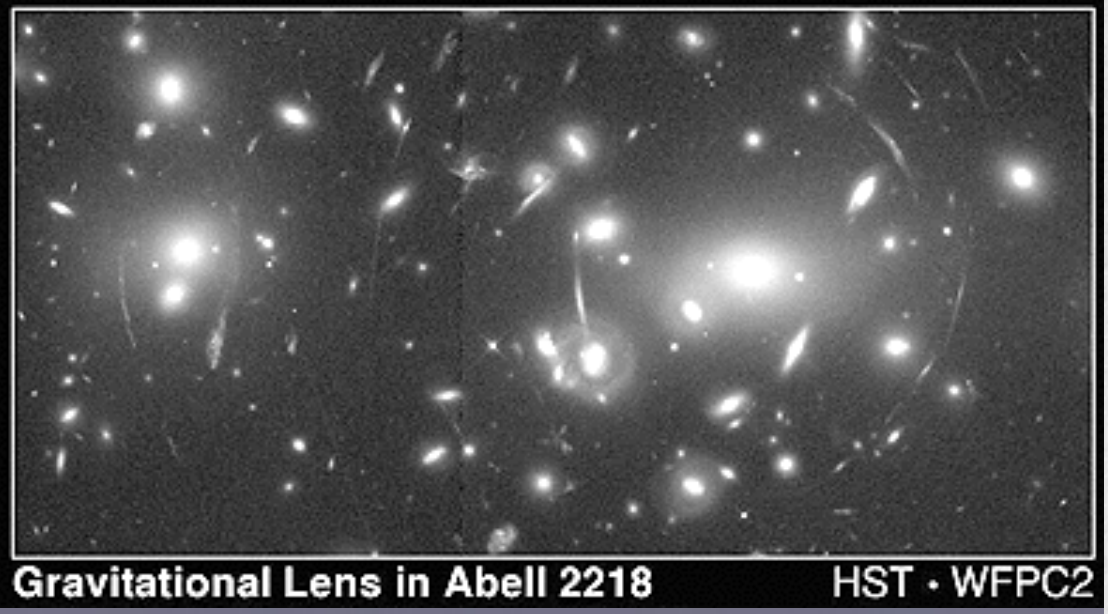

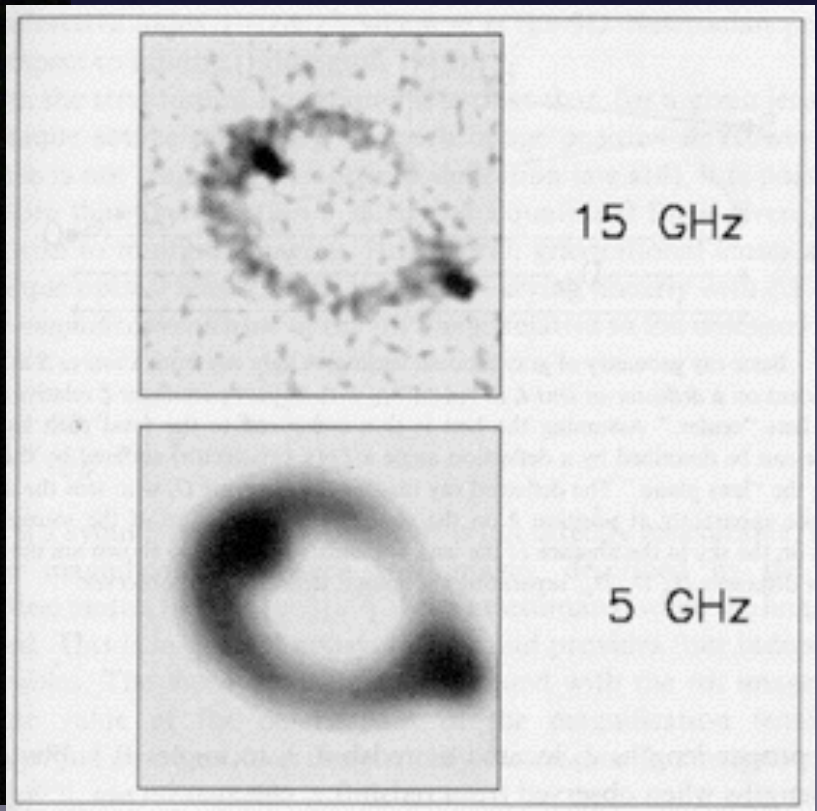

Fig. 1 XMM-Newton and Suzaku light curve of Sw J1644+57 together with the SWIFT-XRT 0.3-to-10-keV light curve for reference (gray) (37, 38).

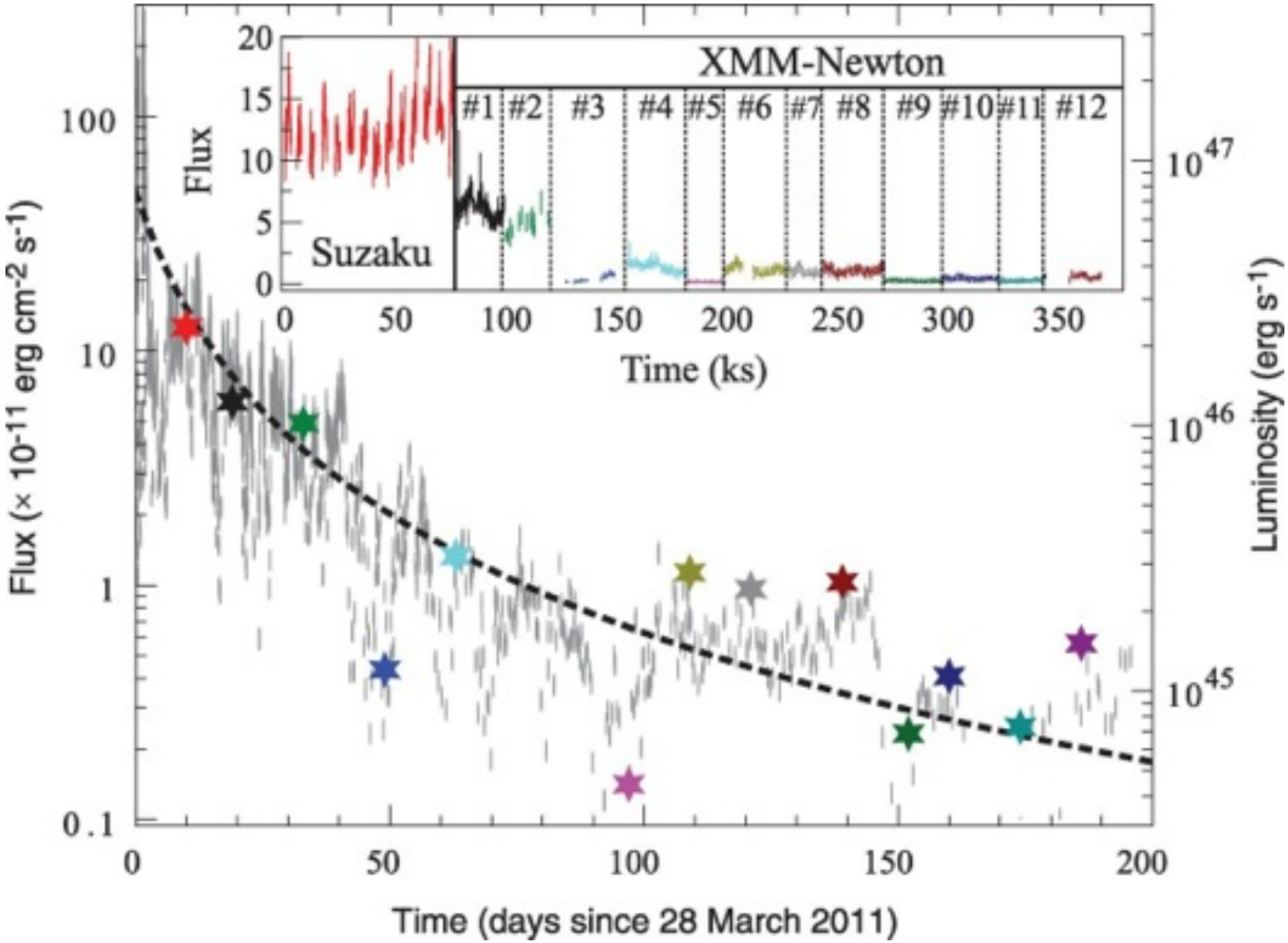

R C Reis et al. Science 2012;337:949-951

Fig. 2 (A) Power spectra for Suzaku and (B) for XMM #1, in the 2- to 10-keV energy range.

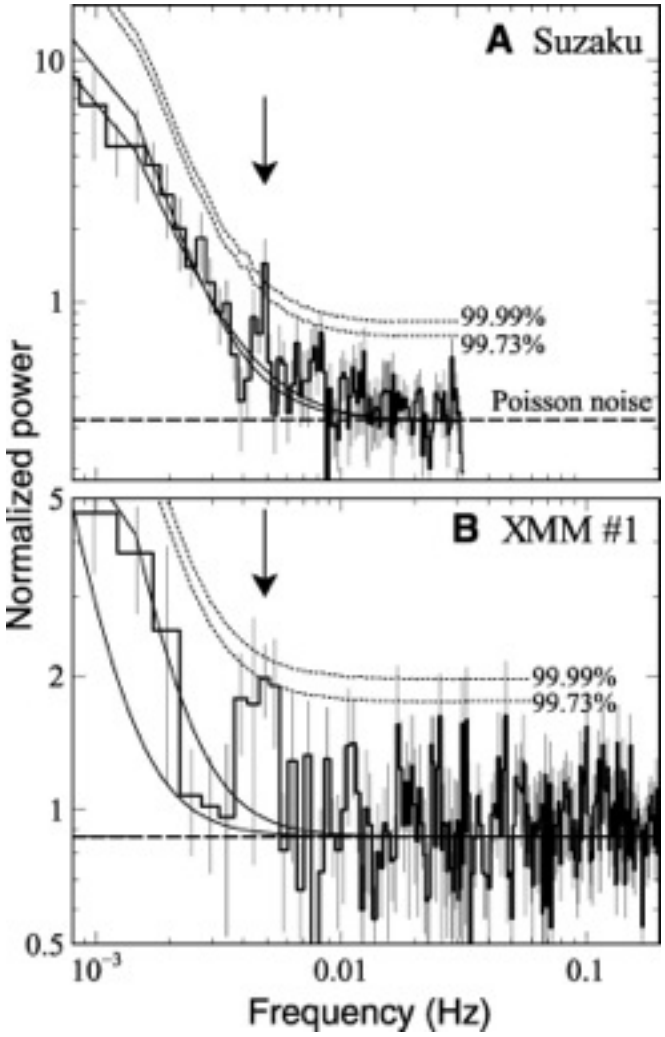

R C Reis et al. Science 2012;337:949-951

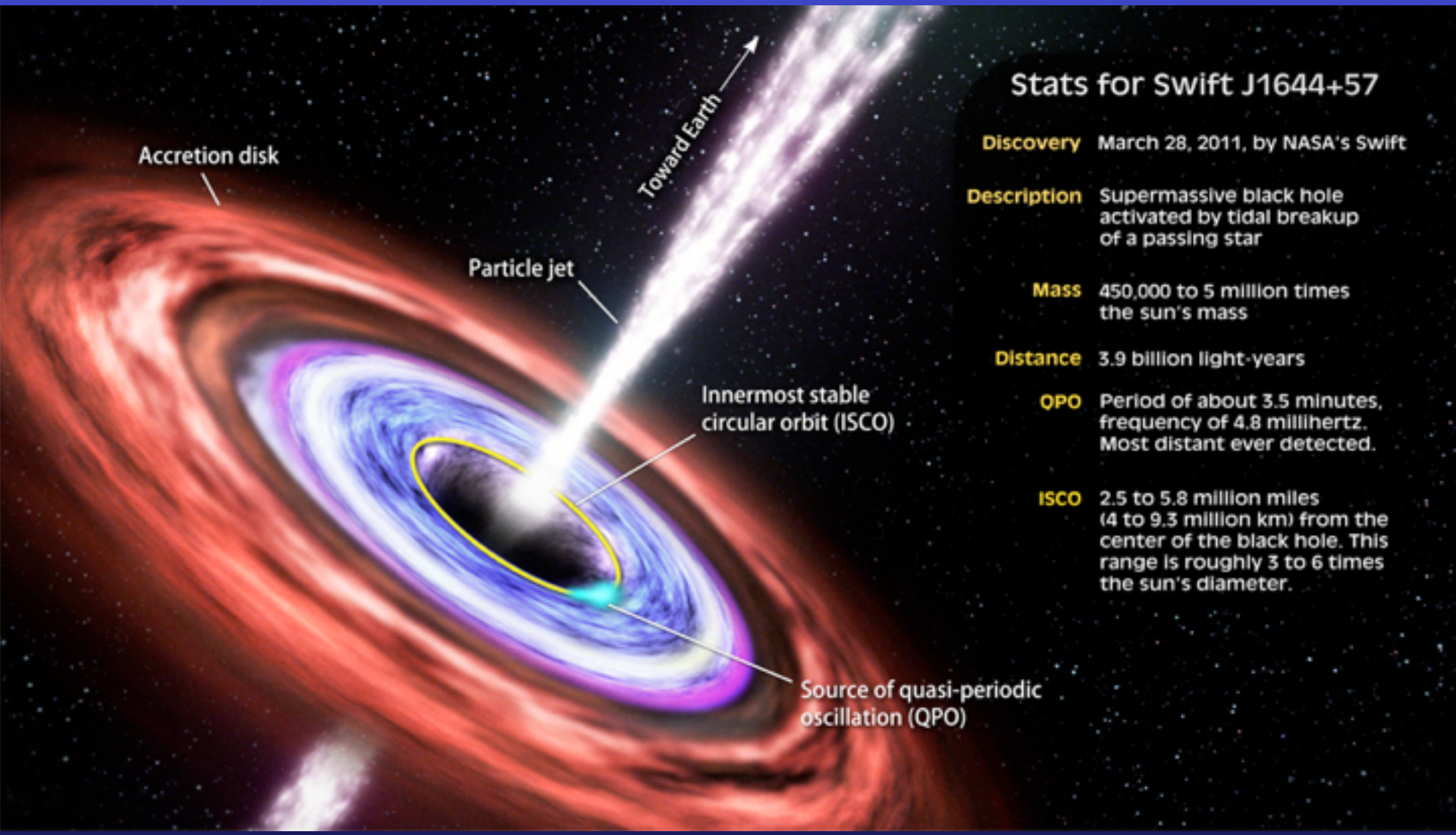
Accretion disk
Toward Earth
Particle jet
Innermost stable circular orbit (ISCO)
Source of quasi-periodic oscillation (QPO)
Stats for Swift J1644+57
Discovery March 28, 2011, by NASA's Swift
Description Supermassive black hole activated by tidal breakup of a passing star
Mass 450,000 to 5 million times the sun's mass
Distance 3.9 billion light-years
QPO Period of about 3.5 minutes, frequency of 4.8 millihertz. Most distant ever detected.
ISCO 2.5 to 5.8 million miles (4 to 9.3 million km) from the center of the black hole. This range is roughly 3 to 6 times the sun's diameter.

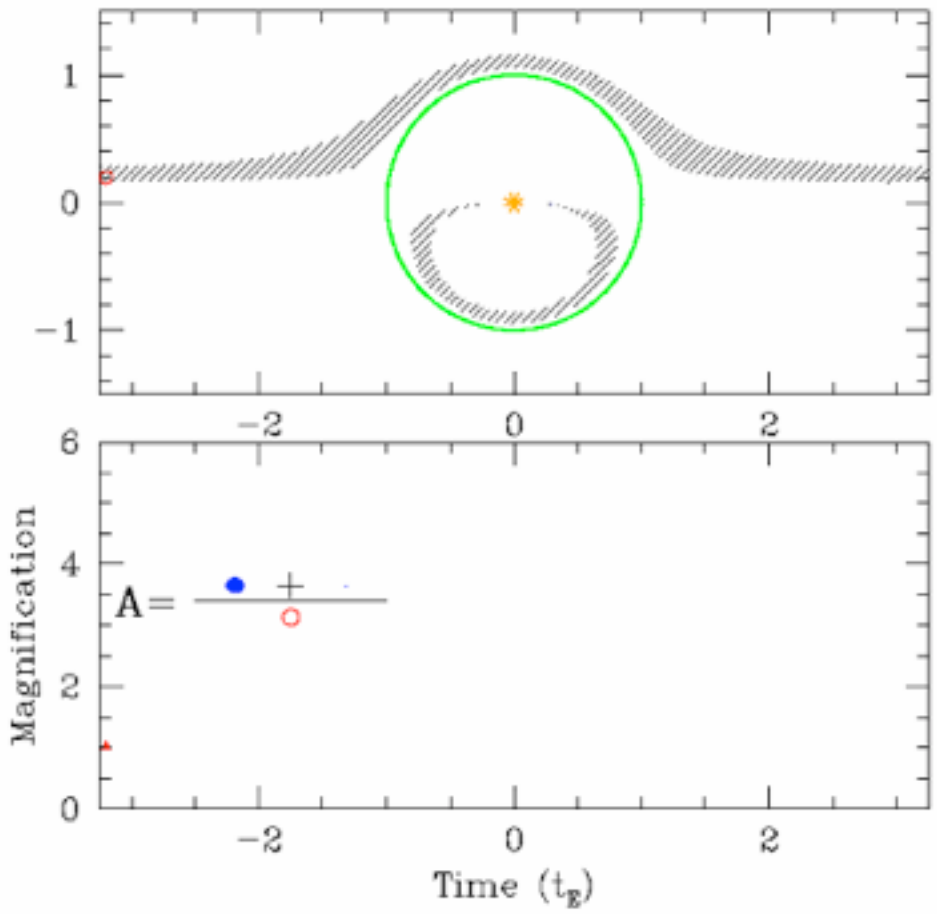

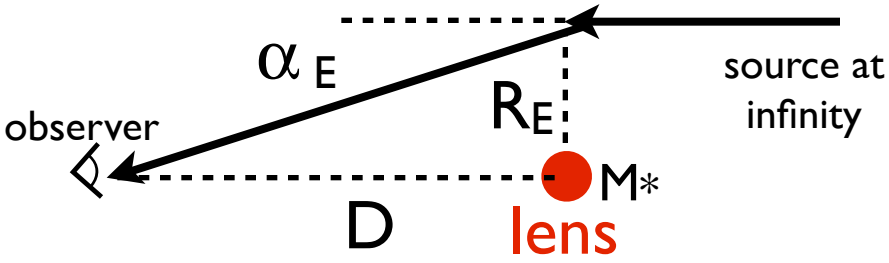

$$\Delta v \sim \frac{GM_*}{R_E^2} \times \frac{2R_E}{c} \qquad \alpha_E \sim \frac{\Delta v}{c} \sim \frac{R_E}{D}$$

$$\alpha_E \sim 1\,\mathrm{mas} \left(\frac{M_*}{M_\odot}\right)^{1/2} \left(\frac{\mathrm{kpc}}{D}\right)^{1/2}$$

$$R_E \sim 1\,\mathrm{AU} \left(\frac{M_*}{M_\odot}\right)^{1/2} \left(\frac{D}{\mathrm{kpc}}\right)^{1/2}$$

$$t_E \sim \frac{R_E}{v_{\mathrm{rel}}} \sim 1\,\mathrm{month} \left(\frac{R_E}{\mathrm{AU}}\right) \left(\frac{30\,\mathrm{km/s}}{v_{\mathrm{rel}}}\right)$$

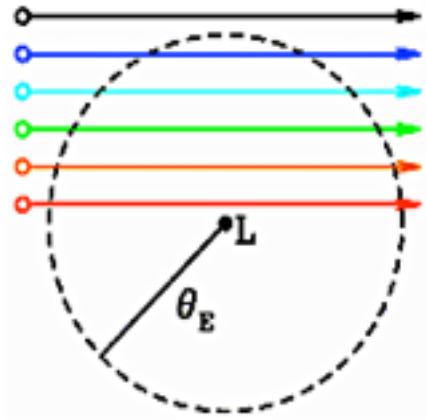

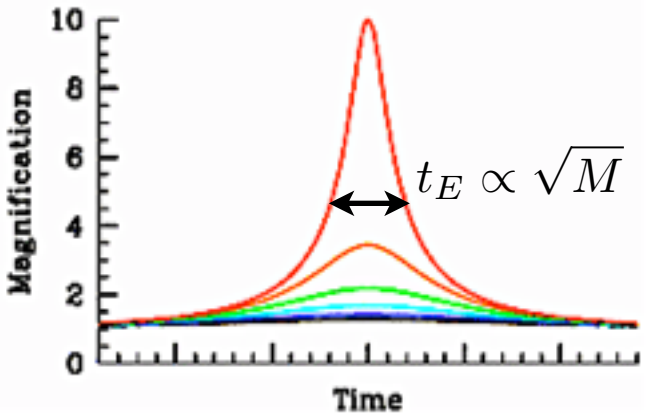

"Microlensing"
= unresolved strong lensing
= measure light curve only

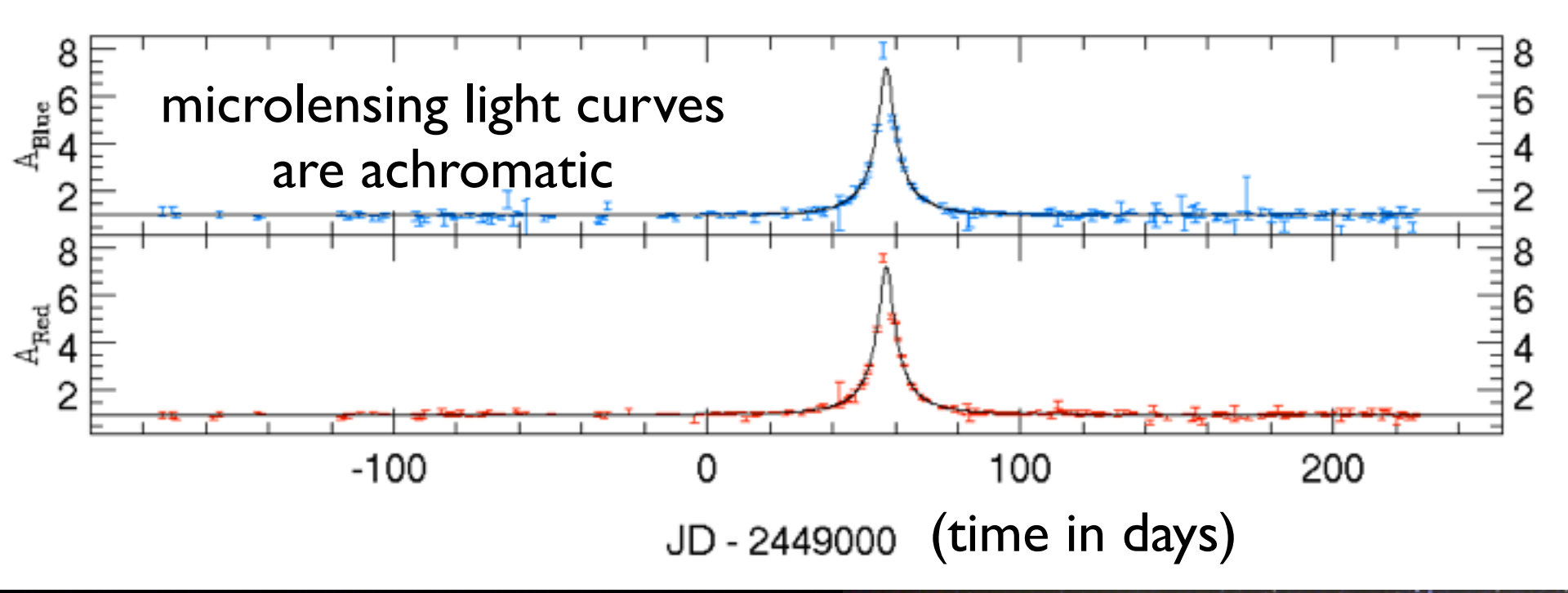

Microlensing surveys stare at dense star fields

Large Magellanic Cloud
(LMC = satellite galaxy of Milky Way)

Galactic Bulge
(of our Milky Way)

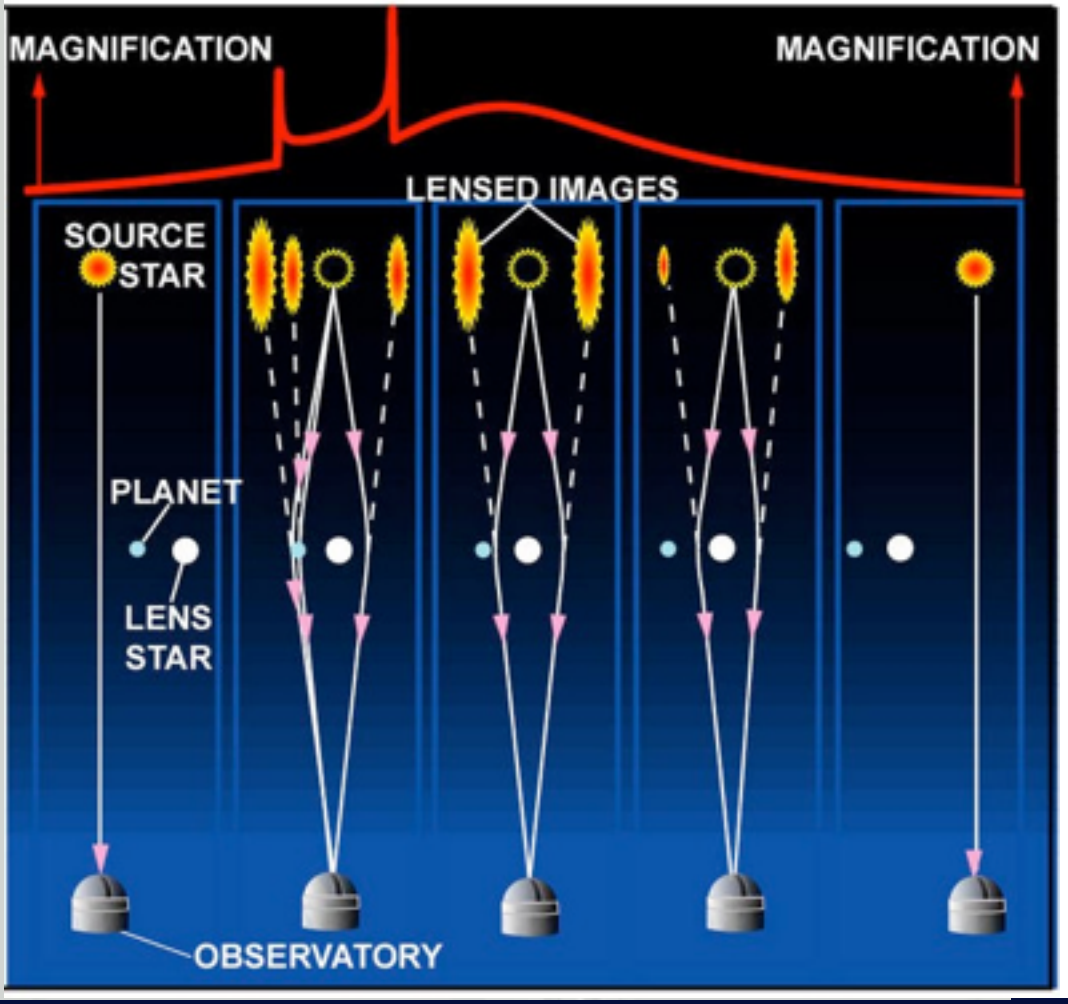

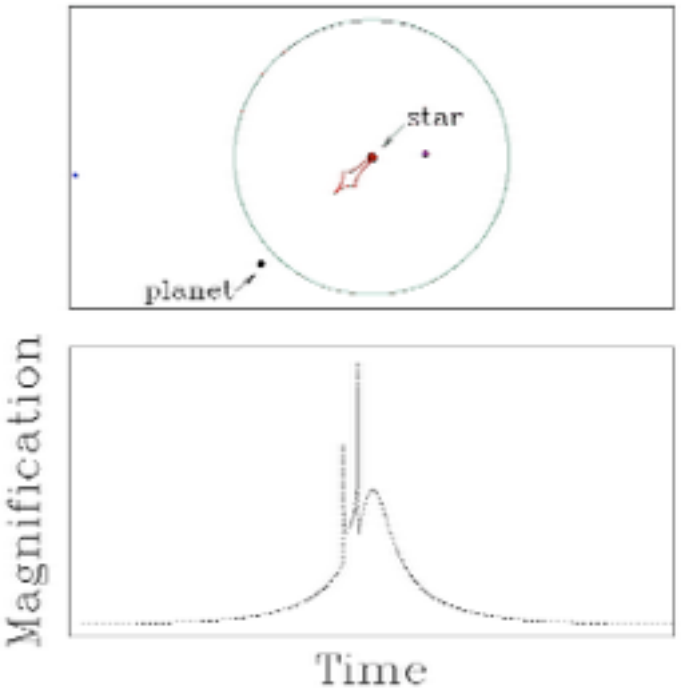

Planetary Microlensing (Binary lens)

$D \approx 5.2^{+0.2}_{-2.9}\,\mathrm{kpc}$ $\qquad$ $a \approx 3.0^{+0.1}_{-1.7}\,\mathrm{AU}$

$M_* \approx 0.36^{+0.03}_{-0.28}\,M_\odot$ $\qquad$ $M \approx 1.5^{+0.1}_{-1.2}\,M_J$

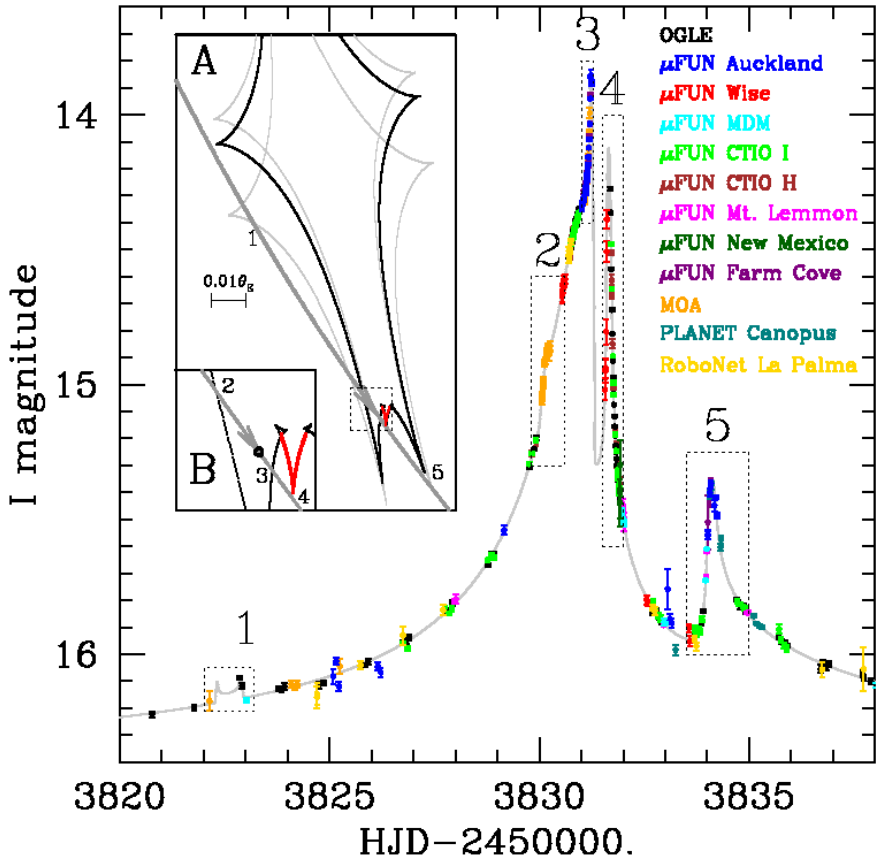

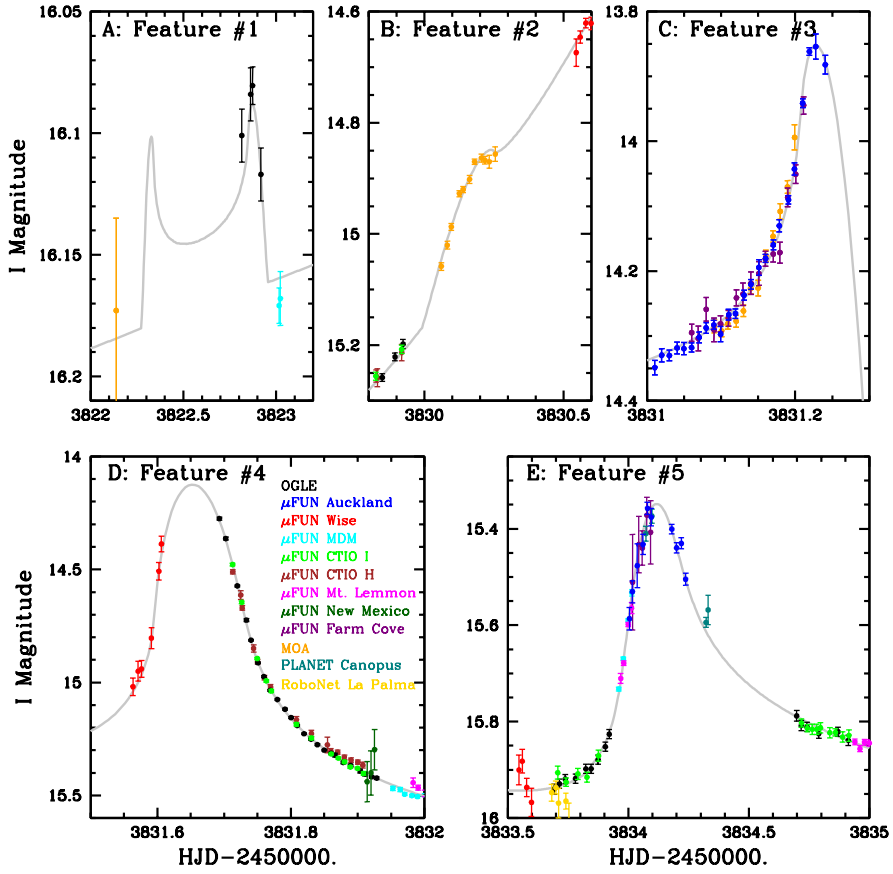

$M_* \approx 0.5 M_\odot$ $D \approx 1.5\,\mathrm{kpc}$

$M_1 \approx 0.71 M_J$ $a_1 \approx 2.3\,\mathrm{AU}$

$M_2 \approx 0.27 M_J$ $a_2 \approx 4.6\,\mathrm{AU}$ $e_2 \approx 0.15^{+0.17}_{-0.10}$

from orbital motion!

Statistics from microlensing

1. At fixed M_*, $dN/dM \propto M^{-1.7}$
2. 20 +/- 10% of stars have 5-15 $M_\oplus$ at a ~ 1.6-4.3 AU
3. For every star 0.08 $M_\odot$ < M_* < 1 $M_\odot$,
   there are ~2 *free-floating* Jupiter-mass objects!

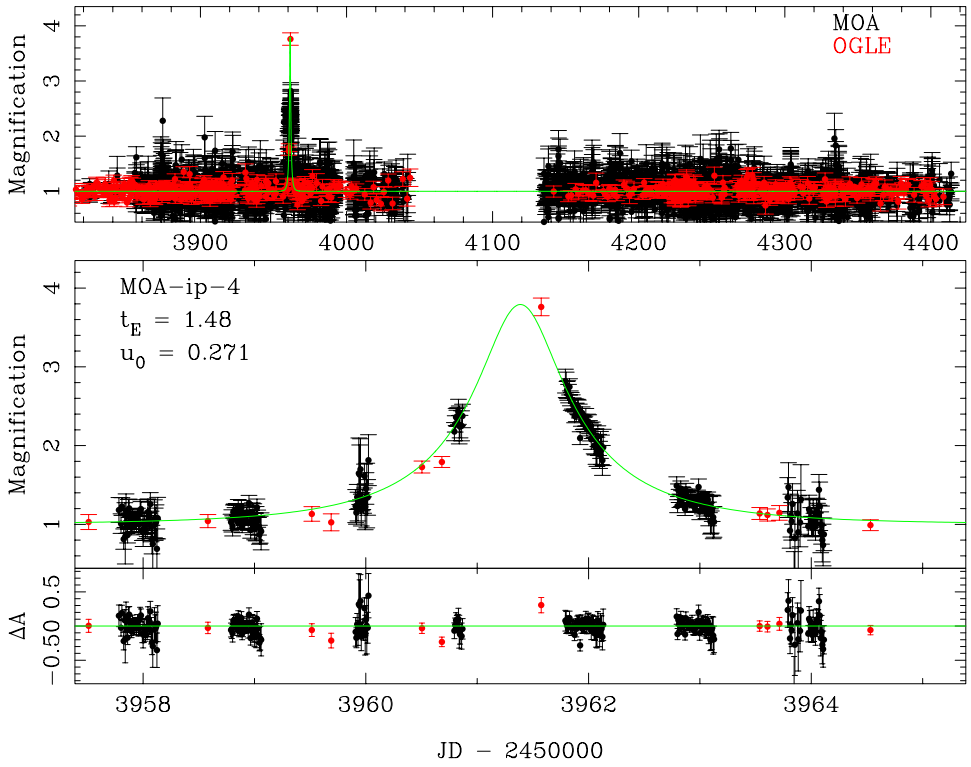

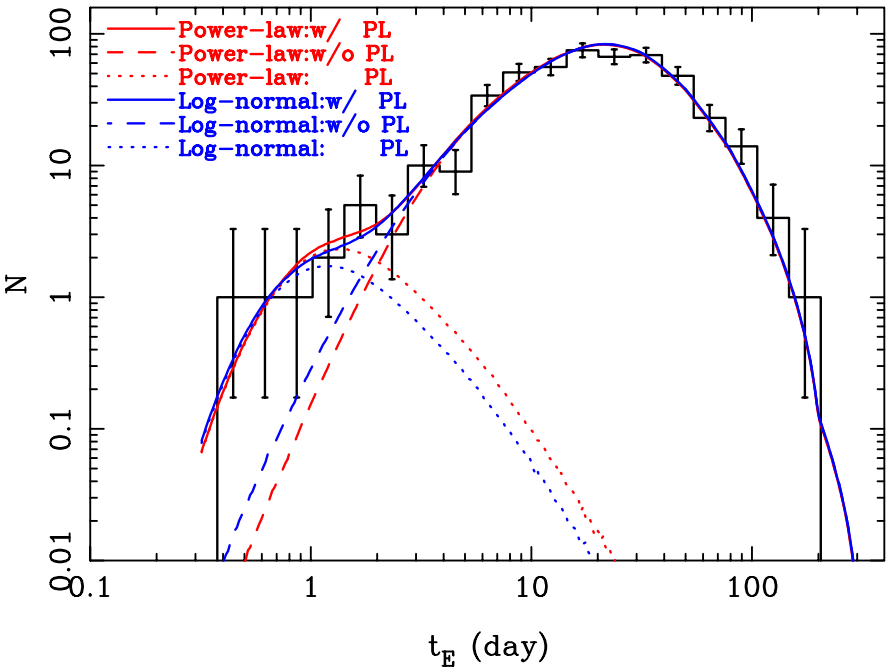


A Long Time Ago
In a Disk Galaxy
Far Far Away

Stars form in interstellar clouds (~1-100 pc in size)

Hot halo gas

Globular cluster

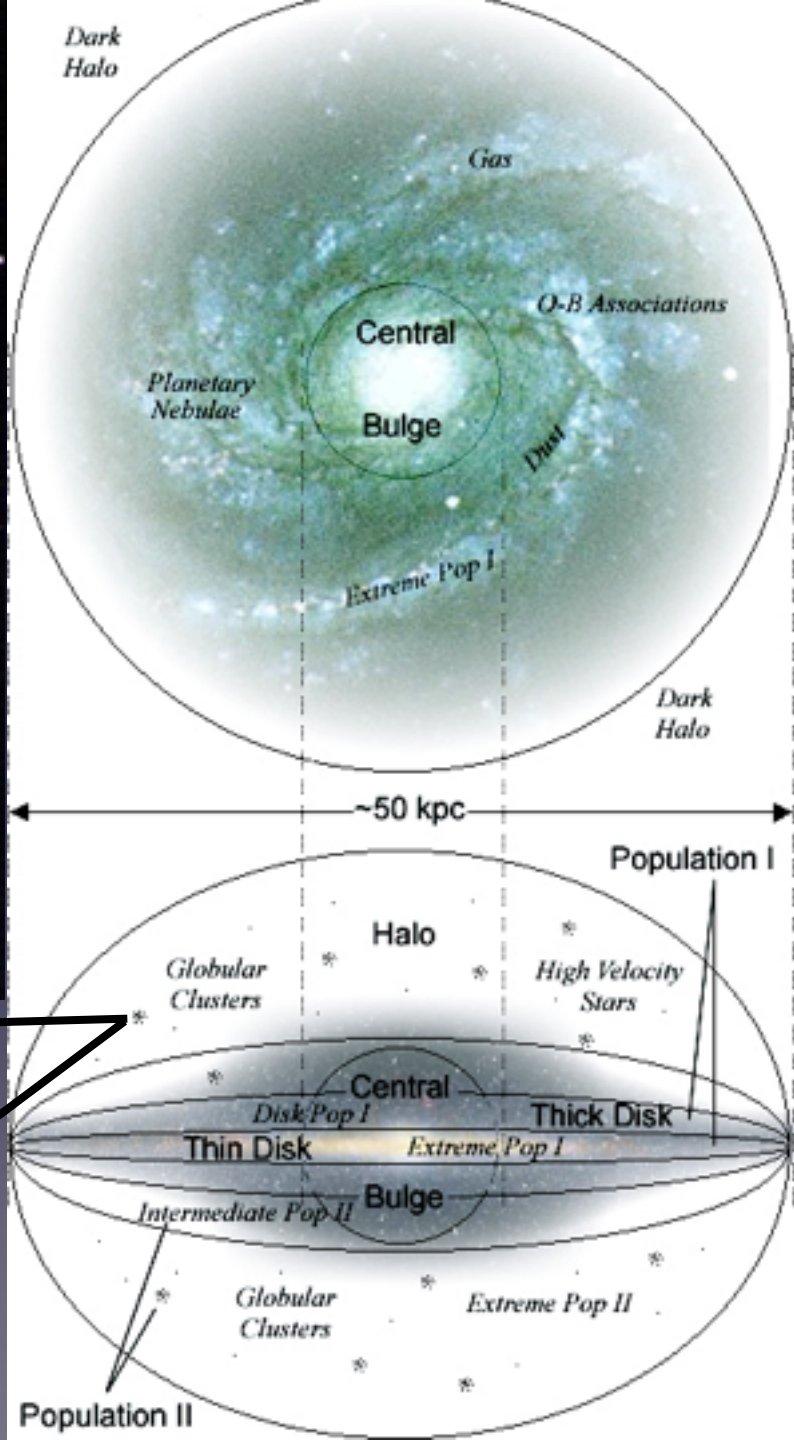


NGC 2207 and IC 2163


The Mice


Stephan's
Quintet

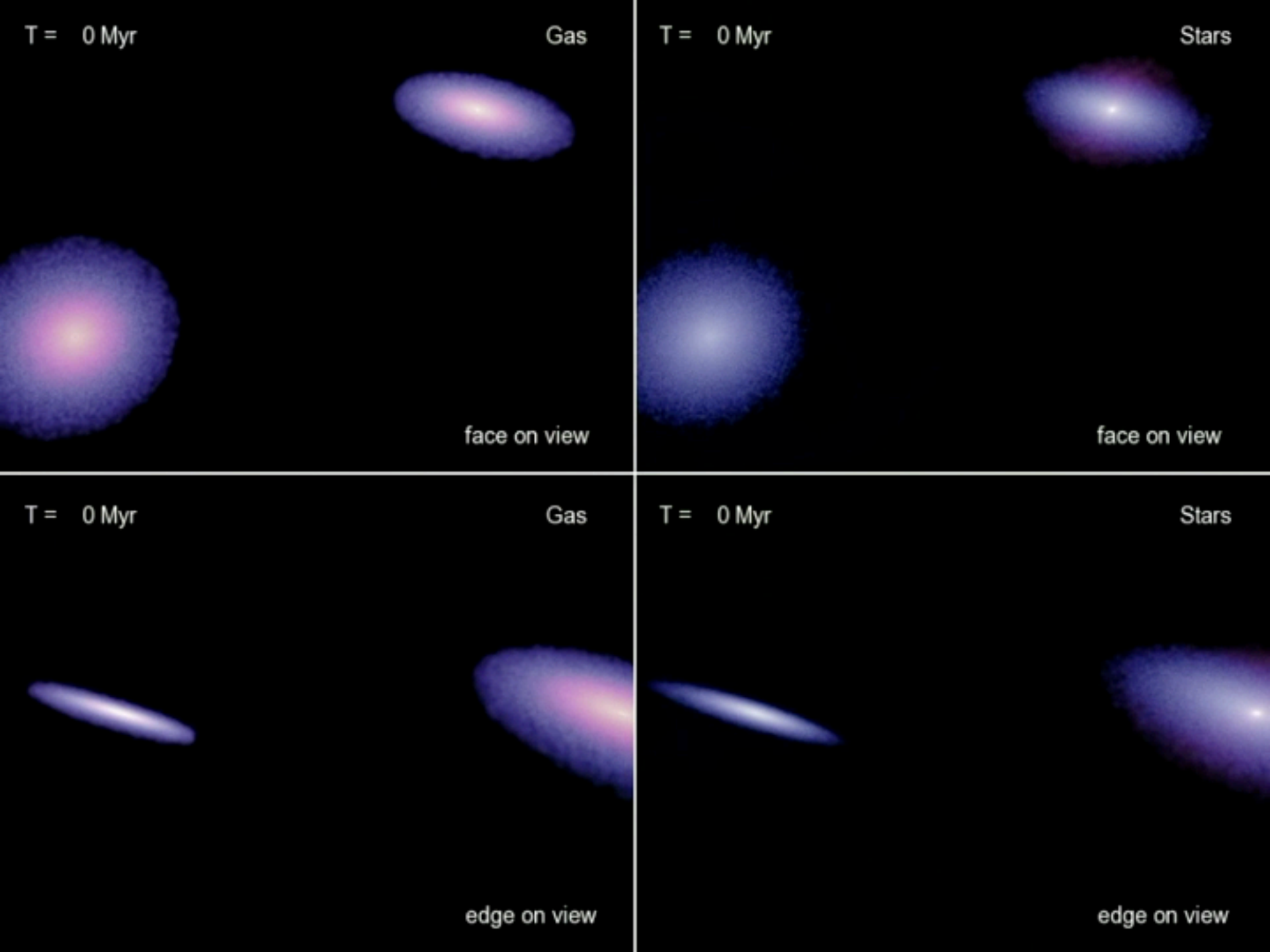
T = 0 Myr
Gas
face on view
T = 0 Myr
Stars
face on view
T = 0 Myr
Gas
edge on view
T = 0 Myr
Stars
edge on view

Disk galaxy
"Late-type galaxy"
"Blue galaxy"
"Star-forming galaxy"

Elliptical galaxy
"Early-type galaxy"
"Red galaxy"
"Red and dead"


Galaxy Cluster
Massive Ellipticals Inside
Less Massive Disks Outside

Differential Rotation

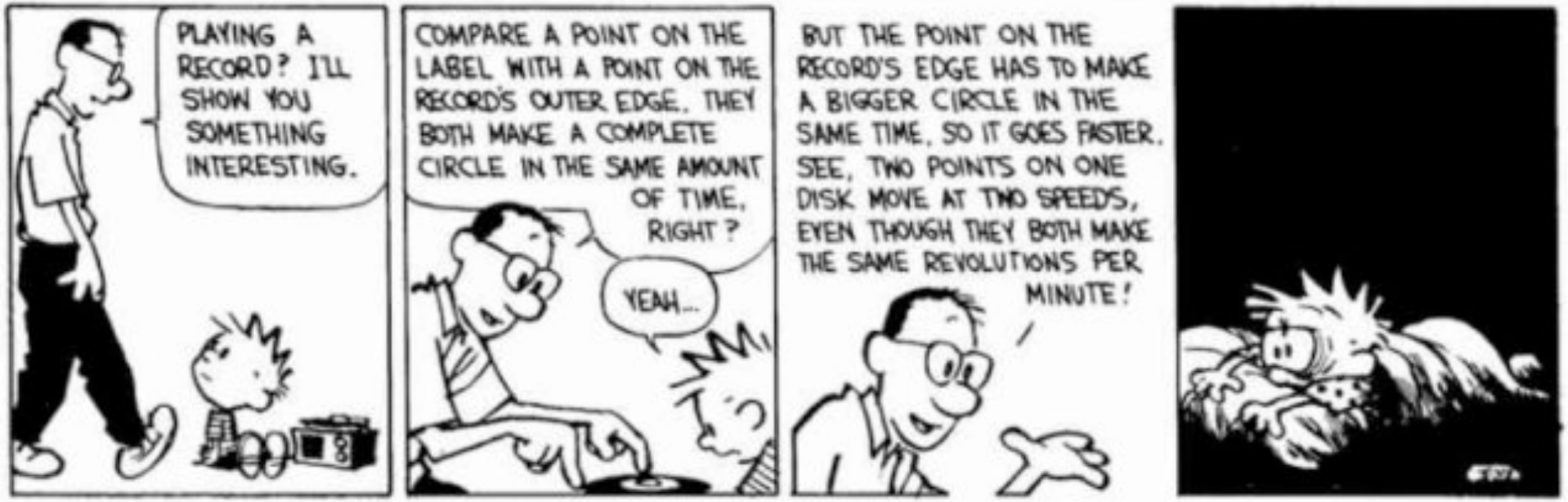

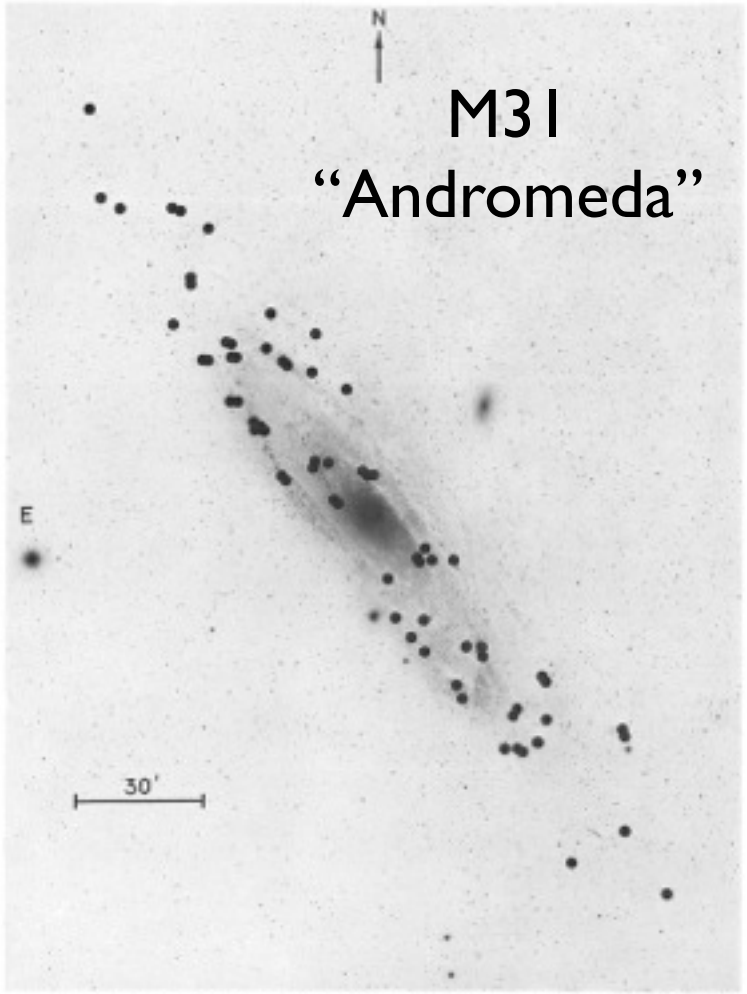

M31
"Andromeda"

FIG. 1.—Identification chart for emission regions in M31 for which velocities have been obtained. Palomar 48-inch Schmidt ultraviolet photograph, 103a0 plate + UG 1 filter, courtesy of Dr. S. van den Bergh.

RUBIN AND FORD (see page 380)

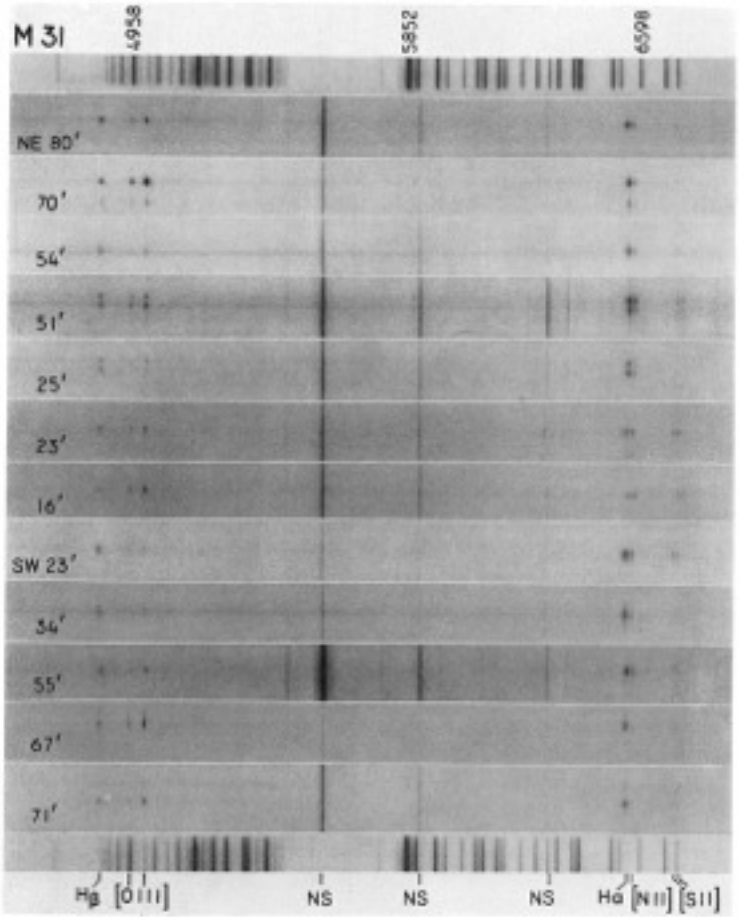

FIG. 2.—Representative spectra of emission regions in M31, arranged according to distance from center. Lines crossing the spectra are nightsky lines. Comparison spectrum is Ne + Fe, original dispersion 135 Å mm^{-1} = 6 km sec^{-1} μ^{-1} at Hα. Principal emission lines are indicated.

RUBIN AND FORD (see page 381)

Many of the brighter emission regions in M31 are large, complex associations of emission regions and OB stars. However, there are also completely isolated Strömgren spheres. In an effort to obtain spectra from all parts of M31, we have generally observed no more than two regions within a single association, and have observed some of the isolated regions. In Table 1, column (9), we have classified the observed regions according to their membership in the M31 OB associations as defined by van den Bergh (1964). Fourteen of the regions we have observed are not in OB associations; the remaining fifty-three regions are distributed in thirty-four associations. Seventeen associations have velocities from two or more regions; for all association members the average deviation from the mean association velocity is 10 km sec^{-1}, or just equal to the average internal error in the radial velocity of an emission region. We conclude that the line-of-sight component of the velocity dispersion within an association is less than ± 10 km sec^{-1}, or less than 15 km sec^{-1} projected to a circular-velocity component in the plane of M31.

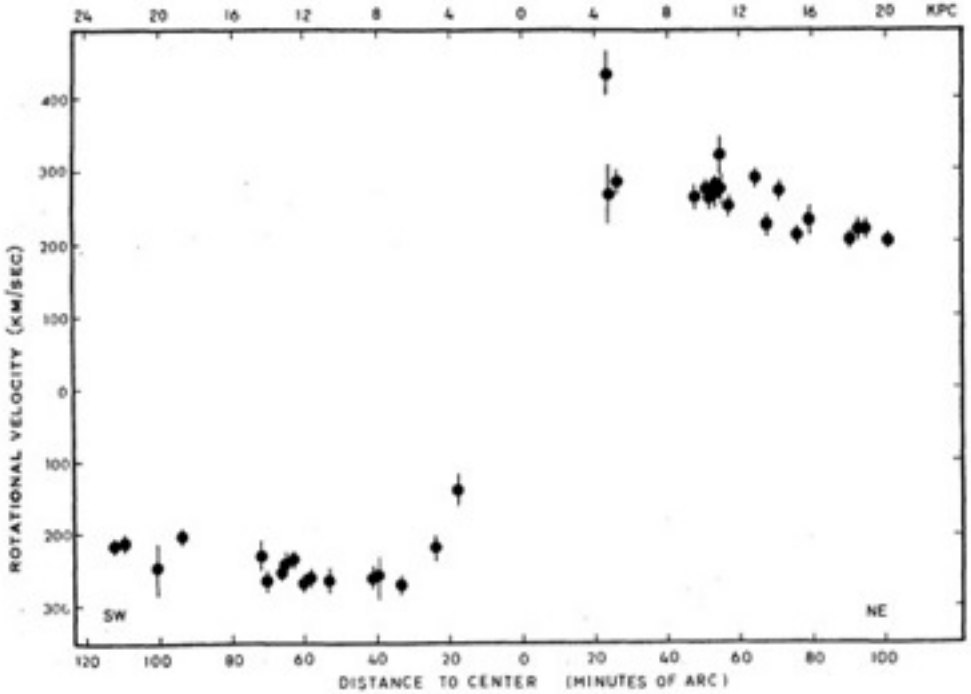

FIG. 4.—Mean rotation velocities for thirty-four OB associations plus three outer regions in M31, as a function of distance from the center. Error bars indicate average error of the velocity of the association, calculated from the velocities of individual emission regions in the association, or from the observational errors, whichever are larger.

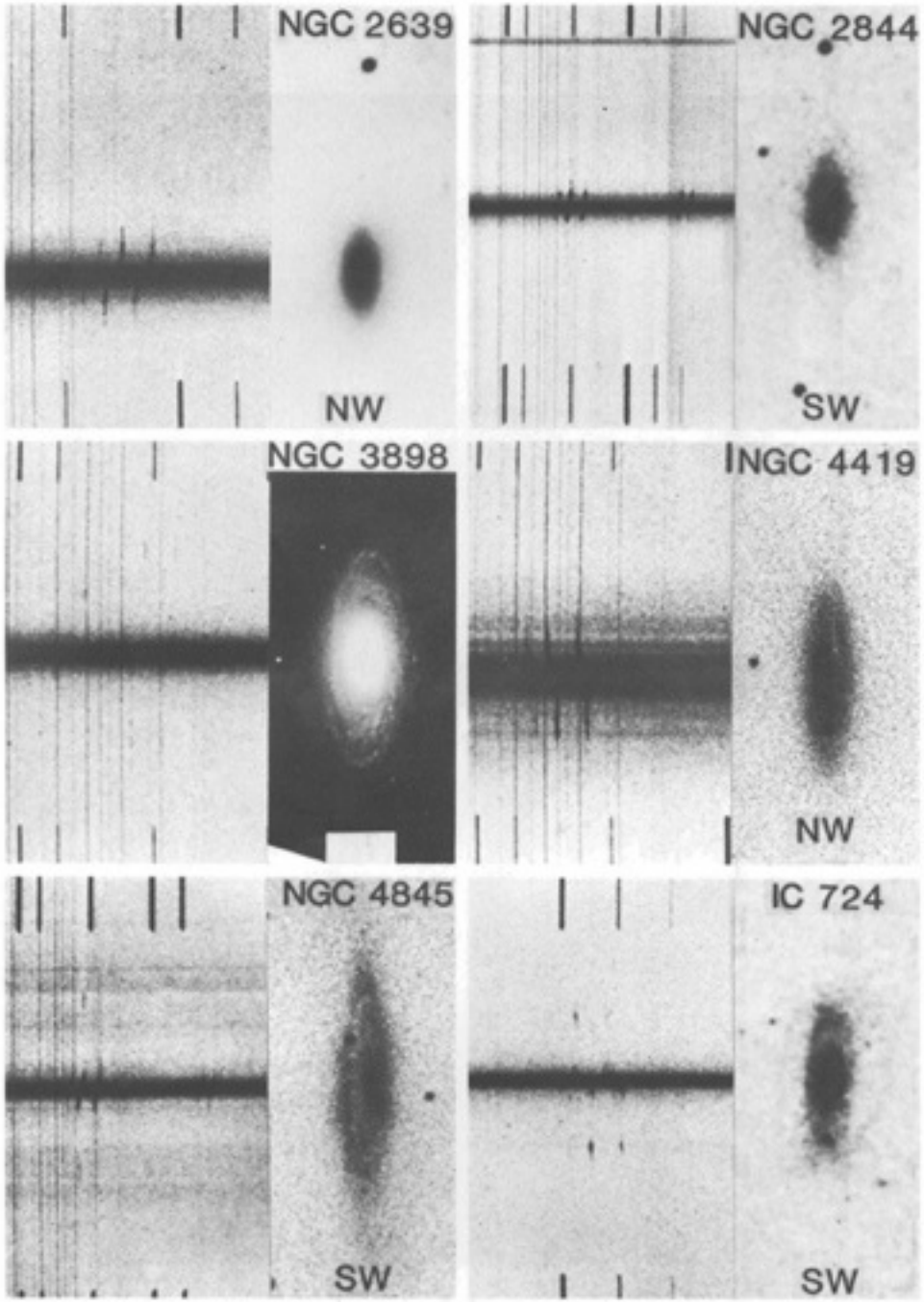
NGC 2639
NW
NGC 2844
SW
NGC 3898
NGC 4419
NW
NGC 4845
SW
IC 724
SW

FIG. 1a

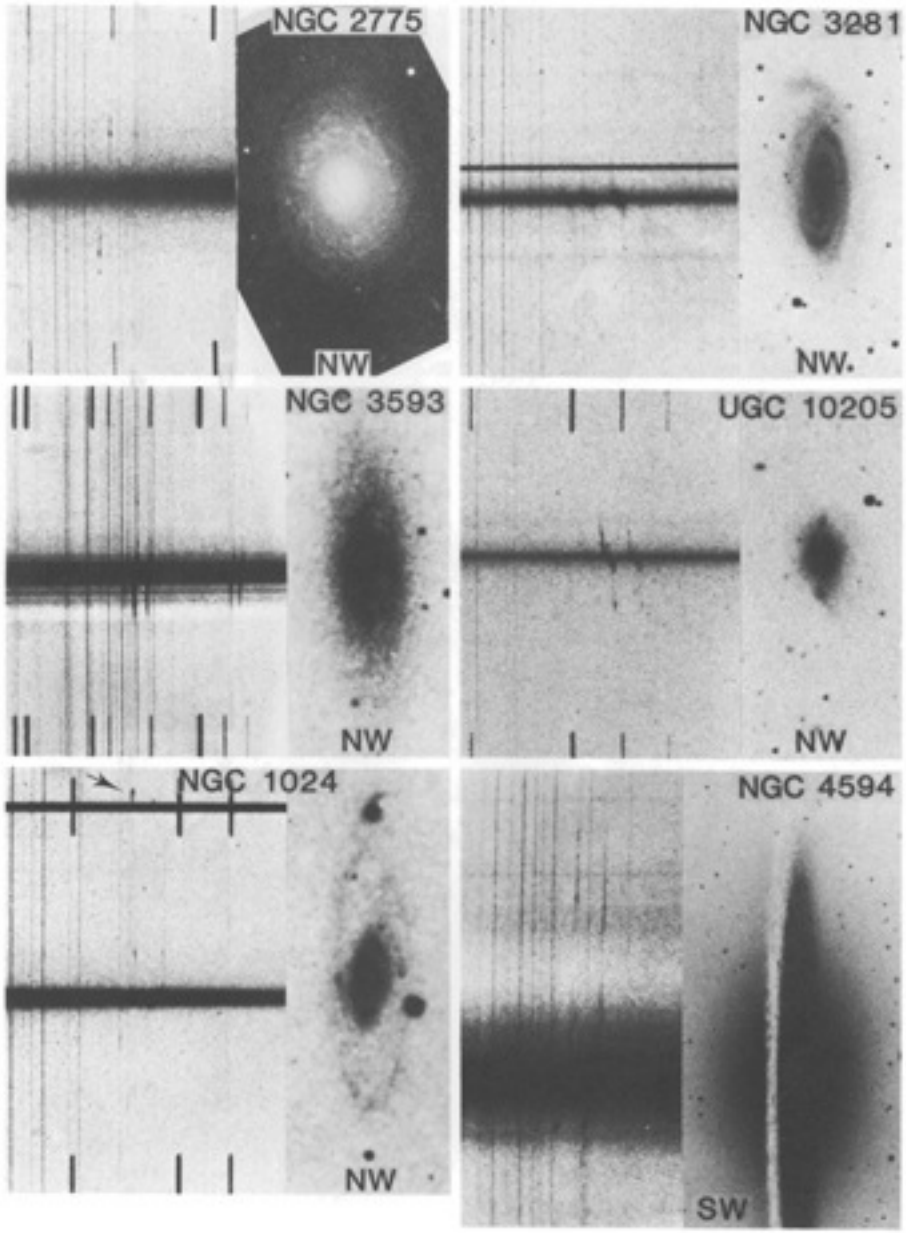
NGC 2775
NW
NGC 3281
NW.
NGC 3593
NW
UGC 10205
NW
NGC 1024
NW
NGC 4594
SW

FIG. 1b

Rotation Curves of Disk Galaxies

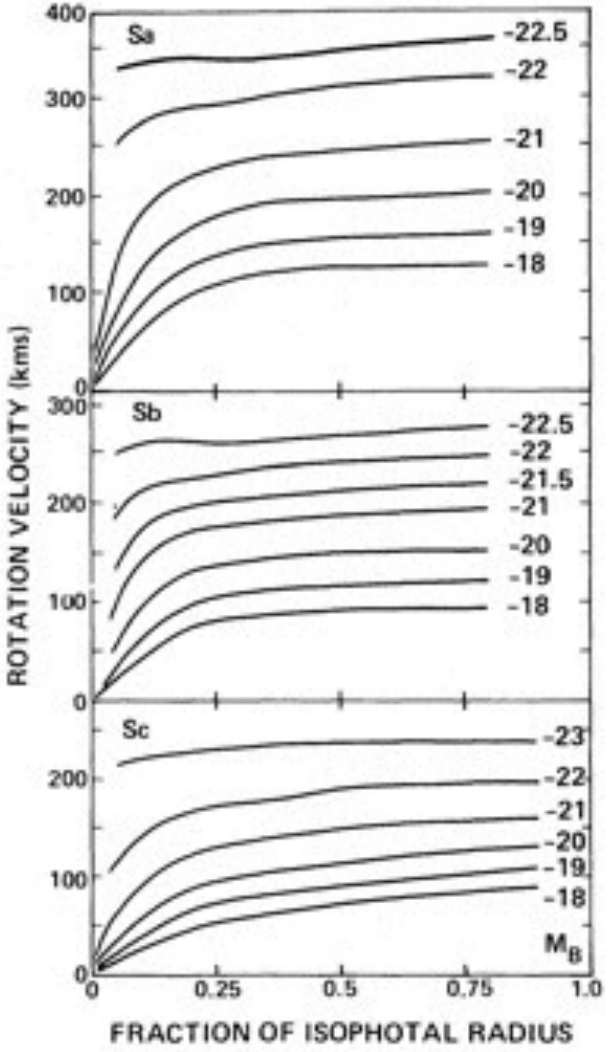

FIG. 4.—Synthetic rotation curves showing average smoothed rotation velocity as a function of fraction of isophotal radius, R_{25}, for (*top*) Sa galaxies of successive luminosities, (*middle*) Sb galaxies, and (*bottom*) Sc galaxies. The procedure for synthesizing these curves is described in Appendix B.

optical galaxy. As we discuss below in connection with $\mathcal{M}/L$ ratios, the nonluminous component must contribute to the overall gravitational potential at all radii. These observations suggest that the forms of the distributions of mass within the more extended halos are similar except for radial and/or density scale factors, independent of the morphology of the optical galaxy.

IV. COMPARATIVE INTEGRATED PROPERTIES OF THE Sa, Sb, AND Sc PROGRAM GALAXIES

In this section, we compare integral properties of Sa, Sb, and Sc galaxies which we have studied. Rotational velocities for the Sa, Sb (Paper II), and Sc (Papers I and III) galaxies are tabulated in Appendix A.

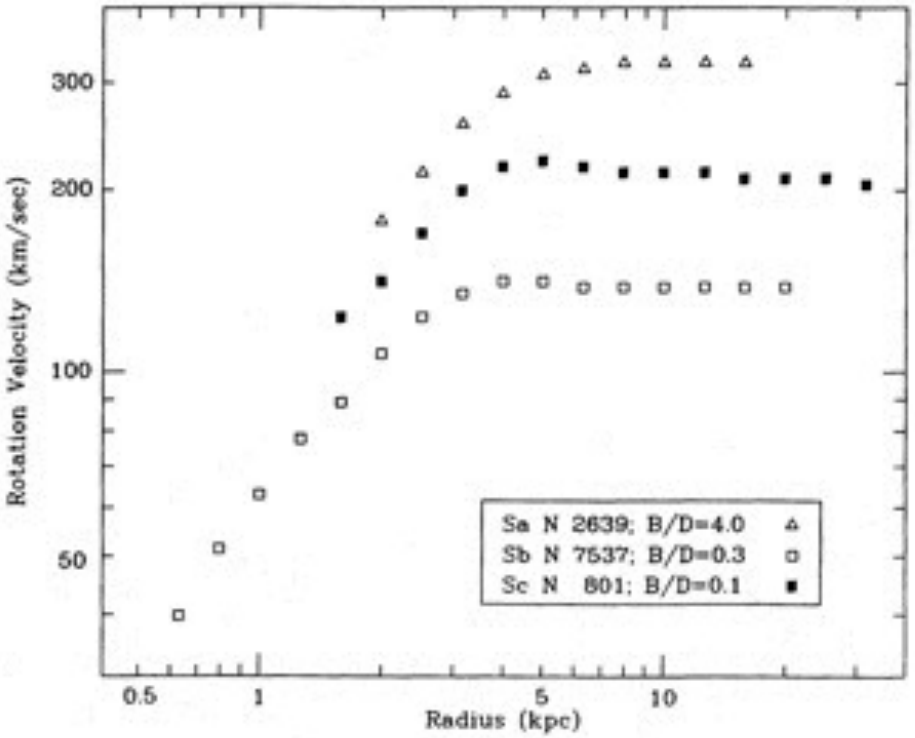

Rubin et al. 1985

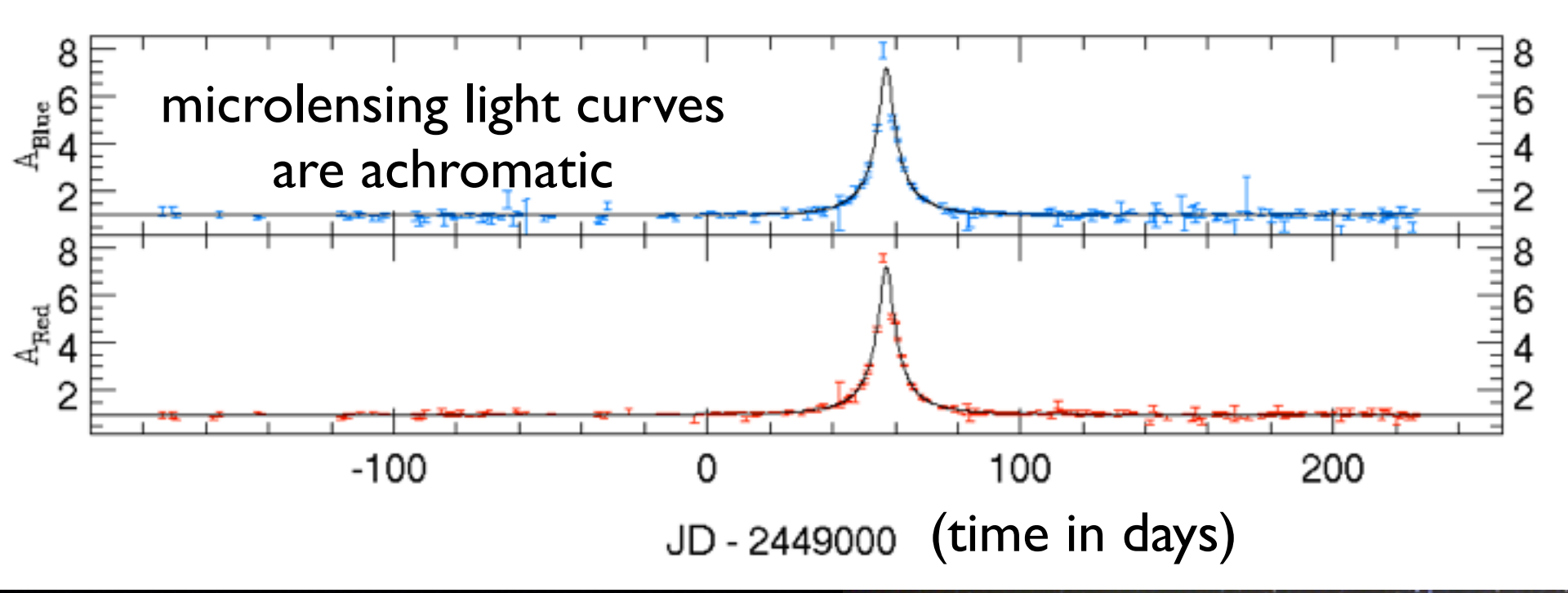

Microlensing surveys stare at dense star fields

Large Magellanic Cloud
(LMC = satellite galaxy of Milky Way)

Galactic Bulge
(of our Milky Way)

Dark Matter Candidates

Alternative to WIMP → MACHO

MACHO = MAssive Compact Halo Object

Try to find MACHOs using gravitational microlensing

I. MACHO survey of Large and Small Magellanic Clouds

II. OGLE = Optical Gravitational Lensing Experiment

III. EROS = Experience de Recherche des Objets Sombres

IV. AGAPE = Andromeda Gravitational Amplification Pixel Experiment

Dark Matter Candidates

WIMP = Weakly Interacting Massive Particle

WIMPs feel gravity

WIMPs might also feel the weak nuclear force
e.g., radioactive decay like ^{14}C into ^{14}N= conversion of neutron into proton
e.g., pp chain in Sun = conversion of proton to neutron
range ~ 10^{-15} cm (incredibly small!)

Are WIMPS "hot" or "cold"?

- "hot" = near light speed = "relativistic"
- low mass
- hot dark matter is known to exist
  e.g., neutrino: non-zero mass < 1 eV
- but hot dark matter doesn't clump to form galaxies

- "cold" ($v << c$) = "non-relativistic"
- high mass (maybe ~100 GeV)
- many cold dark matter particles predicted, none (yet) detected
- nicely clumps to form galaxies

XENON100: The TPC Assembly

- *x10 fiducial mass of XENON10*
- *x100 less back than XENON10*

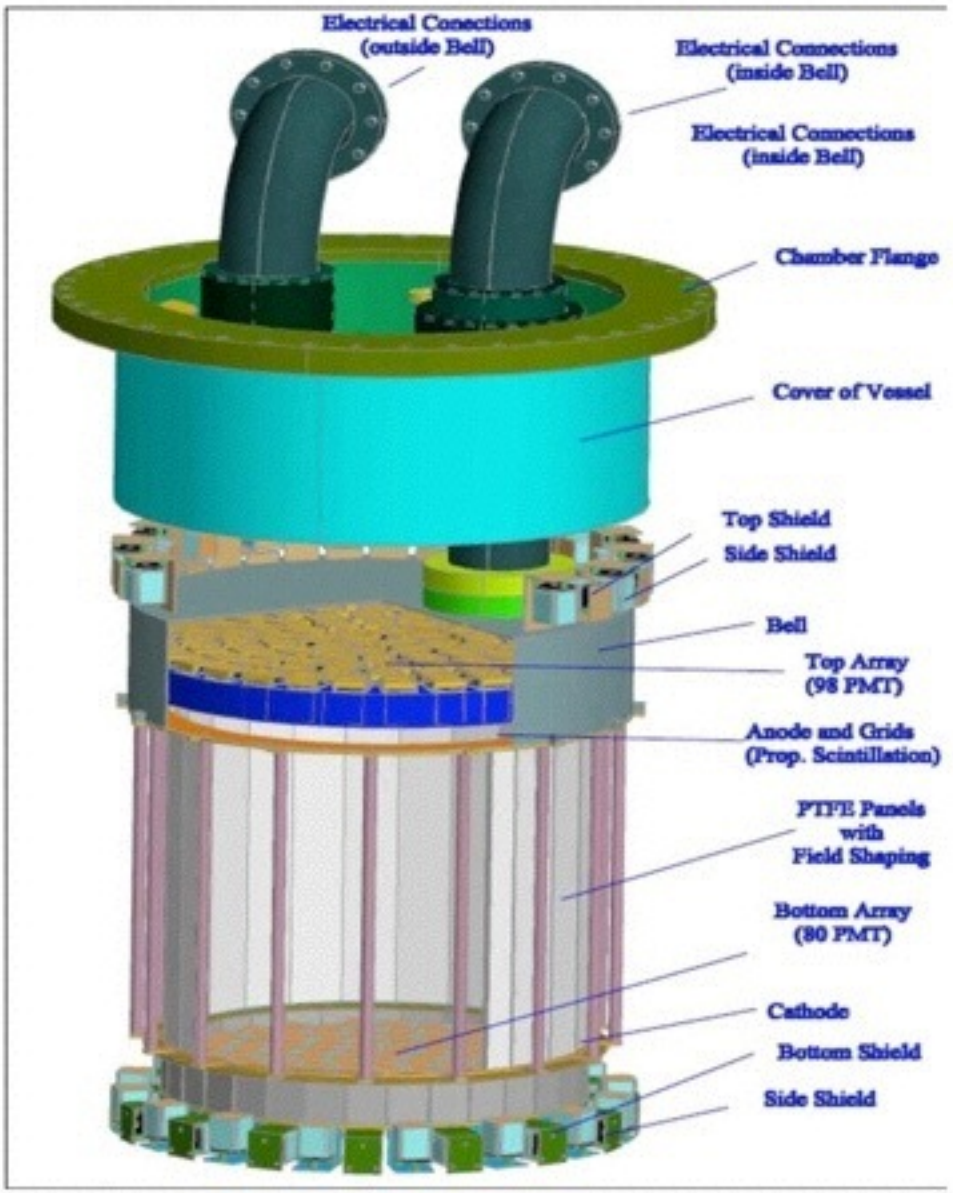

XENON100 @ LNGS

1.4 km of rock (3100 mwe)muon intensity is approximately 1/(m^2 h)

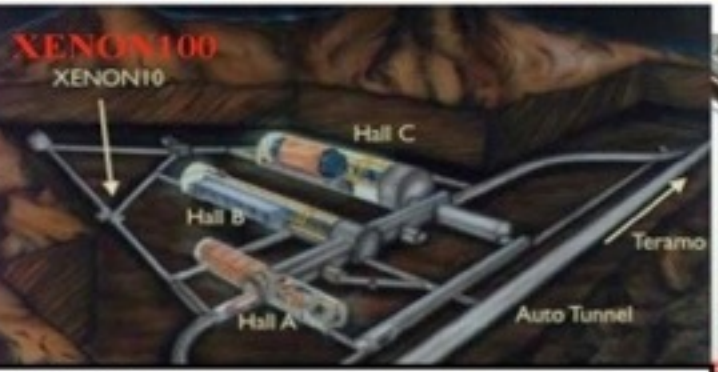

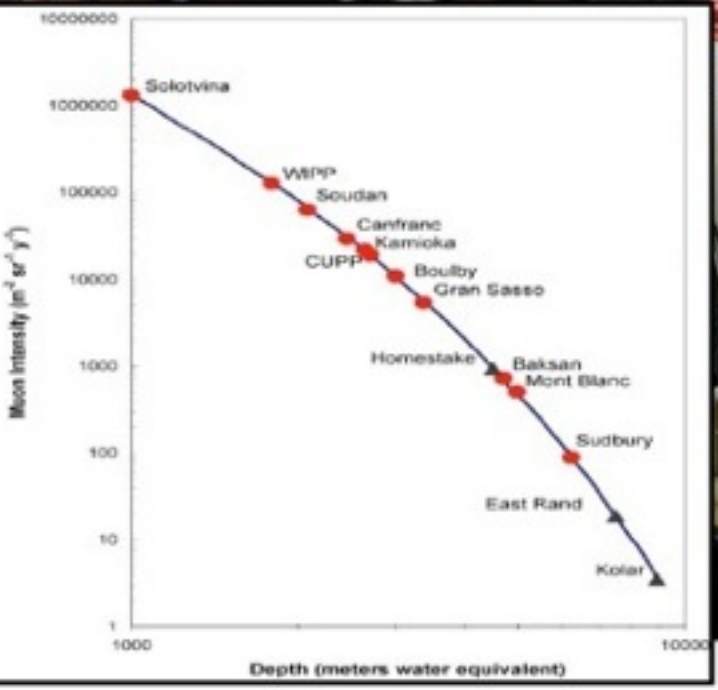


World Wide Experiments for Dark Matter
Direct Detection
YangYang
KIMS
Kamioka
XMASS
Homestake
LUX
SNOLAB
DEAP/CLEAN
PICASSO
Soudan
CDMS
Boulby
ZEPLIN
DRIFT
Frejus/
Modane
EDELWEISS
Canfranc
ArDM
ANAIS
Gran Sasso
CRESST
DAMA/LIBRA
WARP
XENON

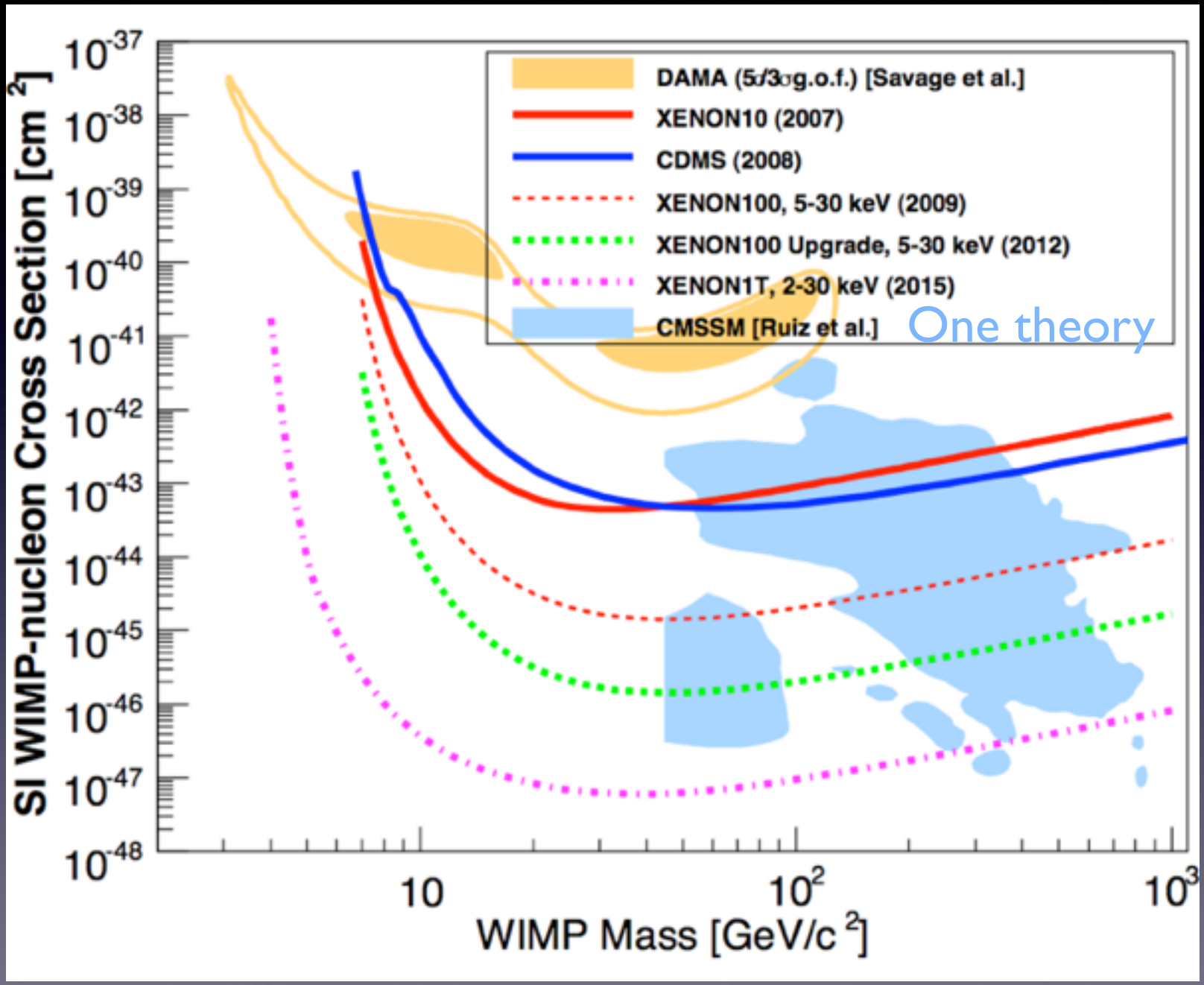
DAMA (5σ/3σg.o.f.) [Savage et al.]
XENON10 (2007)
CDMS (2008)
XENON100, 5-30 keV (2009)
XENON100 Upgrade, 5-30 keV (2012)
XENON1T, 2-30 keV (2015)
CMSSM [Ruiz et al.]
One theory
SI WIMP-nucleon Cross Section [cm²]
WIMP Mass [GeV/c²]
10⁻³⁷
10⁻³⁸
10⁻³⁹
10⁻⁴⁰
10⁻⁴¹
10⁻⁴²
10⁻⁴³
10⁻⁴⁴
10⁻⁴⁵
10⁻⁴⁶
10⁻⁴⁷
10⁻⁴⁸
10
10²
10³

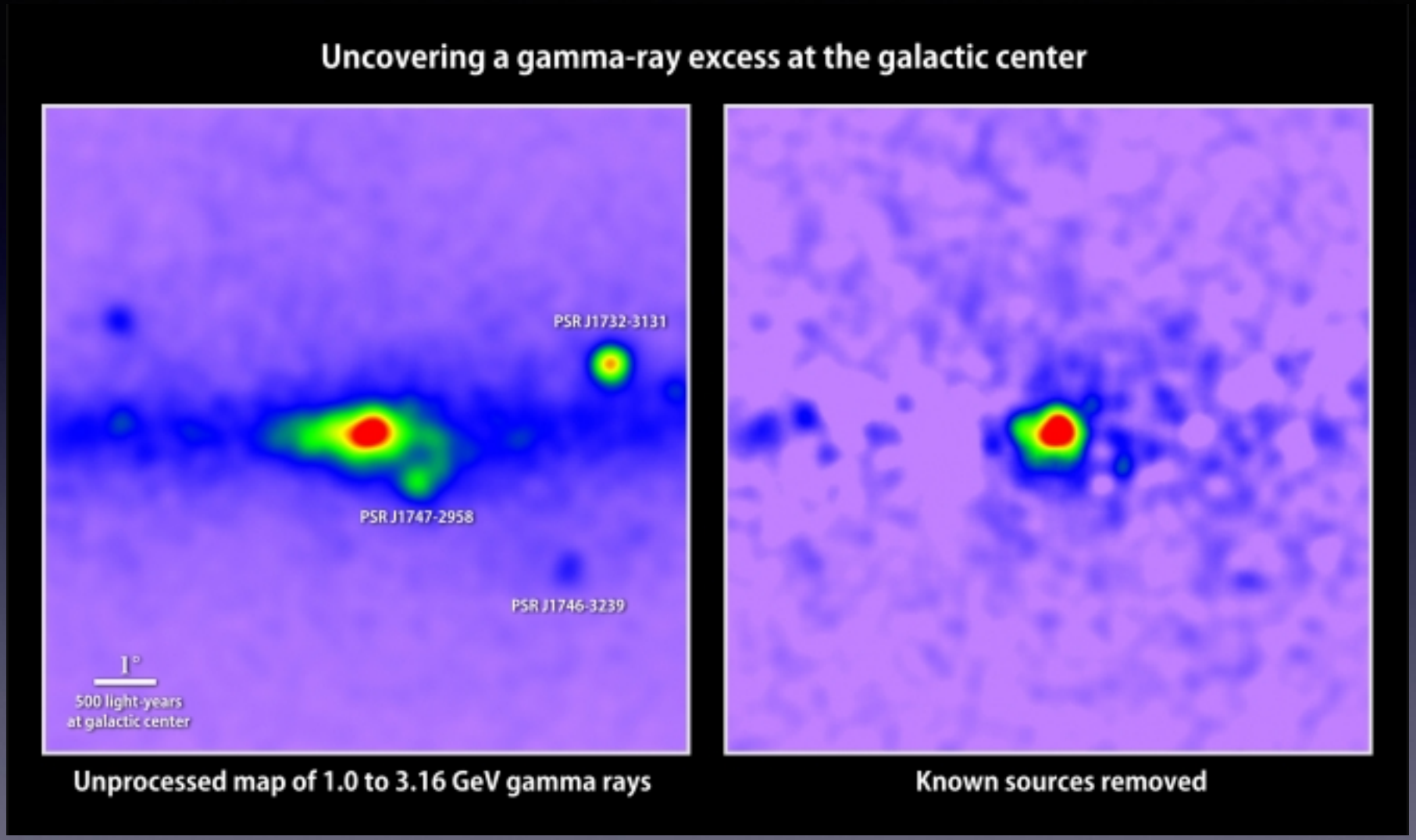

Possible “dark matter self-annihilation signal”

Type Ia supernova as standard candle

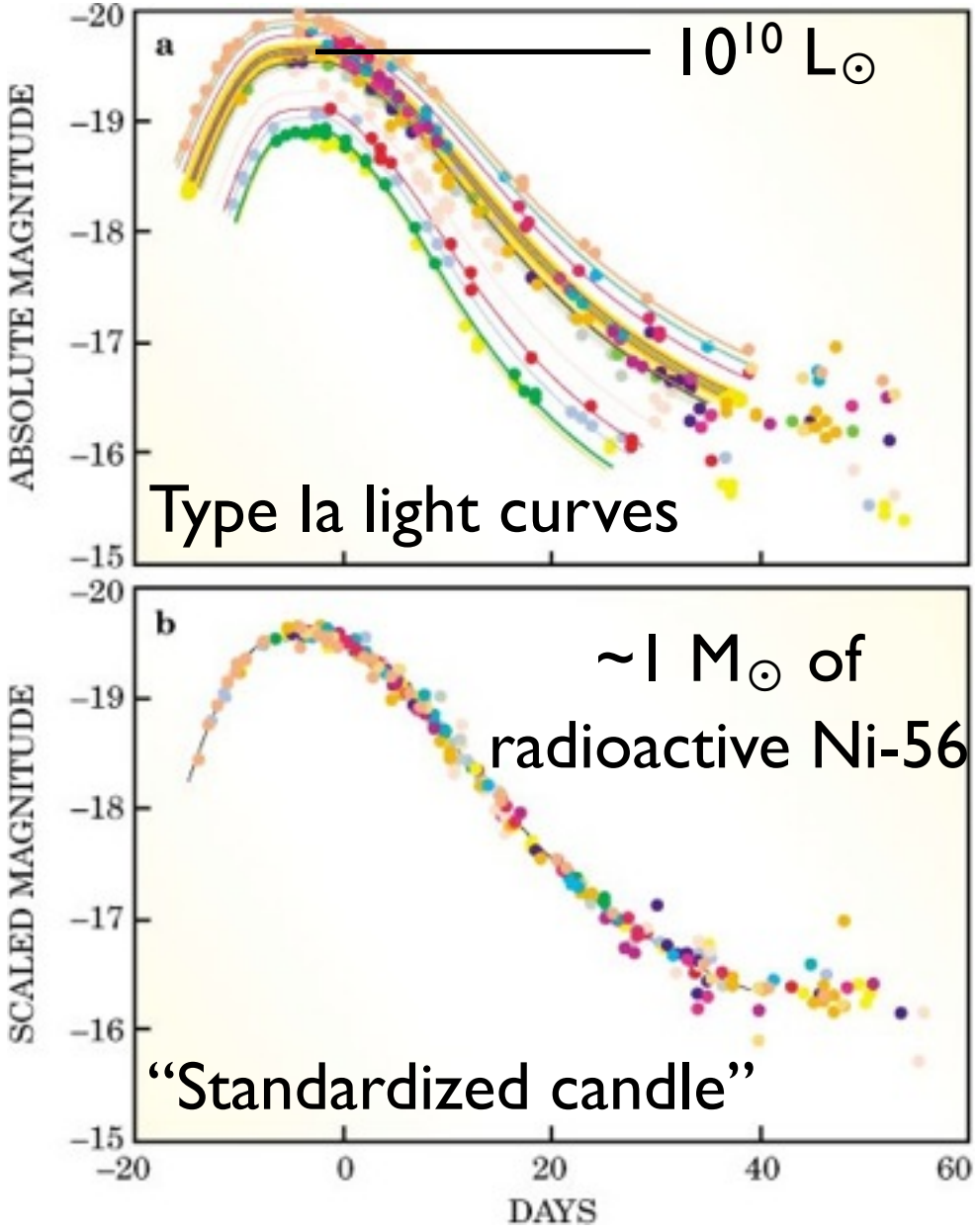

Type Ia Supernova: "Double Degenerate" Progenitor

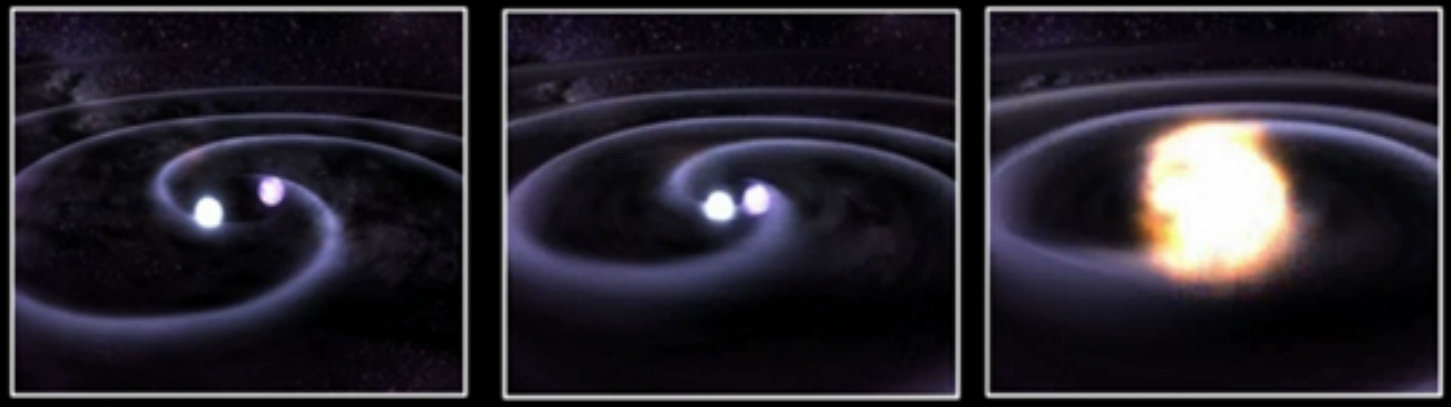

Two white dwarfs merging: C, O fuses to Si fuses to Ni

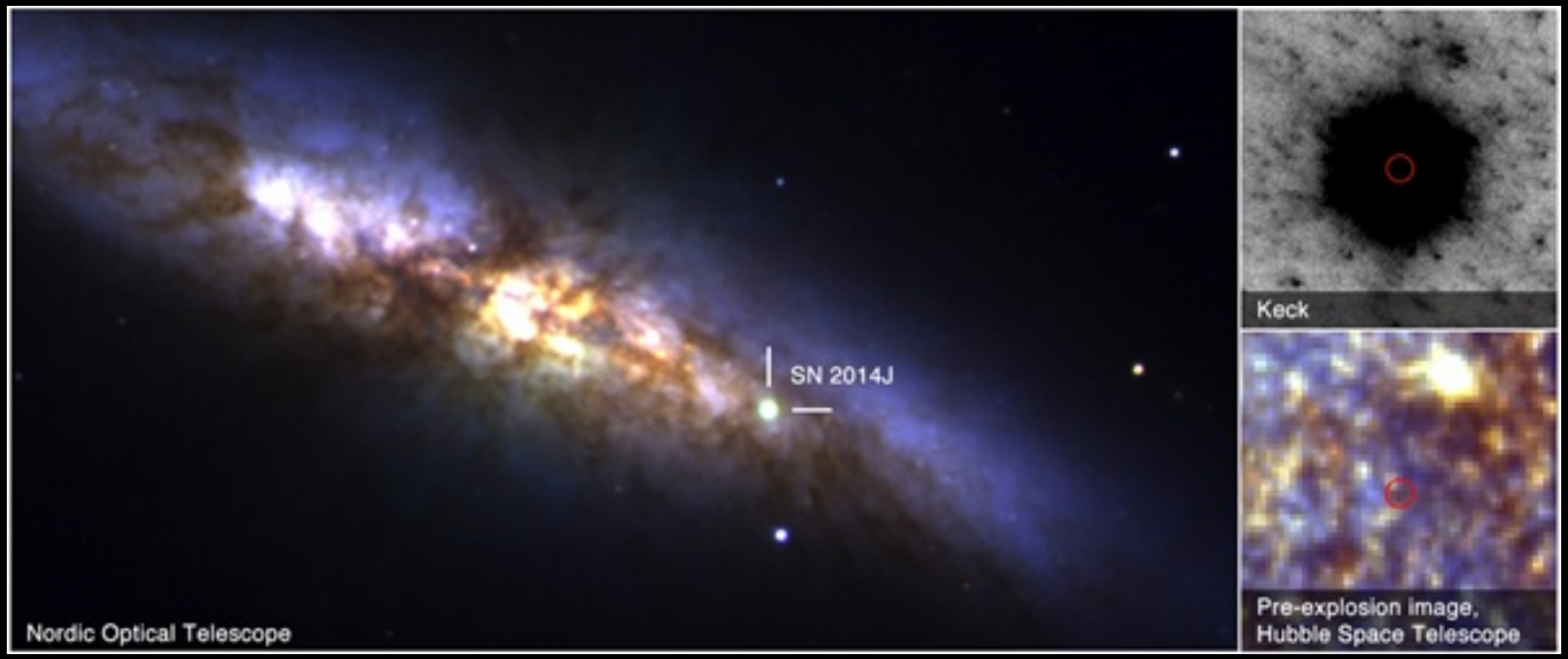

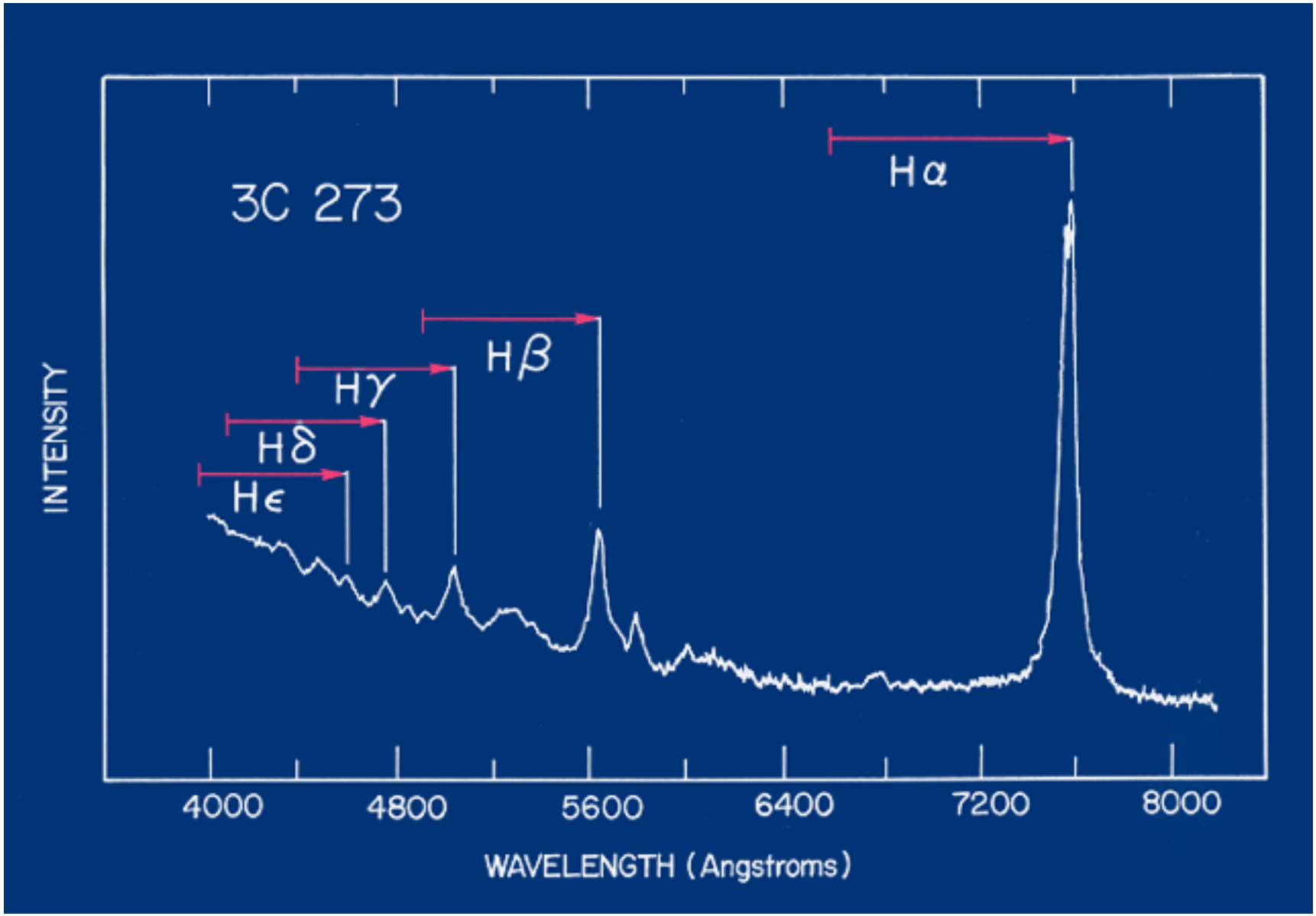

Redshift ⇒ galaxy is receding from us

Hubble's Original Data

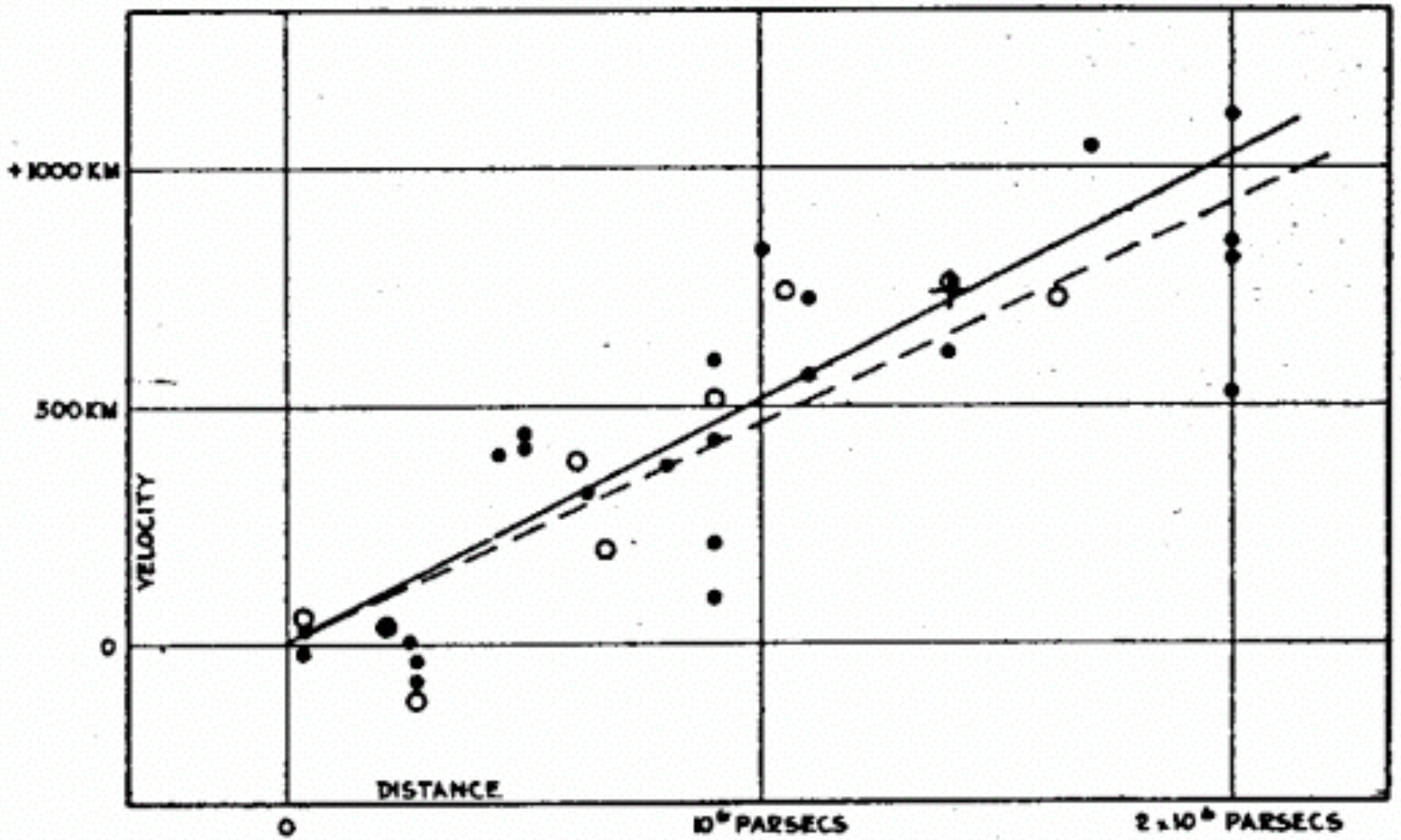

FIGURE 1

local universe = “low-redshift universe” = “low-z”

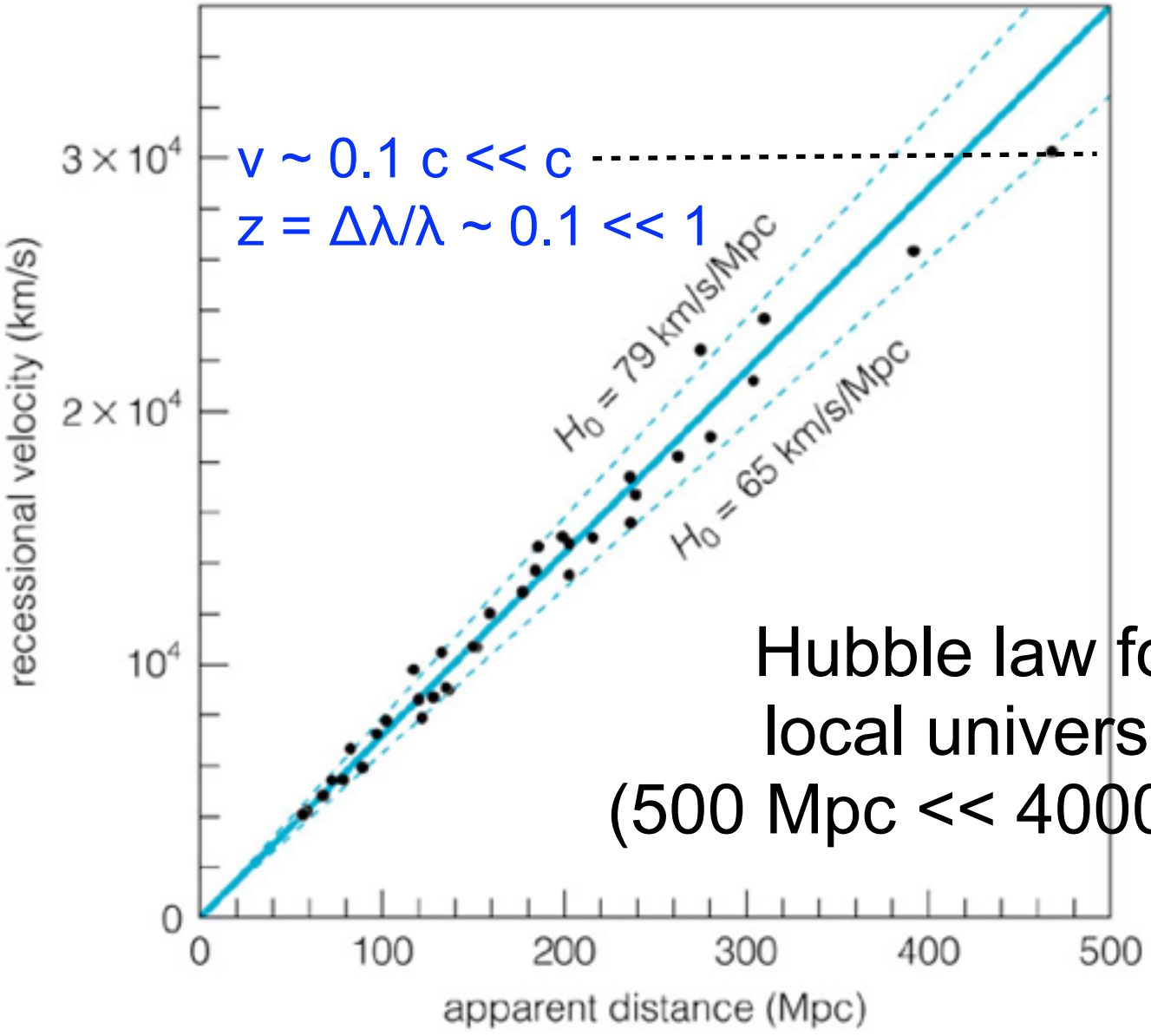

Hubble law for
local universe
(500 Mpc << 4000 Mpc)

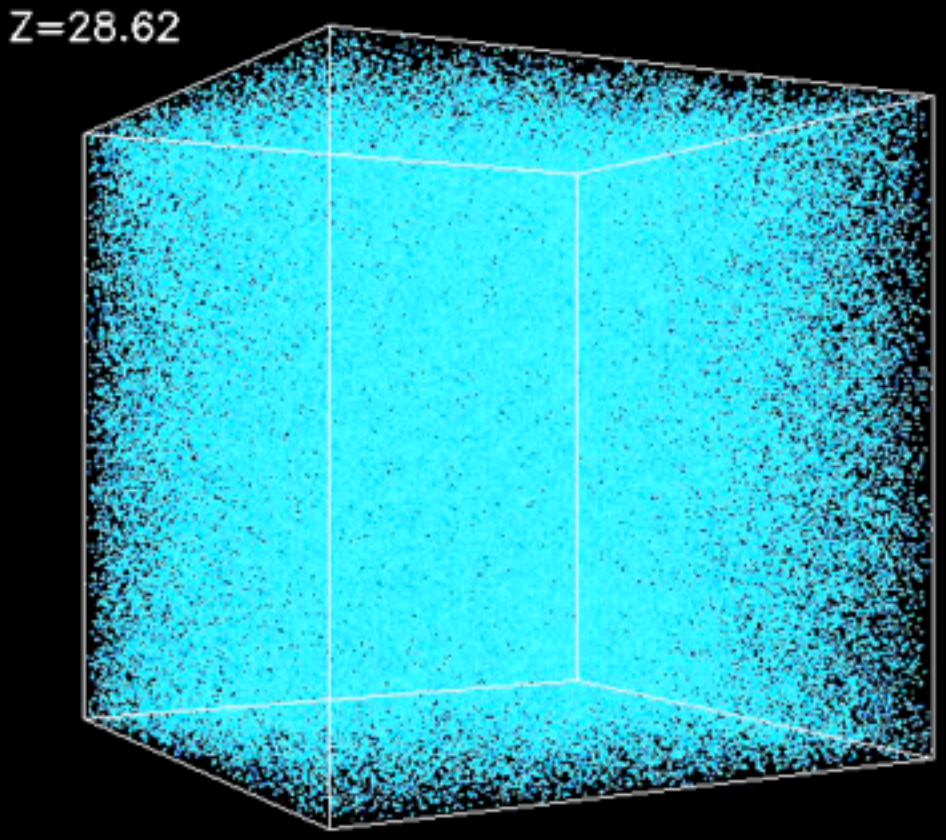
Z=28.62

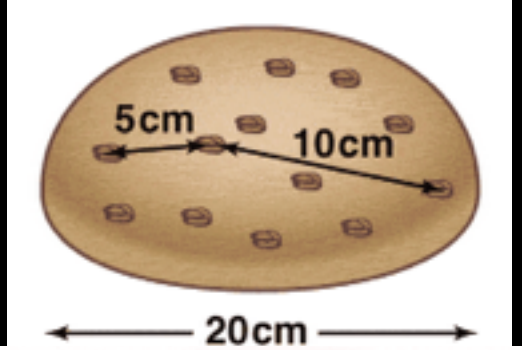
5cm
10cm
20cm

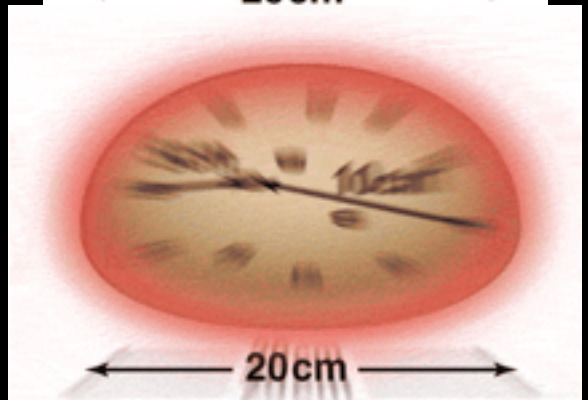
20cm

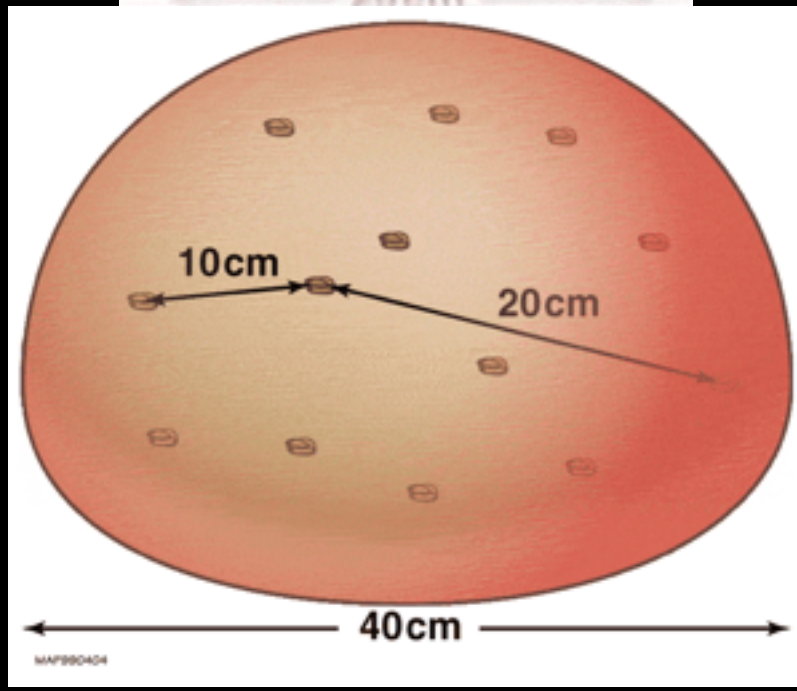
10cm
20cm
40cm

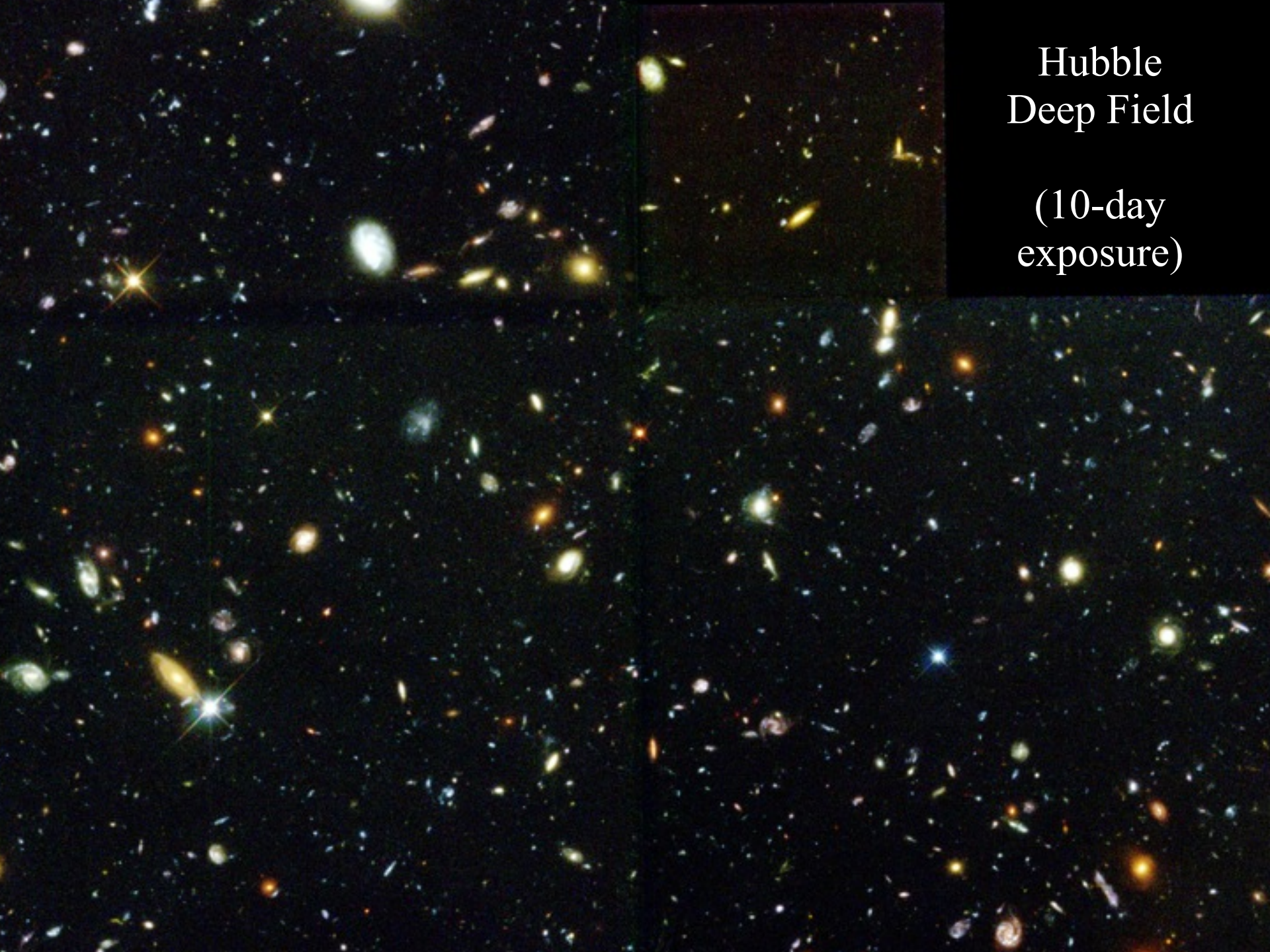
Hubble
Deep Field
(10-day
exposure)

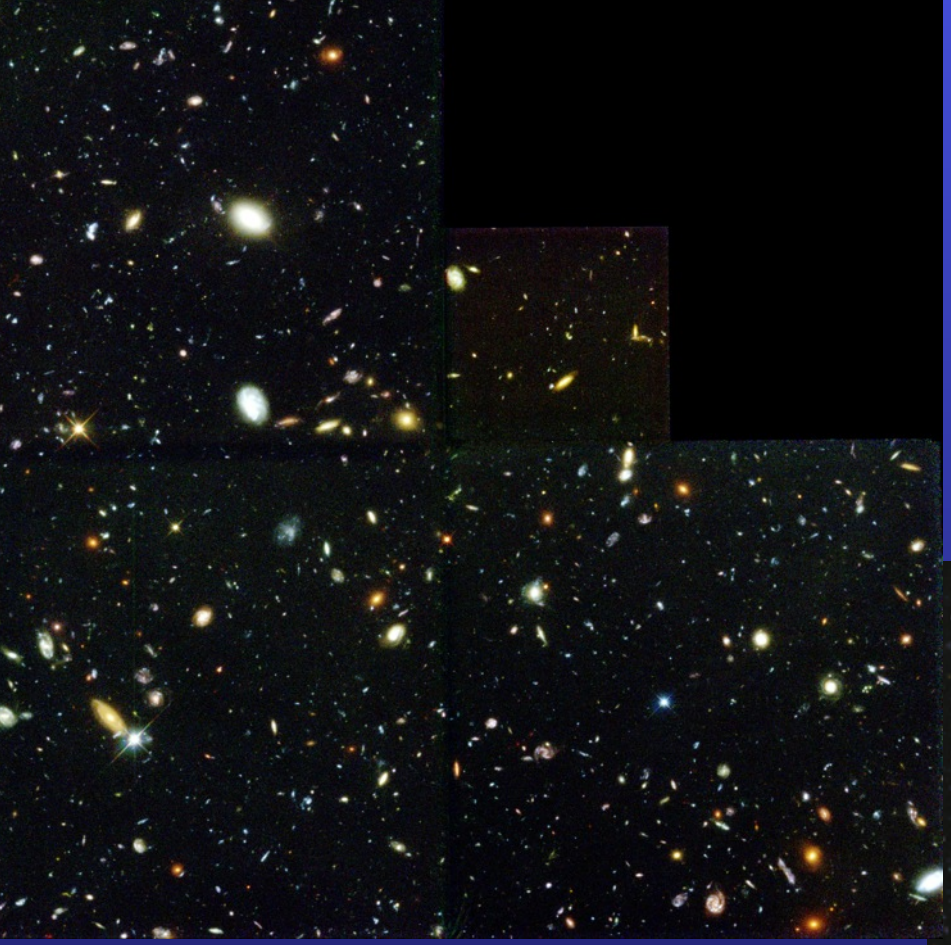

Hubble
eXtreme
Deep Field

(23-day
exposure)

Hubble
Deep Field

(10-day
exposure)

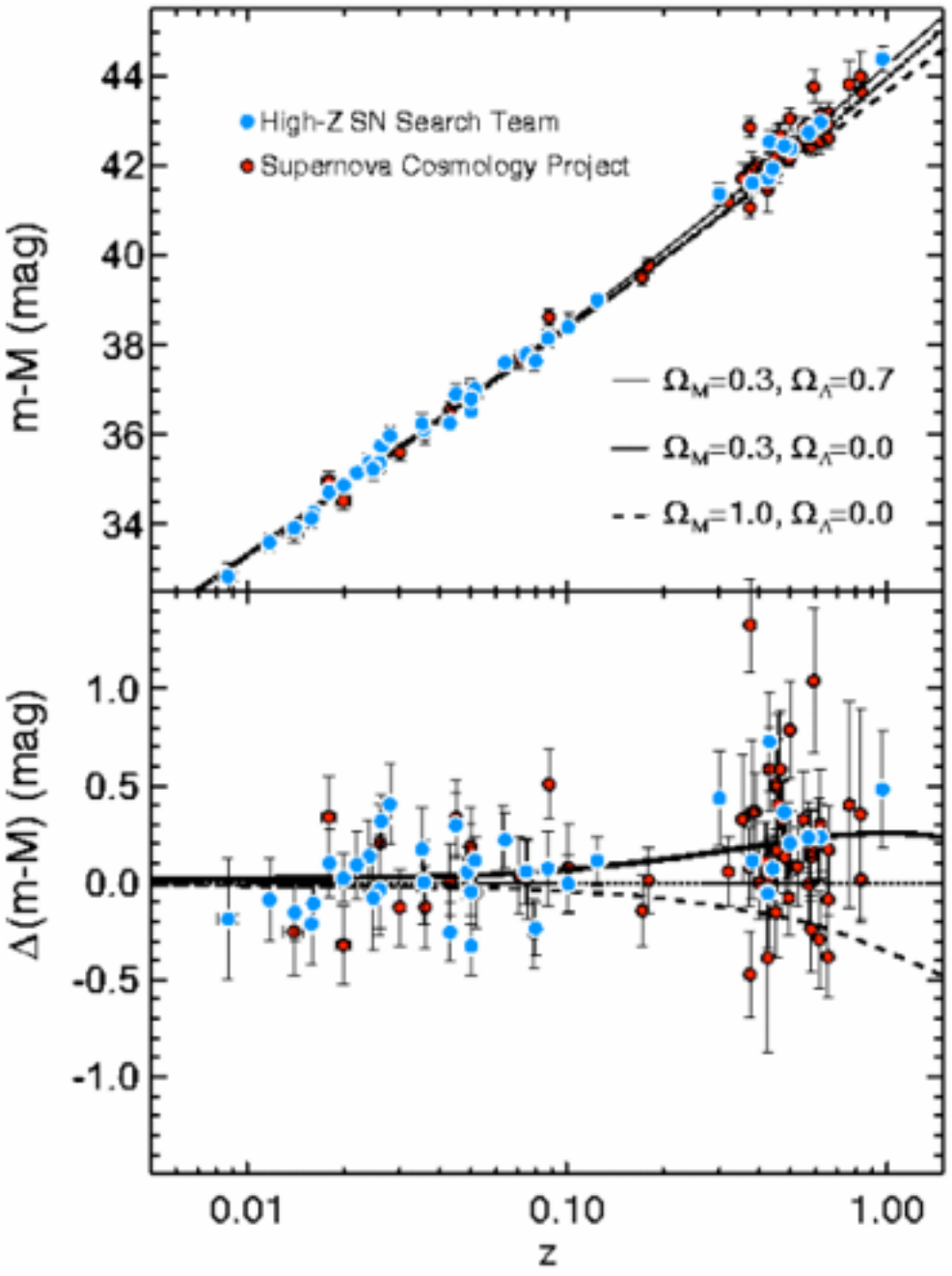

magnitude-redshift relation (a.k.a. generalized Hubble law) shows evidence for positively accelerating universe (old models were typically decelerating)

Evidence for Dark Matter $\Omega_m = 0.26$

Many of the brighter emission regions in M31 are large, complex associations of emission regions and OB stars. However, there are also completely isolated Strömgren spheres. In an effort to obtain spectra from all parts of M31, we have generally observed no more than two regions within a single association, and have observed some of the isolated regions. In Table 1, column (9), we have classified the observed regions according to their membership in the M31 OB associations as defined by van den Bergh (1964). Fourteen of the regions we have observed are not in OB associations; the remaining fifty-three regions are distributed in thirty-four associations. Seventeen associations have velocities from two or more regions; for all association members the average deviation from the mean association velocity is 10 km sec^{-1}, or just equal to the average internal error in the radial velocity of an emission region. We conclude that the line-of-sight component of the velocity dispersion within an association is less than ± 10 km sec^{-1}, or less than 15 km sec^{-1} projected to a circular-velocity component in the plane of M31.

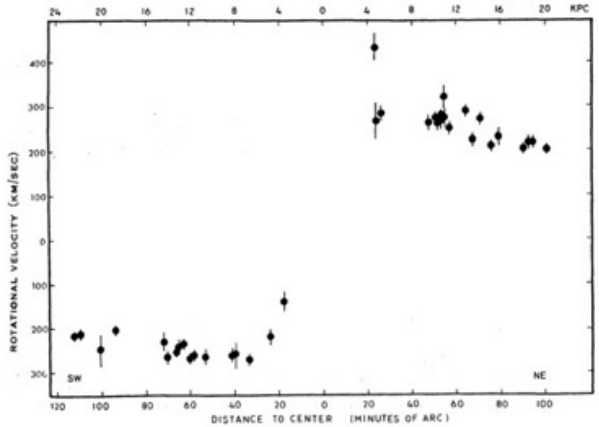

FIG. 4.—Mean rotation velocities for thirty-four OB associations plus three outer regions in M31, as a function of distance from the center. Error bars indicate average error of the velocity of the association, calculated from the velocities of individual emission regions in the association, or from the observational errors, whichever are larger.

Flat Rotation Curves of Individual Galaxies

Gravitational Lensing + Fast Galaxies (1000 km/s) in Galaxy Clusters

Hot Gas in Galaxy Haloes and Galaxy Clusters

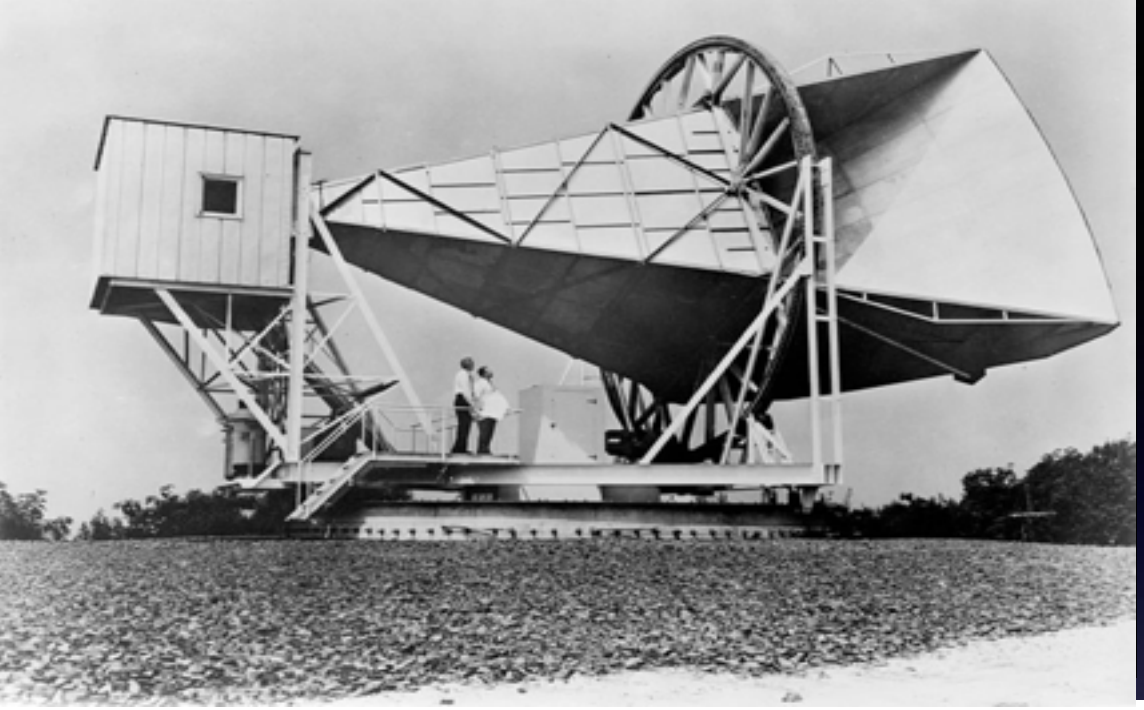

Holmdel
Horn Antenna
(Bell Labs)
7.35 cm wavelength
Penzias & Wilson
1960s

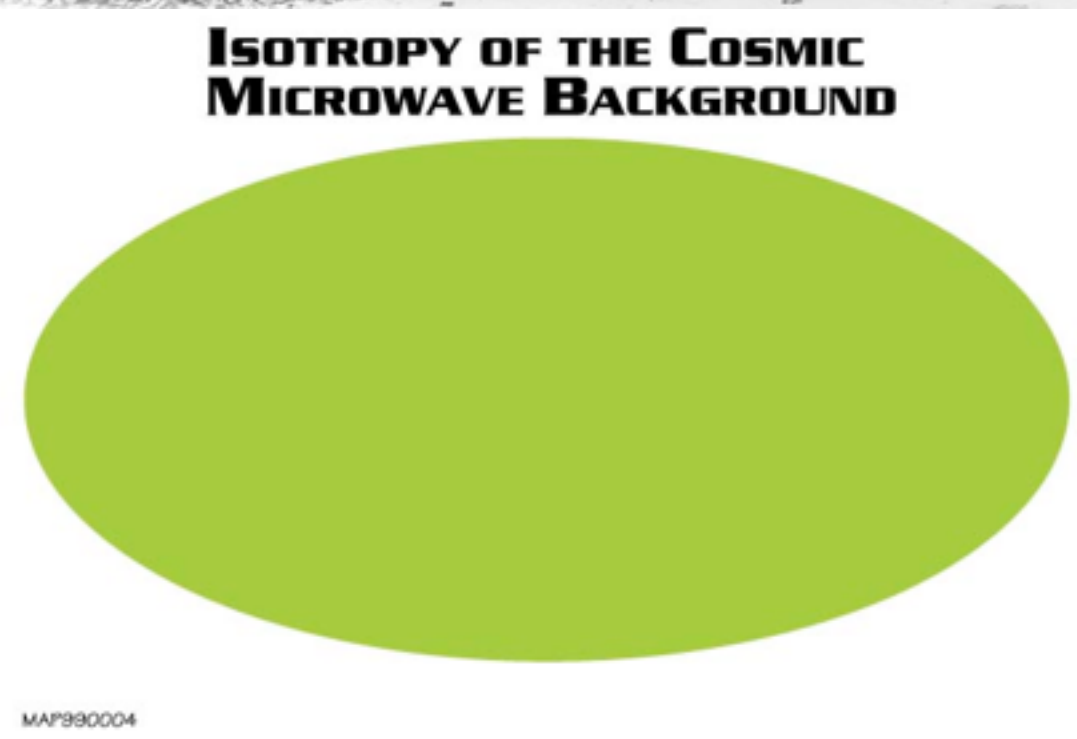

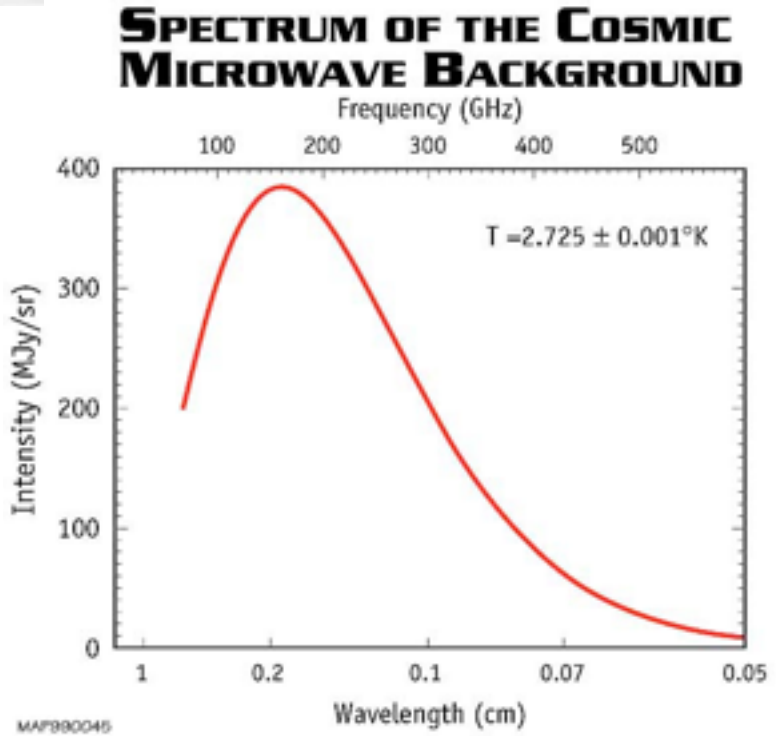

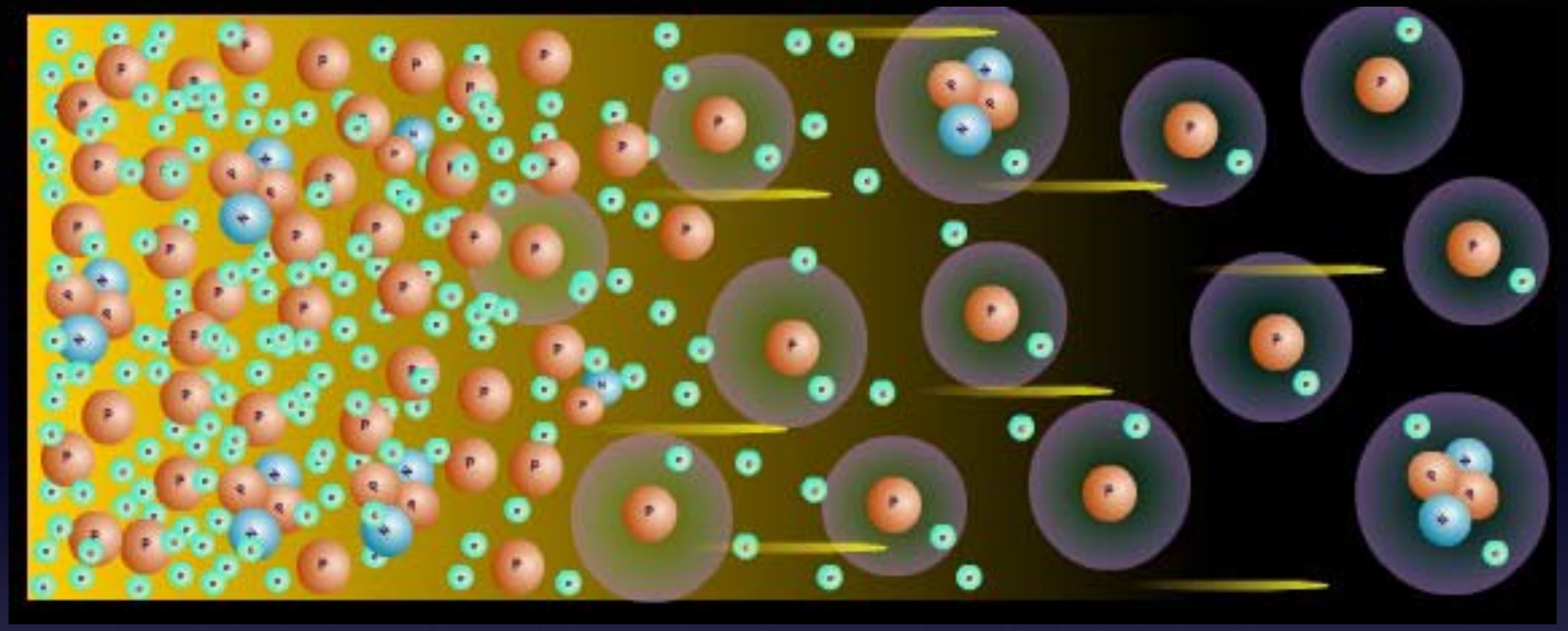

Isotropy of the Cosmic Microwave Background

MAP990004

Peter H. Dana 9/20/94

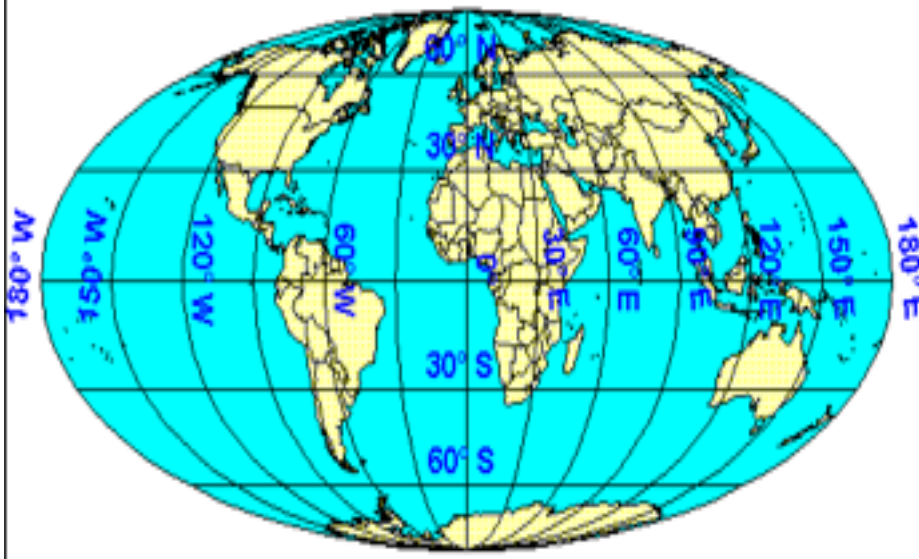

Mollweide Equal-Area

Isotropy of the Cosmic Microwave Background

MAP990004

Spectrum of the Cosmic Microwave Background

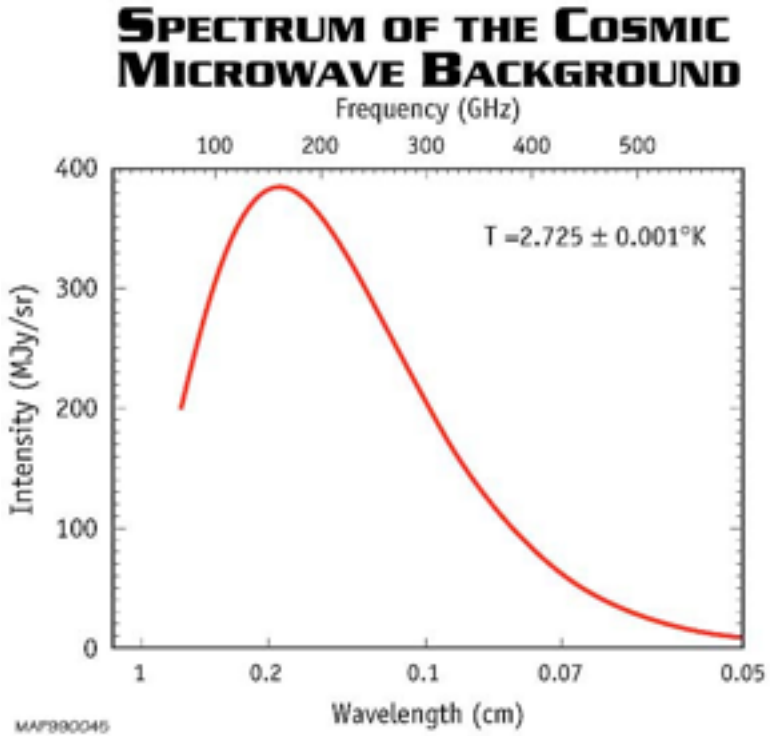

MAP990045

red = 2.726 K blue = 2.724 K

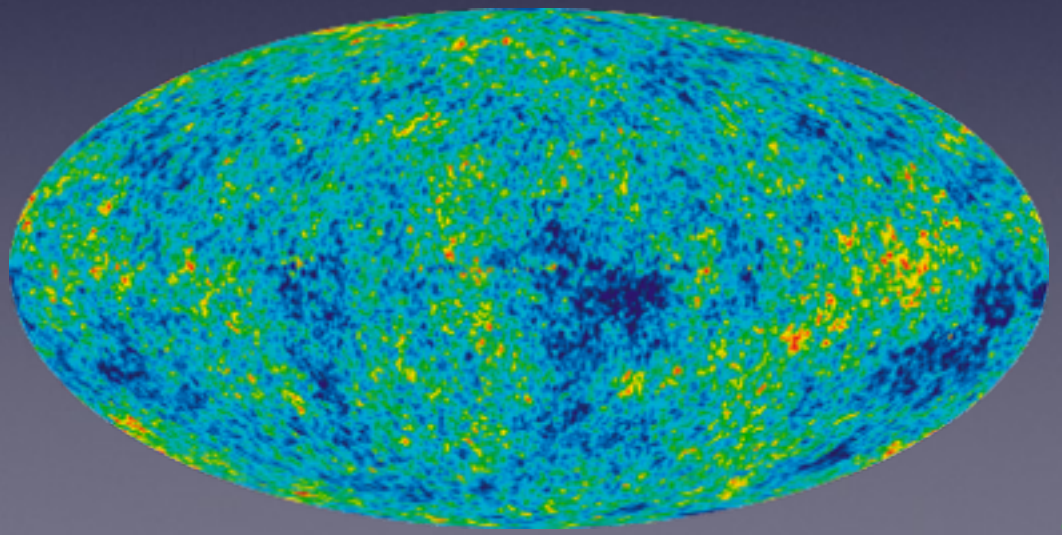

CMB temperature fluctuations
= photons redshifted and blueshifted
by dark matter clumps and voids
at time of recombination

Angular size of dark matter clumps ~ 1°
= horizon size at time of recombination

Clumps originate from
quantum fluctuations in the
inflation energy field,
grown to cosmic proportions by inflation

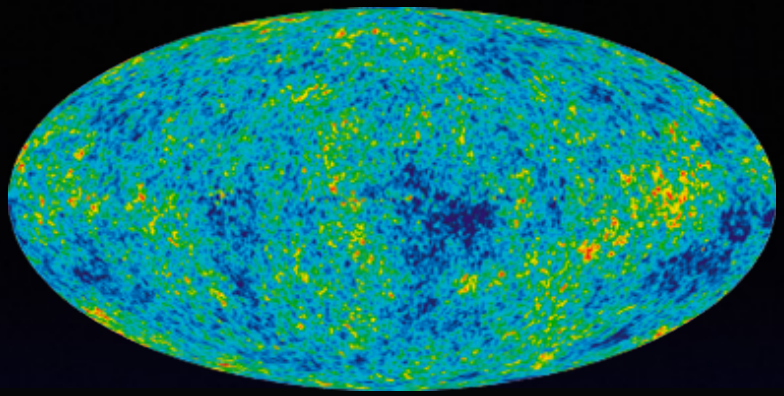

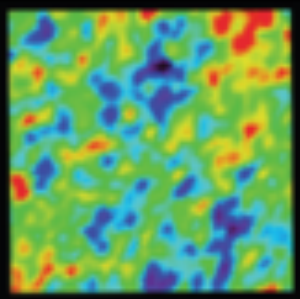

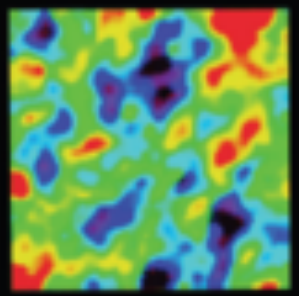

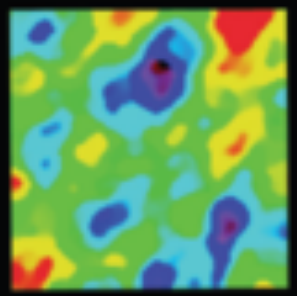

The physical size of the fluctuations is the horizon size at the last scattering surface.

The Consensus Model

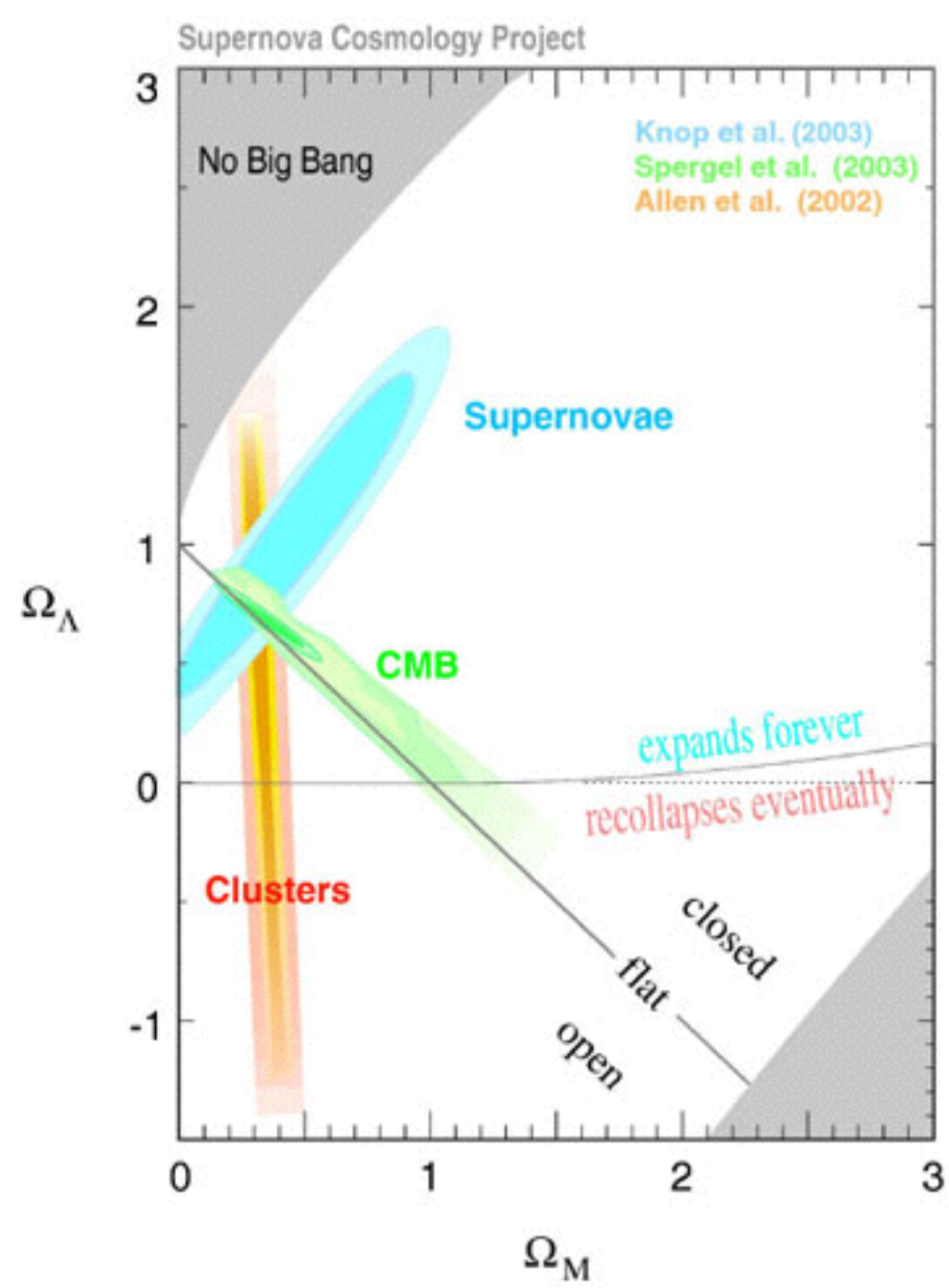

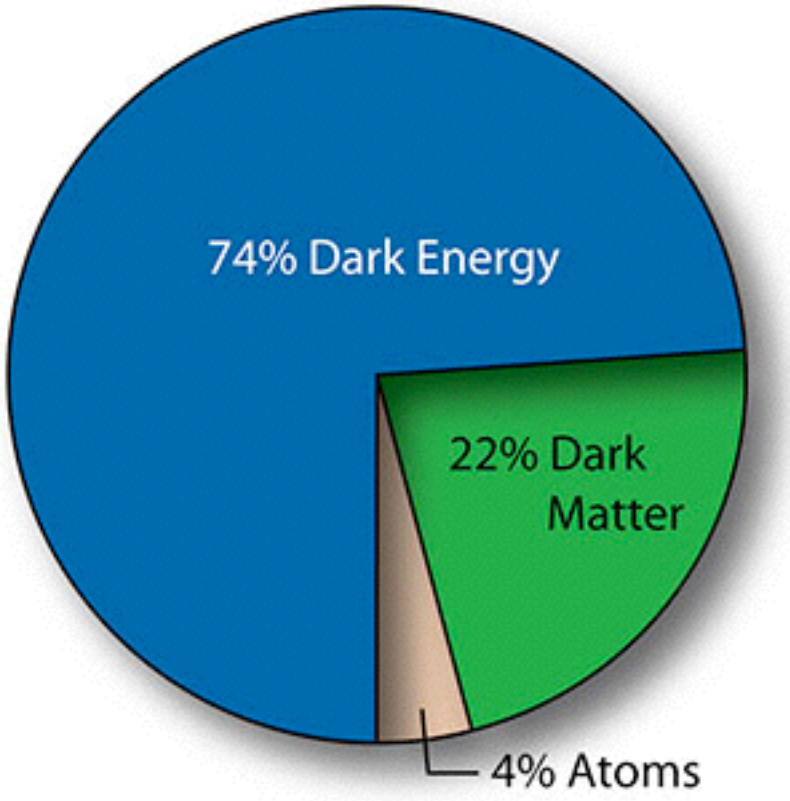

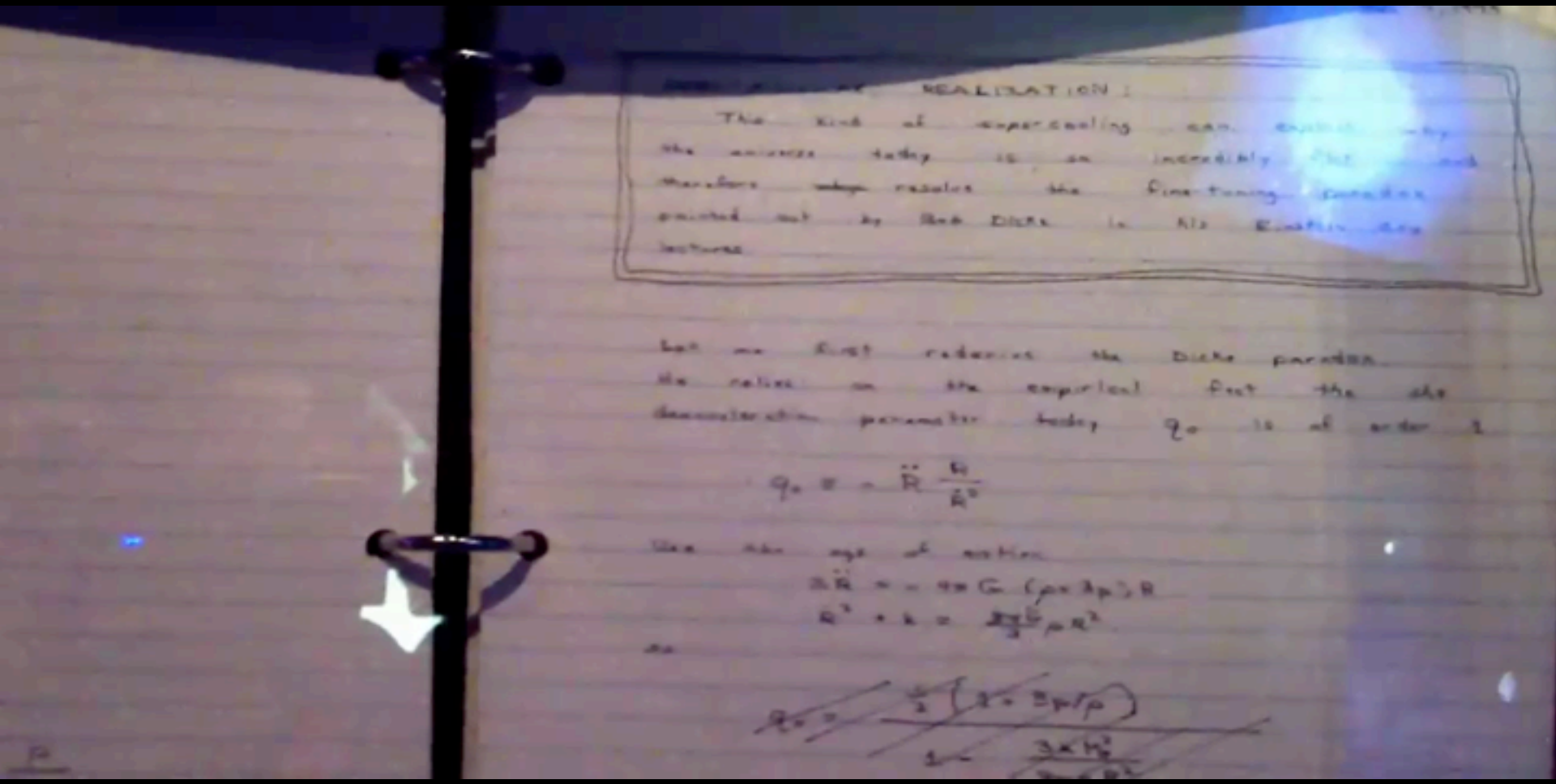

Permanent collection of the Adler Museum (Chicago)

"So, after a few of the most productive hours I had ever spent at my desk, I had learned something remarkable. Would the supercooled phase transition affect the expansion rate of the universe? By 1:00 a.m. I knew the answer: Yes, more than I could have ever imagined."

Supercooled water

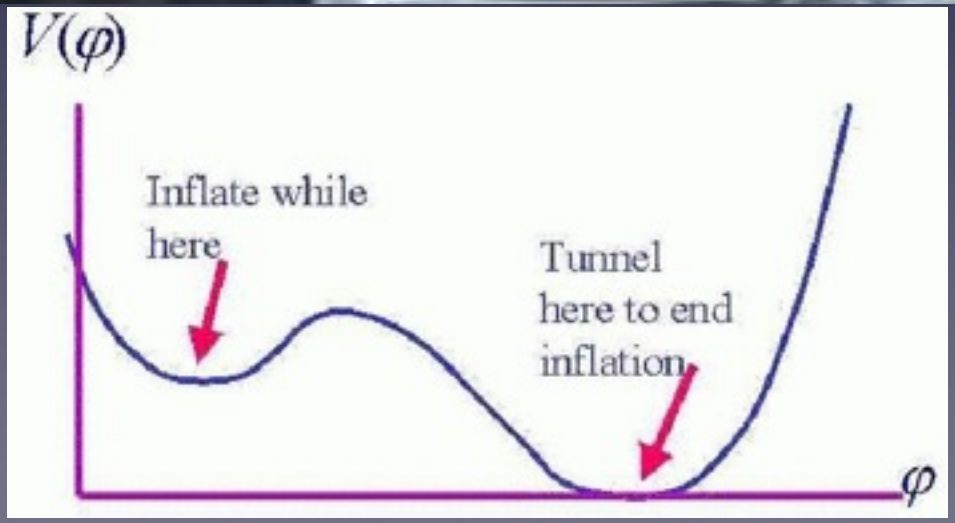

“World’s Messiest Office”
Boston Globe Winner 2005

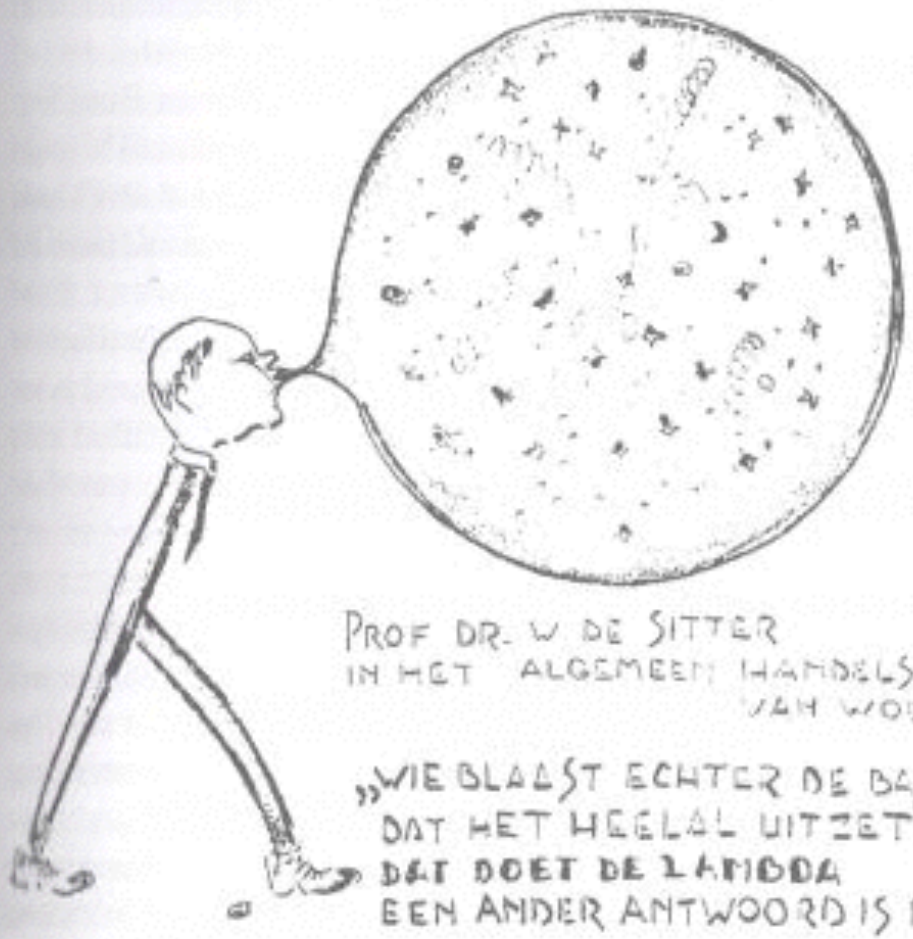

The quote is translated by van der Laan as: "What, however, blows up the ball? What makes the universe expand or swell up? That is done by the Lambda. Another answer cannot be given."

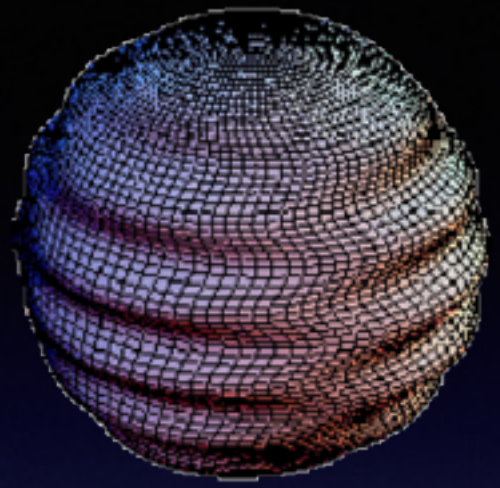

Quantum fluctuations in the gravitational field grow to cosmic proportions during inflation

⇒ Cosmic-scale gravitational waves

Gravitational waves polarize CMB photons

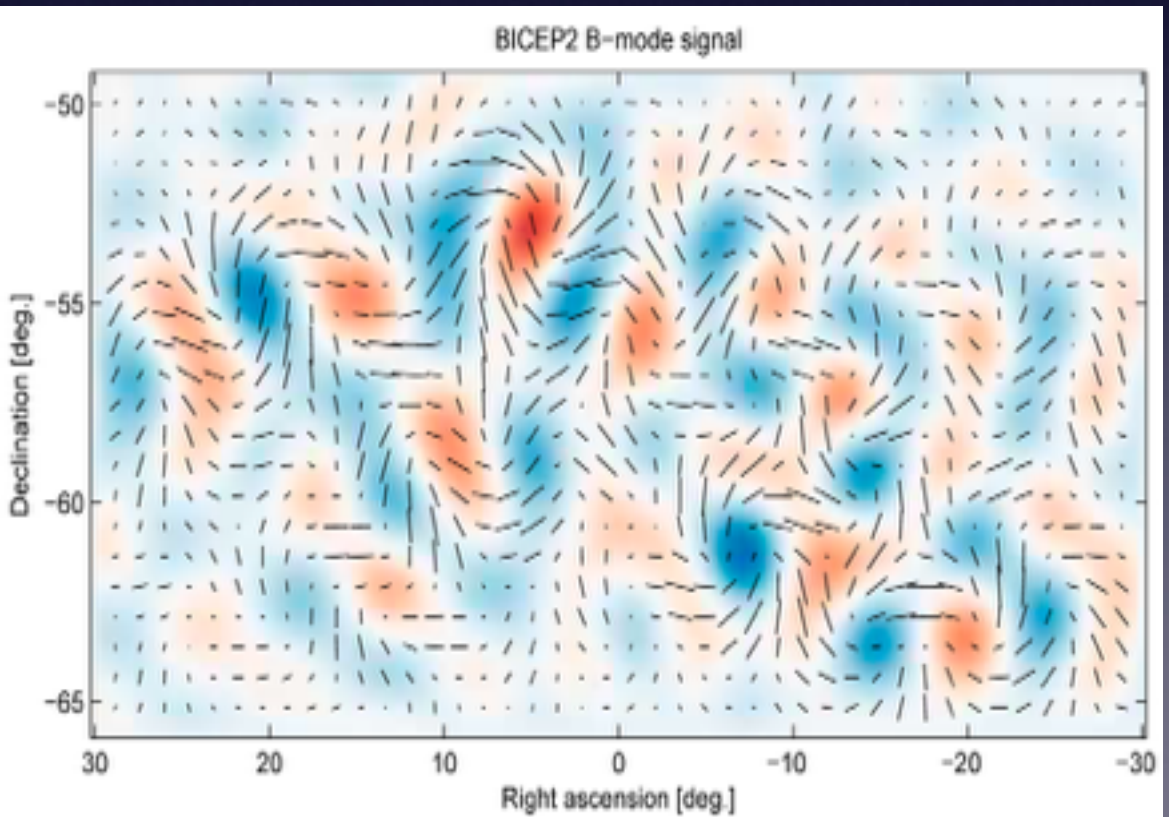

Strength of polarization directly measures

$u_{inflation}$

and by extension

$E_{inflation} \propto (u_{inflation})^{1/4}$

Observed polarization is consistent with

$E_{inflation} \sim E_{GUT} \sim 10^{12}$ TeV

and

$t_{inflation} \sim 10^{-36}$ s

Big Bang Nucleosynthesis

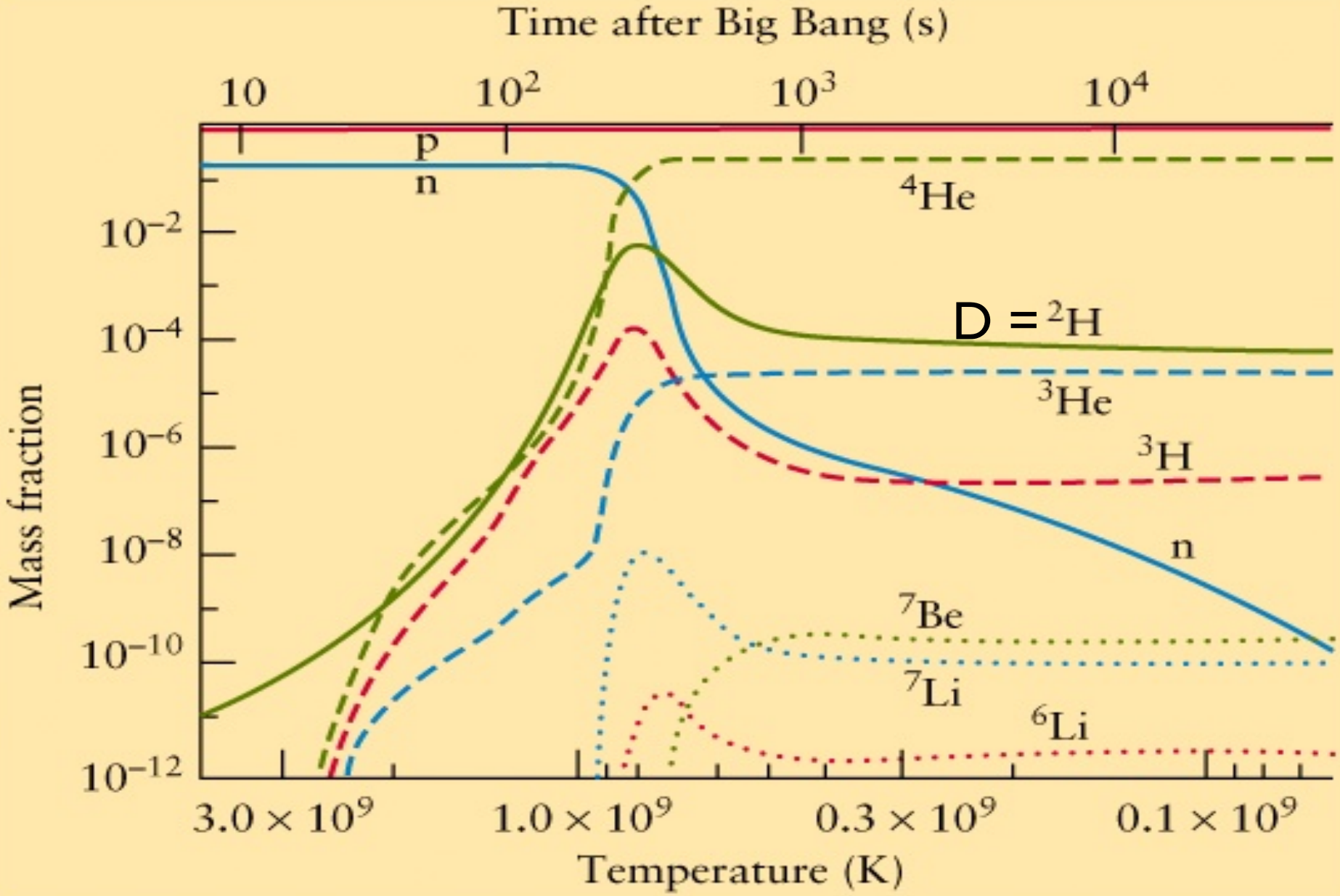

More baryons
⇒ More fusion reactions
⇒ Less deuterium

$\Omega_{baryon,0} = 0.04$

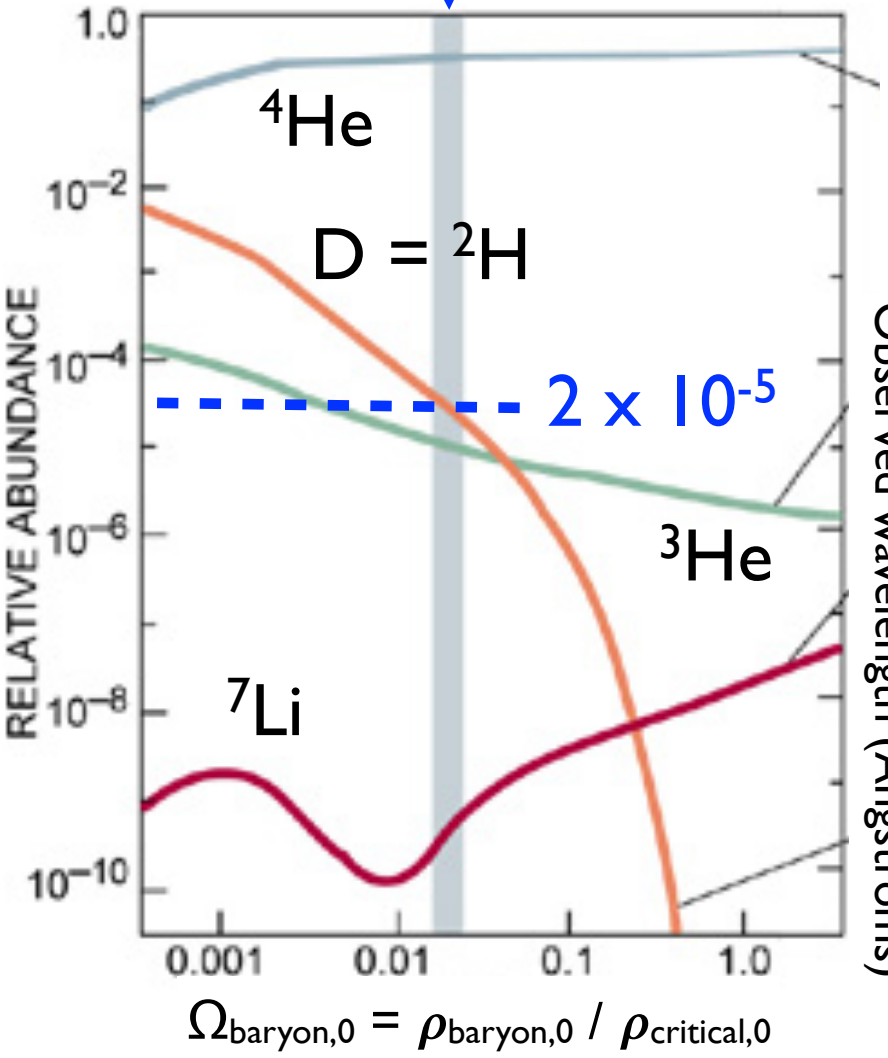

Primordial deuterium abundance measured from Ly-α forest